

# **Investigating the Effects of the Urban Environment on Cyclist Exposure to Near-Roadway Air Pollution**

William Jacob Farrell

Department of Civil Engineering & Applied Mechanics

McGill University, Montréal

August 2014

A thesis submitted to McGill University in partial fulfillment of the requirements of the degree of Master of Engineering in Civil Engineering

© William Jacob Farrell, 2014

# TABLE OF CONTENTS

Abstract .....	v
Résumé.....	vi
List of Figures .....	vii
List of Tables .....	ix
List of Abbreviations .....	x
Acknowledgements.....	xi
Preface & Contribution of Authors.....	xii
Chapter 1 — Introduction.....	1
1.1. Background & Motivation .....	1
1.2. Objectives.....	2
1.3. Summary .....	3
Chapter 2 — The Intersection of Cycling, Air Pollution, Health, and Land Use.....	6
2.1. Introduction .....	6
2.2. Air Pollution & Health .....	6
2.3. Air Pollution Mapping with Land Use Regression Models .....	7
2.4. Exposure & Dosage by Mode of Transportation .....	9
2.5. Cyclist Exposure by Cycling Facility & Route Choice .....	10
2.6. Conclusion.....	11
Chapter 3 —Air Quality Data Collection Methodology .....	12
3.1. Introduction .....	12
3.2. Instruments .....	13
3.2.1. Condensation Particle Counter .....	13
3.2.2. Microaethalometer .....	14
3.2.3. Global Position System Unit .....	14

3.2.4. Digital Camcorder.....	14
3.3. Mobile Data Collection Campaign.....	15
3.3.1. Route Selection .....	15
3.3.2. Project Bicycle.....	19
3.3.3. Data Collection Procedure .....	20
3.4. Fixed Site Data Collection Campaign.....	22
3.4.1. Location Selection .....	22
3.4.2. Data Collection Procedure .....	25
3.5. Conclusion.....	26
Chapter 4 — Mobile Data Processing Methodology.....	27
4.1. Introduction .....	27
4.2. Black Carbon Post-Processing .....	27
4.3. Combining Air Pollution Measurements with Location Data.....	29
4.4. Traffic Data .....	31
4.5. Built Environment Data .....	33
4.5.1. Cycling Infrastructure .....	33
4.5.2. Urban Canyon Effect .....	35
4.5.3. Other Land Use Data .....	36
4.6. Meteorological Data.....	37
4.7. Conclusion.....	38
Chapter 5 — Using Fixed Site Monitoring to Understand the Effects of Built Environment on Air Pollution Concentrations and Dispersion .....	39
5.1. Introduction .....	39
5.2. Methodology .....	40
5.2.1. Developing Explanatory Variables for Overall UFP Levels .....	40

5.2.2.	Two-Sided Measurements .....	42
5.3.	Results .....	43
5.3.1.	Independent Observations.....	43
5.3.2.	Observations Averaged by Site.....	46
5.3.3.	Two-Sided Measurements .....	48
5.4.	Discussion and Conclusion .....	50
Chapter 6	— Generating a Land Use Regression Model With Mobile Measurements .....	53
6.1.	Introduction .....	53
6.2.	Methodology .....	53
6.3.	Results .....	54
6.3.1.	Descriptive analysis .....	54
6.3.2.	Regression analysis.....	61
6.4.	Discussion .....	62
6.5.	Conclusion.....	63
Chapter 7	— Understanding the Effects of Cycling Facility Infrastructure and Route Choice	65
7.1.	Introduction .....	65
7.2.	Methodology .....	65
7.3.	Results .....	67
7.3.1.	Air Pollution Mapping.....	67
7.3.2.	Cycling Facilities Analysis.....	69
7.3.3.	Regression Analysis.....	71
7.4.	Conclusion and Discussion .....	73
Chapter 8	— Conclusion .....	76
8.1.	Implications.....	76

8.1.1. Methodological Implications .....	76
8.1.2. Consequential Implications.....	76
8.2. Limitations .....	77
8.3. Future Work .....	79
8.4. Summary .....	79
References.....	82

## ABSTRACT

This thesis seeks to understand how the built environment and surrounding land use affect variations in near-roadway air pollution. In particular, two air pollutants are investigated: ultrafine particles (UFP) and black carbon (BC). Specifically, the study explores this question in the context of urban cycling. That is, how do factors such as traffic, buildings, and cycling infrastructure affect the concentration of air pollution to which cyclists are exposed?

These answers are sought by way of a large-scale environmental monitoring campaign on the Island of Montreal during the summer of 2012. The campaign is comprised of two components: a mobile measurement portion whereby bicycles equipped with air pollution monitoring equipment cycle across roughly 500 km of unique roadway collecting UFP and BC concentrations, paired with global positioning system (GPS) data which allowed air pollution levels to be associated with the street on which they were collected—and a fixed site monitoring portion whereby research assistants measured pollution and counted traffic volumes and composition for set intervals of time at 73 locations. The overarching objective was to explain the variations in air pollution concentration by meteorological and built environment data, using land-use regression (LUR) analysis techniques. The mobile analysis relies primarily on geographic information systems (GIS) based land-use data while the fixed site analysis relies primarily on field measurements.

Several investigations follow from this general data collection campaign. From the fixed site data a LUR model is developed based on meteorological factors, vehicular volumes and compositions, and built environment characteristics of the roadway corridor. These data also form the basis of a secondary investigation which explains the differences in UFP levels on opposite sides of the same street using wind, urban canyon, and traffic characteristics. Notable findings include support for some meteorological and urban canyon effects on air pollution, the relevance of both vehicular volumes as well as the truck component thereof.

Two investigations arise from the mobile data collection campaign. The first attempts to explain the variations in air pollution using meteorological, land-use, and roadway characteristics, including results from a mesoscopic traffic simulation. The second seeks to understand how the nature of cycling infrastructure and cycling network design affect cyclists' exposure to pollution. In addition to the effects captured in the fixed site analysis, relevant observations include the strong effects of nearby highways, especially for BC, and nearby restaurants, especially for UFP. The latter investigation from the mobile campaign shows that cycling facilities along major roads tend to have higher levels of pollution, however separated cycling infrastructure did reduce exposure to BC, perhaps owing in part from their greater distance from the street centerline. However the strongest reductions in air pollution were observed on multi-use trails, which typically run through parks and are located at substantial distances from the street.

Together, these investigations use a novel methodological framework to unravel the interactions between cycling, the built environment, land use, traffic, and air pollution.

**Keywords:** black carbon; cycling infrastructure; cycling facilities; cyclist exposure; environmental monitoring; land use regression; air pollution exposure; ultrafine particles

## RÉSUMÉ

Cette thèse cherche à comprendre comment la cadre bâti et entourant l'utilisation du sol affectent les variations de la pollution de l'air près de la chaussée. En particulier, deux polluants atmosphériques sont étudiés: les particules ultrafines (UFP) et la suie (BC). Plus précisément, l'étude explore cette question dans le contexte du cyclisme urbain. Autrement dit, comment ne facteurs tels que le trafic, les bâtiments et les infrastructures cyclables affectent la concentration de la pollution de l'air à laquelle sont exposés les cyclistes?

Ces réponses sont recherchées par moyen d'une campagne de surveillance de l'environnement sur l'Île de Montréal au cours de l'été 2012. La campagne est généralement composée de deux éléments: une partie surveillance mobile dans laquelle des vélos équipés d'équipement de surveillance de la pollution de l'air ont parcouru environ 500 km de route unique mesurant des concentrations de particules ultrafines et de suie—et une partie de surveillance sur site fixe, où des assistants de recherche ont mesuré la pollution et ont compté le volume et la composition du trafic pour des intervalles définis de temps à 73 emplacements. L'objectif principal était d'expliquer les variations de la concentration de la pollution de l'air par des données météorologiques et du cadre bâti, en utilisant des techniques d'analyse de régression d'utilisation du sol (LUR). L'analyse mobile repose principalement sur les données de l'utilisation du sol, en forme de systèmes d'information géographique (GIS), tandis que l'analyse de site fixe repose principalement sur des mesures prises sur le site.

Plusieurs enquêtes découlent de la campagne principale. Un modèle de régression de l'utilisation du sol est développé à partir de la campagne sur site fixe. Ce modèle utilise des facteurs météorologiques, le volume routier et sa composition, et les caractéristiques du cadre bâti et de la chaussée. Ces données sont aussi utilisées comme fondement d'une autre enquête, qui explique la différence entre des niveaux d'UFP sur les côtés opposés de la même rue, utilisant les propriétés du vent, du canyon urbain, et du trafic. Des résultats notables incluent un appui pour des effets météorologiques et de canyon urbain sur la pollution de l'air, la pertinence des volumes de véhicules et de la composante de camions de celui-ci.

De plus, la campagne mobile est la fondation de deux autres enquêtes. La première est une explication de la variation dans la pollution de l'air qui utilise des caractéristiques de la météorologie, de l'utilisation du sol, et de la chaussée. Les attributs de la chaussée incluent les résultants d'une simulation mésoscopique du trafic. La deuxième enquête cherche à comprendre comment la nature des infrastructures cyclables et le design du réseau cyclable affectent l'exposition des cyclistes à la pollution. En plus des effets capturés dans l'analyse sur site fixe, des observations pertinentes comprennent les effets importants de la proximité aux autoroutes, en particulier pour la suie et la proximité aux restaurants, en particulier pour les UFP. La dernière enquête de la campagne mobile démontre que le réseau cyclable sur les routes principales tend à avoir des niveaux plus élevés de pollution, mais les pistes cyclables réduisent l'exposition à la suie, peut-être en partie en raison de leur plus grande distance de l'axe de la rue. Toutefois, les réductions les plus fortes de la pollution de l'air ont été observées sur les sentiers polyvalents, qui passent généralement dans des parcs et sont situés à des distances considérables de la rue.

Ensemble, ces enquêtes utilisent un nouveau cadre méthodologique pour démêler les interactions entre le vélo, le cadre bâti, l'utilisation des terres, la circulation, et la pollution de l'air.

**Mots-clés :** exposition de la pollution de l'air; exposition des cyclistes; infrastructure cyclable; model de régression de l'utilisation du sol; particules ultrafines; réseaux cyclables; suie; surveillance de l'environnement

## LIST OF FIGURES

Figure 1.1: Methodological Thesis Outline .....	4
Figure 3.1: A screenshot of the A.I.M. software used to upload UFP data .....	13
Figure 3.2: The extent of the cycled network, shown with parks, the CBD, and what is defined as the downtown region.....	16
Figure 3.3: Project bicycle set-up used for the mobile data collection campaign. ....	19
Figure 3.4: Project Flowchart for the Mobile Measurement Data Collection and Processing .....	22
Figure 3.5: Fixed Monitoring Locations shown atop ambient NO <sub>2</sub> levels in Montreal .....	23
Figure 4.1: Illustration of the ONA Algorithm Based on Light Attenuation.....	28
Figure 4.2: Cumulative Distribution of ONA Averaging Duration, Demarcating the 50 <sup>th</sup> and 90 <sup>th</sup> percentiles .....	29
Figure 4.3 Data were averaged by each trip on each link; for example the red solid circles and hollow circles were both averaged onto the red link, but as two independent observations. All point data were also assigned the properties of the cycling facility (green) that they were cycled on. ....	31
Figure 4.4: Validation of the Simulated Counts against the Manual Counts results in a correlation of $r=0.78$ ( $p<0.0001$ ; $n=214$ ) .....	32
Figure 4.5: Cycling Network Covered in the Mobile Data Collection Campaign.....	35
Figure 4.6: Schematic Diagram of the Urban Canyon Effect .....	36
Figure 5.1: Histogram of $\ln(\text{UFP})$ for each Observation .....	44
Figure 5.2: Histogram of the $\ln(\text{UFP})$ Concentration at Each Site .....	47
Figure 5.3: Histogram of all observations for $\ln( \Delta\text{UFP} )$ measurements.....	49
Figure 6.1: Histogram of the $\ln$ -transformed of all recorded UFP measurements.....	54
Figure 6.2: Histogram of the $\ln$ -transformed of all recorded BC measurements.....	55
Figure 6.3: Spatial Distribution of UFP .....	56
Figure 6.4: Spatial Distribution of BC .....	56
Figure 6.5: Dummy temperature correlations with $\ln(\text{UFP})$ and $\ln(\text{BC})$ .....	58
Figure 6.6 Maximum Pollution Decay over Distance in Intervals of 1 m.....	63
Figure 7.1: A screenshot of the database to illustrate how data were related .....	67
Figure 7.2: UFP concentration maps for the morning period, divided by quartiles; the link results shown are the average of all trips on the link. ....	67



Figure 7.3: BC concentration maps for the morning period, divided by quartiles; the link results shown are the average of all trips on the link. ....	68
Figure 7.4: Box plot of UFP by cycling facility and road type (omitting extreme values) .....	70
Figure 7.5: Box plot of BC by cycling facility and road type (omitting extreme values) .....	71

## LIST OF TABLES

Table 3.1: Cycling Routes Detailed Descriptions .....	17
Table 3.2: Possible Values for the Naming Convention .....	21
Table 3.3: Fixed Site Monitoring Locations .....	24
Table 4.1: Cycling Facility Classifications .....	34
Table 4.2: Photo Examples of the Physical Configuration of Each Designated Facility Type (Google StreetView) .....	34
Table 5.1: Stability Class Calculation Table [shown with data entry codes] (Adapted from Pasquill 1961) .....	41
Table 5.2: Stability Class Descriptions [shown with data entry codes] (Adapted from Pasquill 1961) .....	41
Table 5.3: Descriptive Statistics for Select Variables over all Observations .....	45
Table 5.4: Linear Regression of $\ln(\text{UFP})$ for all Fixed Site Observations ( $R^2=0.3044$ ; $n=200$ ) ..	46
Table 5.5: Descriptive Statistics for Select Variables at Each Site.....	48
Table 5.6: Linear Regression for $\ln(\text{UFP})$ at Each Site ( $R^2=0.6807$ ; $n=73$ ).....	48
Table 5.7: Descriptive Statistics for Two-Sided Variables Used in Regression.....	49
Table 5.8: Linear Regression Analysis for $\ln( \Delta\text{UFP} )$ ( $R^2=0.4739$ ; $n=50$ ).....	50
Table 6.1: Descriptive Statistics for Air Quality Data.....	55
Table 6.2: Descriptive Statistics for Meteorological Variables .....	57
Table 6.3: Univariate Regression Results for Built Environment Variables .....	59
Table 6.4: Linear Regression for $\ln(\text{UFP})$ Mobile Measurements ( $R^2 = 0.3401$ ; $n = 16,745$ ) .....	61
Table 6.5: Linear Regression for $\ln(\text{BC})$ Mobile Measurements ( $R^2 = 0.2009$ ; $n = 13,217$ ) .....	61
Table 7.1: Air Pollution Variability .....	68
Table 7.2: Pollution, Traffic, and Distance from Road by Cycling Facility Class .....	69
Table 7.3: Descriptive Statistics for Regression Variables Considered .....	72
Table 7.4: Linear Regression for $\ln(\text{UFP})$ ( $n=17,516$ ; $R^2=0.223$ ) .....	72
Table 7.5: Linear Regression for $\ln(\text{BC})$ ( $n=13,335$ ; $R^2=0.153$ ) .....	73

## LIST OF ABBREVIATIONS

AIM Aerosol Instrument Manager

AMT Agence métropolitaine de transport

BC Black Carbon

BE Built Environment

CBD Central Business District

CMA Census Metropolitan Area

CPC Condensation Particle Counter

GIS Geographic Information Systems

GPS Global Positioning System

IQR Interquartile Region

LN Natural Logarithm

LUR Land-Use Regression

NO<sub>2</sub> Nitrogen Dioxide

PM<sub>#</sub> Particulate Matter of  $\varnothing \leq \# \mu\text{m}$

S.D. Standard Deviation

S.E. Standard Error

UFP Ultrafine Particles

v/c Volume/Capacity Ratio

## ACKNOWLEDGEMENTS

I would first like to thank the research assistants, some of whom cycled over 1,000 km in the course of this exercise, for their extraordinary data collection and compilation efforts: Noel Brownlie, Bernard Moulins, Julien Neves-Pelchat, Graeme Pickett, Rhokho Kim, Rebecca Luck, Nicolas Truong, and Mohamad Zukari. I also thank Timothy Sider for providing the vehicular volume results from the mesoscopic traffic simulation. Next I would like to thank the Transportation Research at McGill (TRAM) group for providing the bicycle network data vital to this thesis. I would also like thank the National Sciences and Engineering Research Council of Canada (NSERC) and the Canadian Institute of Health Research (CIHR) for their Collaborative Health Research Projects (CHRP) grant, which has made this study financially possible. Additionally, I thank McGill University and Health Canada for providing the resources required for these studies.

Next, I would like to extend my deep gratitude to my friends and colleagues in the research group for consistently making this time such an amazing experience—specifically, Ahsan Alam, Sabreena Anowar, Golnaz Ghafgazi, Maryam Shekarrizfard, Timothy Sider, and Shamsunnahar Yasmin. Furthermore, I am grateful for all of my other friends in Transportation Engineering, Urban Planning, and elsewhere in the McGill community for making this time truly wonderful.

My sincere thanks to all of the great professors and collaborators who have deeply contributed to my knowledge and appreciation of their respective expertise—specifically Professor Naveen Eluru, Professor Mark Goldberg, Dr. Scott Weichenthal, Professor Ahmed El-Geneidy, Professor Luis Miranda-Moreno, Professor Thomas Naylor, and Professor Peter Brown.

Of course I am enormously thankful to the immeasurable love and support from my parents, William and Nancy, my brother Eric, and my sister Beth.

Finally, I am truly indebted to unparalleled support and guidance of my supervisor, Professor Marianne Hatzopoulou, with whom I have had the tremendous privilege of working. Undoubtedly, without her unwavering confidence in my ability, I would have had neither the opportunity to pursue this degree nor the endurance to complete it.

## **PREFACE & CONTRIBUTION OF AUTHORS**

The thesis to follow represents the culmination of a large-scale data collection effort carried out in order to assess the near roadway air pollution to which urban cyclists are exposed. The study is funded by the Collaborative Health Research Projects (CHRP) grant, which itself is a joint effort of the National Sciences and Engineering Research Council of Canada (NSERC) and the Canadian Institute of Health Research (CIHR). This thesis represents a portion of the overall project, which is to not only assess the air pollution exposure, but to understand their acute health impacts as well.

I would first like to note the vital contributions of the research assistants: Noel Brownlie, Bernard Moulins, Julien Neves-Pelchat, Graeme Pickett, Rhokho Kim, Rebecca Luck, Nicolas Truong, and Mohamad Zukari. Not only did they collect the entirety of the data presented, they have undergone tremendous efforts to process and compile it as well. This includes the calculations for the Optimized Noise Averaging of the mobile black carbon results. I would also like to acknowledge the contribution of classmates Marie-Jacqueline Bower, Sara Fitzpatrick, and Kevin Kwateng Amanin for their assistance in preparing some of these data for a class presentation.

Most of the content in this thesis has been adapted from works either submitted to or drafts in preparation for academic conferences and journals. However these manuscripts have been heavily edited and expanded upon in order to properly conform to the thesis format. All of these manuscripts have been prepared collaboratively with the primary investigator and my supervisor, Professor Marianne Hatzopoulou, as well as Health Canada Research Scientist, Dr. Scott Weichenthal, from the Air Health Effects Science Division, and Professor Mark Goldberg, from the Department of Clinical Epidemiology at the McGill University Health Centre. Although their guidance and revisions have been truly invaluable, I have drafted the content within this thesis.

I will outline in more detail now which sections of the thesis are associated with each publication. Part of the introduction was adapted from a manuscript accepted for the 92<sup>nd</sup> Annual Meeting of the Transportation Research Board (Farrell et al. 2013). The data used in Chapter 5, including the graphic in Figure 3.5, was first used for a journal submission primarily authored by Dr. Scott Weichenthal (Weichenthal et al. 2014). However, the data has been reinterpreted and is now authored by myself. Chapter 6 is primarily derived from an accepted manuscript to the 93<sup>rd</sup> Annual Meeting of the Transportation Research Board (Farrell et al. 2014a), which itself is currently being adapted for a journal submission. The mesoscopic traffic simulation data used in

these chapters was developed primarily by Timothy Sider (Sider, Alam, et al. 2013). Parts of the literature review, the methodology, and the entirety of Chapter 7 are drawn from a paper accepted at the World Symposium on Land Use and Transportation (WSTLUR) conference (Farrell et al. 2014b) and later submitted to the Journal of Transport and Land Use Research (JTLU).

I would also like to acknowledge the contributions of Jean-Philippe Lafleur and Gabriel Damant-Sirois for their assistance in proofreading and editing the French translation of this abstract.

## CHAPTER 1 — INTRODUCTION

### 1.1. Background & Motivation

In recent years, municipalities across the world have sought to promote cycling, in part as an effort to reduce traffic-related air pollution and to increase health and fitness among their residents. Particularly, dedicated cycling infrastructure and low-cost bicycle rental programs are now popular in major cities around the world including Montreal, Barcelona, Paris, Mexico City, and London (Rojas-Rueda et al. 2011). However, due to the close proximity of cyclists to vehicular exhaust, in combination with higher rates of inhalation and increased time spent on the road, cyclists may in fact experience higher exposure to some common traffic pollutants than motorists (de Nazelle and Rodríguez 2009).

The City of Montreal has made considerable investments in cycling facilities since 1995 when the provincial government of Quebec adopted official bicycle policies with the goal of increasing the mode share and safety of cycling through the incorporation of cycling facilities in all new road projects (Pucher and Buehler 2005). The fruits of this investment have been documented by Vélo Québec (2010) in their quinquennial report stating that between 2005 and 2010 the city saw a 10% increase in cycling trips. This increase can be seen among cyclists of all ages, for both utilitarian and leisure trips. In that same time, 160 km of bikeways were added to the cycling network. Furthermore, the increase in the breadth and connectivity of the cycling network has increased users' actual and perceived safety, the latter being an important determinant for the choice of cycling as a transport mode (Larsen, Patterson, and El-Geneidy 2013; Lusk et al. 2011).

However, in a recent evaluation of air pollution along cycling facilities in Montreal, Strauss et al. (2012) found that the facilities that attract the highest volumes of cyclists are also the ones that are characterized by the highest air pollution levels. Yet the study did not explain the variability in pollution levels across cycling facilities nor did it examine the determinants of air pollution exposure. Here we need more literature on cyclist exposure to air pollution and exposure across modes to set the stage as to why this research is important. In order to inform the development of new policies affecting the expansion of the bicycle network, it is important to capture detailed information on the factors influencing cyclists' exposure as well as to understand the spatial variability of air pollution across the Montreal bike network.

This thesis presents the experimental design and results of a large-scale data collection exercise aimed at understanding the determinants of cyclists' exposure to air pollution in Montreal along a wide range of bicycle facilities, neighborhoods, roadway configurations, and times of day. For instance, how advantageous is it to cycle on a small, local street rather than a primary thoroughfare? Does the street alignment of a cycling facility influence the cyclists' pollution exposure? Most importantly, how can this knowledge be applied in order to design a cycling network that will reduce these impediments so that those who choose a pollution-free means of transport will not unjustly suffer a disproportionate effect of harmful motor vehicle generated air pollution?

## **1.2. Objectives**

Building on the strengths of a trans-disciplinary team of researchers with expertise in transportation engineering and planning, air quality modelling, personal exposure to air pollution, as well as epidemiology, a three-year research project has been underway in the City of Montreal. The overall goals of the project include the provision of essential information to develop innovative policies and guidelines to better design cycling infrastructure and information systems that will assist in minimizing exposure to air pollution among cyclists and other road users. The project includes two major data collection exercises, responding to the overarching research objectives:

- 1) In a wide survey of air pollution levels across Montreal roads, to identify factors affecting exposure and to determine how cycling facility type, traffic, built environment, and meteorology affect exposure
- 2) In a panel study of bicyclists:
  - i. to determine changes in levels of exposure to air pollution according to bicycle routes and traffic volumes
  - ii. to determine whether cyclists' exposure to air pollution is associated with decreased respiratory and cardiovascular function

This thesis is concerned primarily with the first component of this larger mission. That is to say, it does not deal specifically with health-related effects of air pollution, despite this topic remaining an important contextual component for the motivation of this study.



Ultimately, extensive field measurements and geospatial analysis are used in order to better understand the components of the built environment which affect one's personal exposure to these air pollutants. Specifically, two pollutants are measured: UFP and BC. Both pollutants are forms of particulate matter (PM) with the former referring to PM less than 0.1  $\mu\text{m}$  in diameter and the latter referring to PM comprised of pure carbon. They are associated with characteristics related to traffic volume, land-use, and the design of cycling infrastructure. A total of approximately 500 km of roads are covered in this survey with a focus on the most popular cycling corridors within the study region.

The objectives of this thesis are as follows:

1. to determine the levels of UFP and BC that users of the road network are exposed to in Montreal, with a particular emphasis on cyclists within the designated cycling network
2. to explain the variations in these levels in terms of the land-use, road characteristics, and built environment using a land-use regression statistical model
3. to test a novel methodological framework (mobile monitoring) that maximizes the spatial extent of data collection efforts
4. to evaluate this methodology by comparing it to more conventional techniques (fixed site monitoring)

### **1.3. Summary**

The thesis continues with a literature review of several topics related to the intersection of air quality, land-use, and cycling. Specifically it outlines the well-documented associations between transportation-generated air pollution and health, including more recent studies pertaining to the pollutants examined in this thesis. Next is an overview on the practice of using land-use regression models predictors of air pollution. Following this, the differences in exposure and dosage between various modes of transit are discussed, which lead into how these built environment characteristics are affected by cycling infrastructure and route choice.

Chapter 3 introduces the framework of the air quality data collection campaign that serves as the foundation of all further analysis. The data collection can be conceptually divided into two

components: a mobile measurement campaign and a fixed site measurement campaign. Figure 1.1 illustrates how the initial data collection methodology feeds into the following chapters.

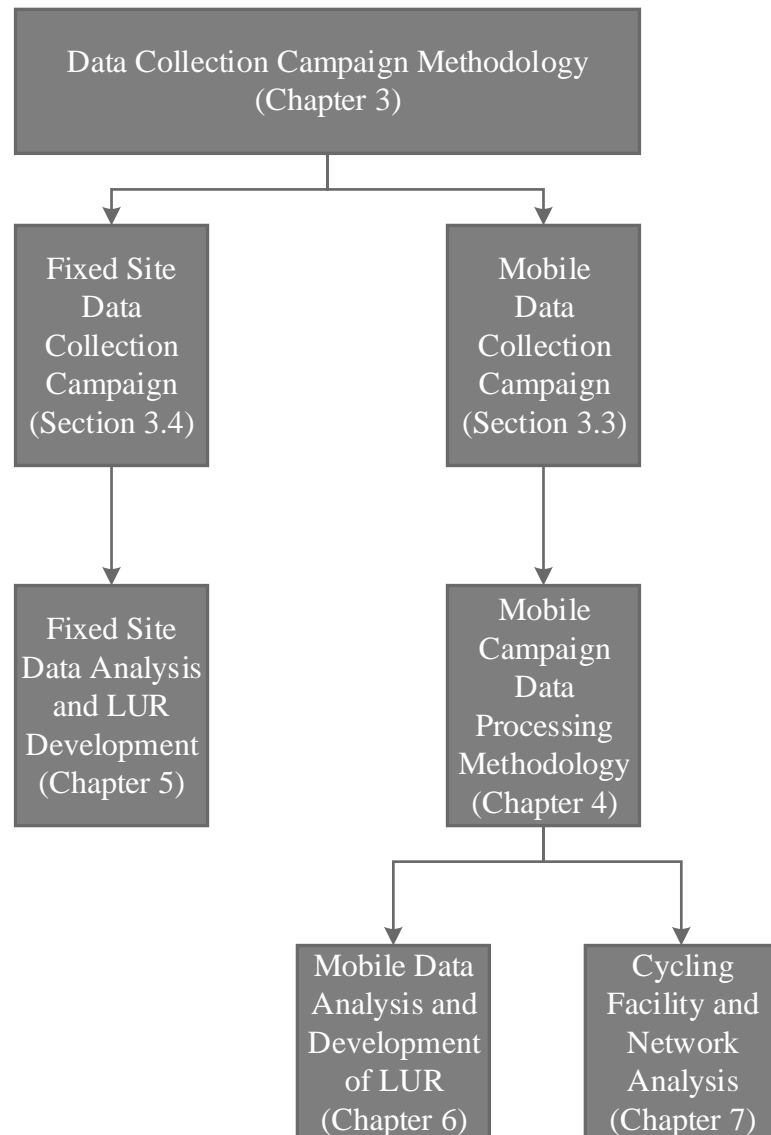


*Figure 1.1: Methodological Thesis Outline*

Chapter 4 discusses the various aspects of data processing that are common to the ensuing analyses. Each following chapter differs somewhat in its processing and interpretation of the data, however their similarities are sufficient to warrant a unified explanation. This chapter also includes

the ways that various land-use, road, cycling, and meteorological characteristics are incorporated into the analysis.

Chapter 5 concerns the fixed site data collection campaign, which was primarily intended to provide a baseline for analysis and validate the more experimental aspects of the mobile campaign. In addition, the nature of this methodology lends itself to a more detailed analysis of a more limited spatial extent. Furthermore, this data collection methodology allowed us to capture associations that are not able to be quantified in a large-scale model.

Chapter 6 is focused on the mobile measurement campaign as it relates to built environment characteristics as well as meteorology. This chapter develops a land use regression model based on attributes mostly ascertained through GIS analysis.

Chapter 7 is concerned with the elements of the mobile measurement campaign pertaining specifically to cyclist exposure to air pollution and how this may be affected by the specific cycling infrastructure and route choices of the cyclists.

The concluding chapter discusses the implications of this research as well as limitations and areas that would benefit from additional work. It also provides a brief summary of the topics discussed in the thesis.

## **CHAPTER 2 — THE INTERSECTION OF CYCLING, AIR POLLUTION, HEALTH, AND LAND USE**

### **2.1. Introduction**

The intersection of air pollution, health, transportation and land use forms a complex topic, yet one that has been extensively studied from many perspectives. Some aspects have been active topics of research for decades, yet others are emerging fields. The literature review begins in Section 2.2 with an overview of the relationship between air pollution and human health, especially in regard to the pollutants to be further examined in this thesis. Section 2.3 describes a well-established method of estimating air pollution levels across a geographic region based on known land use characteristics. Following this, Section 2.4 explores a growing number of studies which attempt to establish the different levels of personal exposure to and dosage of air pollution based on the mode of transport. Finally, Section 2.5 examines the relatively nascent field of determining how these land use characteristics, including cycling facility design, specifically affect the exposure of cyclists to air pollution.

### **2.2. Air Pollution & Health**

Traffic-related air pollution has a large impact on the health of urban populations. There is ample evidence which establishes a causal link between chronic exposure to ambient air pollution and the incidence of and mortality from cardiovascular disease (especially ischemic heart disease) and lung cancer (Brook et al. 2004; Chen, Goldberg, and Villeneuve 2008). As well, there are overwhelming data implicating acute exposures to air pollution causing a variety of immediate health effects (Pope 2000; Dockery 2001; Pope and Dockery 2006). There is no escape from air pollution, especially in large urban areas, although there are small-scale variations that depend on traffic, land use, and other factors.

Particulate matter (PM) is among the most heavily studied air pollutants and has long been known to cause negative health outcomes including increased mortality and morbidity (Samet et al. 2000; Katsouyanni et al. 2001; Brunekreef and Holgate 2002). PM<sub>10</sub>, or PM with diameter less than 10  $\mu\text{m}$  can penetrate the lower respiratory system while PM<sub>2.5</sub> can penetrate the gas-exchange regions of the lungs (Brunekreef and Holgate 2002). More recently, two manifestations of PM,

ultrafine particles (UFP) and black carbon (BC) have been the subject of considerable attention among air pollution and health researchers.

UFP is an order of magnitude smaller than  $PM_{2.5}$ , with a maximum diameter of 0.1  $\mu m$ , while its total surface area is up to a thousand times greater per unit mass than  $PM_{2.5}$  (Berghmans et al. 2009). Its size allows it to penetrate much more deeply into the lungs and lung tissue and its surface area causes more interaction with the tissue at the cellular level. Because of these factors, it has been suggested that conventional environmental monitoring measures accounting only for PM mass are insufficient to fully understand personal PM exposure (Martins et al. 2010). UFP has been linked to a number of negative acute and chronic health outcomes, among them, oxidative-stress induced DNA damage (Li et al. 2002; Calderón-Garcidueñas et al. 2008), reduced heart rate variability (Weichenthal et al. 2011), and inflammation of the cardiovascular and respiratory systems (Card et al. 2008; Jacobs et al. 2010; Strak et al. 2010). BC, also known as soot, is primarily caused by diesel traffic and is known to contribute a positive forcing to anthropogenic climate change. It too is linked to cardiovascular and respiratory inflammation (Jansen et al. 2005; Highwood and Kinnersley 2006). BC and UFP are also both associated with a decrease in peak expiratory flow rate (Zuurbier et al. 2011).

### **2.3. Air Pollution Mapping with Land Use Regression Models**

Land use regression (LUR) models associate a sample of air pollution measurements with a set of relevant land use characteristics which describe the location at which the measurement was taken. Locations are typically distributed across the study region and located within a variety of geographical contexts. The geographical attributes associated with each measurement location are then used as explanatory variables in a regression model for the pollutant in question. These models allow researchers to estimate high resolution regional air quality maps as a function of these explanatory characteristics.

LUR modelling is a very well-established technique for assessing the variations in local air pollution concentrations based on a limited number of sampling stations. It was first introduced in the pollution mapping context by the trans-European *Small Variations in Air Quality And Health* (SAVIAH) study almost two decades ago as a response to growing concern about traffic-related air pollution in urban centers (Collins, Smallbone, and Briggs 1995). This seminal research campaign sought to address the limitations of two other methods of determining small-scale

variation in urban air pollution: the cruder approach of spatial interpolation and the more computationally intensive method of modeling air dispersion. By making use of the rising power of geographic information systems (GIS), their spatial estimates were able to provide a better model fit than simple interpolation and resulted in comparable results to the far more difficult dispersion modelling techniques available (Briggs et al. 1997; 2000). This and other early LURs repeated in cities across the world tended to use a common marker of traffic-related air pollution, nitrogen dioxide (NO<sub>2</sub>), as the dependent variable due in part to its high spatial variability, relative temporal stability, and ease of passive measurement techniques (Gilbert et al. 2005; Ross et al. 2006; Sahsuvaroglu et al. 2006; Henderson 2007).

Since their inception, a number of meta-analyses and other investigations have supported the general reliability of LUR methods while also pointing towards their limitations. These studies show that among the strongest predictors of traffic were road type, traffic count, and land cover, along with natural characteristics such as climate and geography (Ryan and LeMasters 2007; Hoek et al. 2008; Health Effects Institute 2010). However, air pollution varies greatly both spatially and temporally (Crouse, Goldberg, and Ross 2009), and as such, model fit usually increases based on the diversity of site selection more so than the number of sites (Ryan and LeMasters 2007). In fact, Johnson et al. (2010) show that the model fit tends to decrease with an increase in sampling locations, yet the reverse was true with respect to how well these models performed when applied to datasets not included in the initial analysis. The duration of sampling also remains a significant limitation in LURs as monitoring is typically conducted with one to four surveys of one or two weeks each (Hoek et al. 2008; Johnson et al. 2010). Model fit tends to improve with longer sampling; however by averaging this greater variability studies sacrifice temporal resolution for models with ostensibly better predictive power. Ryan and LeMasters (2007) found model fit values typically ranged from an R<sup>2</sup> value of 0.54 to 0.81.

Despite these limitations, LURs remain an important tool in predicting exposure to air pollution. In recent years, the technique has been expanded to include the two pollutants of interest in this investigation: UFP and BC. These particles are increasingly used as markers of traffic-related air pollution, however their extremely high spatiotemporal variability make them especially difficult to model effectively. These studies show strong evidence that UFP and BC are correlated with traffic density, and especially truck traffic, and are inversely related to temperature and wind

speed (Kaur and Nieuwenhuijsen 2009; Berghmans et al. 2009; Sider, Goulet-Langlois, et al. 2013; Abernethy et al. 2013; Hatzopoulou et al. 2013). Additionally, many road geometry and land use variables have also shown strong correlations with air pollution concentrations. Distance to major cross-street (Rivera et al. 2012), distance to the nearest road (Hoek et al. 2011), fast food restaurants (Abernethy et al. 2013), distance to a seaport, and population and building density (Abernethy et al. 2013; Hoek et al. 2011), among others have all shown correlations with either UFP, BC, or both.

More recent LURs have taken advantage of improvements in instrument technology, especially UFP, where mobile monitoring equipment has only recently become available (Weichenthal et al. 2011; Hatzopoulou et al. 2013). Mobile monitoring has also been utilized in order to establish the difference in exposure by transport mode, a topic to be further explained in Section 2.4.

## **2.4. Exposure & Dosage by Mode of Transportation**

Both UFP and BC are associated with traffic emissions and therefore are elevated in near-road environments. Near roadway air pollution is a problem affecting all users of the street, considering that travel accounts for a disproportionately large fraction of personal daily exposure to air pollution (de Nazelle et al. 2012; Dons et al. 2012). Research that investigates the interactions between the built environment, active transportation, and air quality has focused on monitoring personal exposure in transport micro-environments, showing air pollution exposure to be elevated not only for pedestrians and cyclists but also for drivers and transit riders. Briggs et al. (2008) showed that mean exposures while walking were greatly in excess of those while driving. Tsai et al. (2008) found that motorcycle commuters were exposed to the highest concentrations and car commuters to the lowest while bus commuters' longer commuting time resulted in high exposures. In a review of personal exposure studies, Kaur et al. (2007) noted that most studies found higher in-vehicle exposures compared to pedestrians.

Indeed, the vast majority of research is converging on the understanding that air pollution exposure levels are greater in motorized vehicles than in active modes of transport for UFP (Boogaard et al. 2009; Kaur and Nieuwenhuijsen 2009; de Nazelle et al. 2012; Kingham et al. 2013) and BC (Highwood and Kinnersley 2006; de Nazelle et al. 2012; Dons et al. 2012), however results may differ when analyzing different pollutants. There are many reasons for the differences

in research findings, namely variations in the environmental context, monitoring methods, meteorology, vehicle ventilation and most importantly exposure duration and breathing rates which have not been consistently taken into account.

However, a distinction must be drawn between exposure and dosage. While exposure refers to the concentrations in a given environment, dosage refers more specifically to the actual amount of pollution deposited in the body; in the case of air pollution this occurs via inhalation. Due to the nature of cycling, and to a lesser extent walking, personal dosage for the same level of exposure for both UFP (Berghmans et al. 2009; Int Panis et al. 2010; de Nazelle et al. 2012) and BC (de Nazelle et al. 2012; Dons et al. 2012) may be up to twice as high during active transport. This is primarily due to increased minute ventilation rates of cyclists, which could be over four times greater than drivers and passengers of motorized transportation (Int Panis et al. 2010). This difference reinforces the imperative to better mitigate the air pollution to which cyclists are exposed in the first place.

## **2.5. Cyclist Exposure by Cycling Facility & Route Choice**

Recent research suggests a strong association between the built environment and physical activity, implying that compact urban areas contribute to decreased automobile dependency and increased walking and cycling (Frank et al. 2007; 2008). Cycling is an increasingly popular choice for urban residents in North America, and cities are accordingly expanding their cycling infrastructure to accommodate this demand. However, planning an effective cycling network is a difficult task, demanding consideration of a large number of factors. Safety, comfort, accessibility, demand, cost, and maintenance must all be paid due attention, and all have been studied much in the literature and in practice. Yet, there is a startling dearth of literature seeking to determine a set of best practices for designing cycling networks with respect to cyclists' exposure to harmful pollutants. Due to their proximity to traffic, high respiration rates, and longer journeys, cyclists are at risk of being exposed to higher concentrations of air pollution as compared to other users of the road system.

Despite this, the promotion of cycling facilities and development of cycling networks is done with little regard to cyclists' exposure to air pollution. However, a number of studies are beginning to emerge highlighting the effect that route choice has on pollution exposure. Streets with higher traffic volumes are associated with higher UFP (Boogaard et al. 2009; Kaur and



Nieuwenhuijsen 2009; Kingham et al. 2013) and BC (Dons et al. 2013). Research that assesses the factors affecting overall exposure found that traffic density and dispersion characteristics of the road (Briggs et al. 2008), pavement position and the side of road walked upon (Kaur, Nieuwenhuijsen, and Colvile 2005), as well as traffic volumes, wind speed, and operation of the clearway (Greaves, Issarayangyun, and Liu 2008) as significant predictors of exposure.

Regarding the actual facility type, very little research has been conducted, and that which has been currently lacks decisive results. One study has shown that more popular cycling routes were characterized by higher exposure to NO<sub>2</sub>, a common marker of traffic-related air pollution, based on a land use regression model (Strauss et al. 2012). Some particularly recent studies have shown that cycle tracks, which are physically separated from traffic, may in fact have a modest reduction of UFP (Hatzopoulou et al. 2013; Kingham et al. 2013) and BC (Hatzopoulou et al. 2013) concentrations. The manipulation of natural pollutant dispersion patterns in urban street canyons—known as passive control of air emissions—through low boundary walls (McNabola, Broderick, and Gill 2008), trees (Buccolieri et al. 2009), and noise barriers (King, Murphy, and McNabola 2009) has shown promising results. Note however, that under certain conditions passive controls have been shown to significantly increase concentrations on the roadway (Baldauf et al. 2008).

## **2.6. Conclusion**

The intersecting disciplines of environmental monitoring, epidemiology, and urban design are all vitally important if efforts to encourage utilitarian cycling are to continue. It should be made clear however that despite the elevated risks of negative health outcomes pertaining to air pollution, the benefit of the physical activity required for cycling allows it to remain an overall healthier alternative to more sedentary modes of transport, even in light of risks of physical injury and air pollution exposure (Rojas-Rueda et al. 2011). So while it should be acknowledged that cycling remains an overall healthy activity, this ought not result in complacency with preventable risks, including the dangers of inhaling traffic-related air pollution. This especially as cycling continues to be encouraged as a positive force for the environment and personal health.

The geostatistical modeling techniques described in Section 2.3 are currently among the most reliable methods researchers today have in explaining the spatiotemporal variation in air pollution. This, combined with the known health effects described in Section 2.2 and the increased

dosage faced by cyclists as described in Section 2.4 establish the academic groundwork that comprises the motivation behind this research project. However, as Section 2.5 establishes, there is currently little research done with regard to how the built environment and cycling network affects this particularly vulnerable transportation choice. If cycling is to be promoted as part of an environmental and public health agenda, then reasonable measures should be taken in order to curb cyclists' exposure to the very pollutants that they themselves are helping to reduce, whilst avoiding the increase of their own risk of respiratory and cardiovascular ailments.

## **CHAPTER 3 —AIR QUALITY DATA COLLECTION METHODOLOGY**

### **3.1. Introduction**

The core of this thesis is premised on an extensive air quality data collection campaign conducted during the summer of 2012. Planning and scheduling took place in May of that year and field work was conducted during June and July. The study was located across the Island of Montreal in Quebec, Canada, and was primarily headquartered at the downtown campus of McGill University. The principal intent was to capture the relationship between air quality and the built environment by taking measurements at locations that varied in land use, road characteristics, and cycling facility design. Specifically, two traffic-related air pollutants were measured: UFP and BC. The study primarily consisted of two parallel streams:

- 1) Conducting a spatially extensive mobile air quality data collection campaign
- 2) Obtaining more detailed information at a number of stationary data collection sites

The chapter begins with Section 3.2 describing the various instruments used in the course of this research project. Section 3.3 details the data collection methodology used for the mobile component of the project, and serves as the foundation for Chapter 6 and Chapter 7. Section 3.4 describes the data collection methodology of the fixed site component and serves as the foundation for Chapter 5. For reference, Figure 1.1 outlines the relationship between these chapters and the results of these methodologies. Chapter 3 concludes with Section 3.5, which explains how these methods support the remainder of the thesis.

## 3.2. Instruments

### 3.2.1. Condensation Particle Counter

A portable condensation particle counter (CPC Model 3007, TSI) was used to measure UFP concentrations. Due to the minuscule size of ultra-fine particles ( $\leq 0.1 \mu\text{m}$ ), conventional mass concentration measurements are not possible. Instead, air passes through an alcohol-soaked wick, allowing the alcohol to condense around the particle, thus increasing its size so that it can be measured using conventional optical techniques in the form of a particle count concentration ( $\#/\text{cm}^3$ ). In recent years, portable CPCs have greatly expanded researchers' capacity for the mobile measurement of UFP.

The instrument was able to record at a frequency of 1 Hz. Instruments were zeroed weekly by placing an air filter over the intake to ensure that the baseline was correct. Data were logged in the memory of the instrument and, following each trip, were uploaded to a server as a C07 file using the manufacturer's software, Aerosol Instrument Manager (AIM), pictured in Figure 3.1. Following this, the C07 files were exported as XLS files using the timestamp as the data point time format.

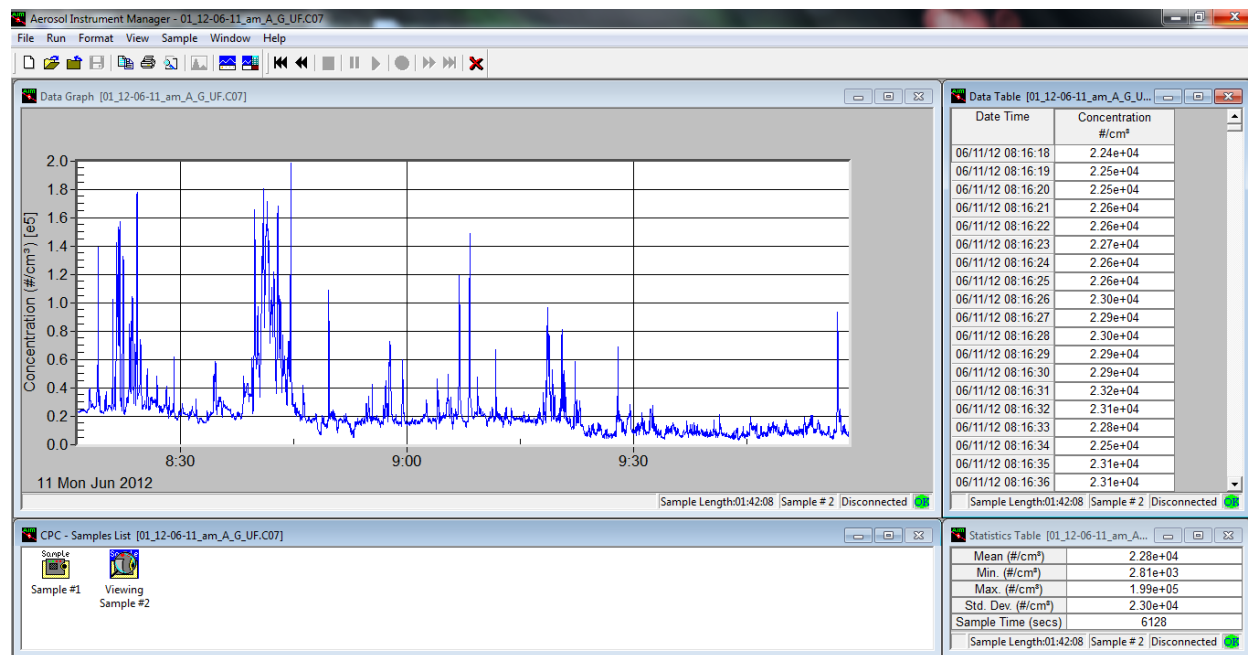


Figure 3.1: A screenshot of the A.I.M. software used to upload UFP data

### 3.2.2. *Microaethalometer*

A microaethalometer (MicroAeth AE51, Magee Scientific) was used to measure the concentration of BC. Air passes through a filter where BC particles are deposited. A light is shown on the filter measuring the change in light attenuation caused by the soot deposits. From this, a mass concentration is recorded in nanograms per cubic meter ( $\text{ng}/\text{m}^3$ ).

The microaethelometer was able to record data at a frequency of 1 Hz, however noise and negative readings required results to be averaged according to a process described further in section 4.2. Filters were replaced prior to use each morning. After each use, data stored in the memory of the instrument were uploaded to a server. The files could be opened directly with Microsoft Excel and were then saved in XLSX format.

### 3.2.3. *Global Position System Unit*

In order to record information such as location, speed, and temperature, a commercially available GPS unit (Edge 800, Garmin) was used for the mobile data collection campaign. Furthermore, area maps and pre-defined routes were uploaded to the device and displayed on a screen to guide the research assistants along the intended measurement routes.

The instrument was able to record readings at a frequency of 1 Hz. Data were uploaded to the manufacturer's website, Garmin Connect, which provided a visualization and summary of each trip. Files were subsequently downloaded to the server. These could then be exported as either TCX or GPX files, each of which contained slightly different information. Both were then saved as XLSX files.

### 3.2.4. *Digital Camcorder*

Select trips were supplemented by a commercially available video camcorder (Hero2, GoPro) affixed to either the helmet or the handle bars of one of the research assistants during the mobile data collection campaign. With a  $170^\circ$  wide-angle lens, the camera was able to create a visual record of the surrounding traffic and land use characteristics for a number of the pre-defined routes. The camera recorded high-definition footage (720p) at 60 frames per second. Although this information did not contribute to the investigations to follow, it allows for the possibility of future work to more closely examine the real-time effects for a sub-sample of the data collected.

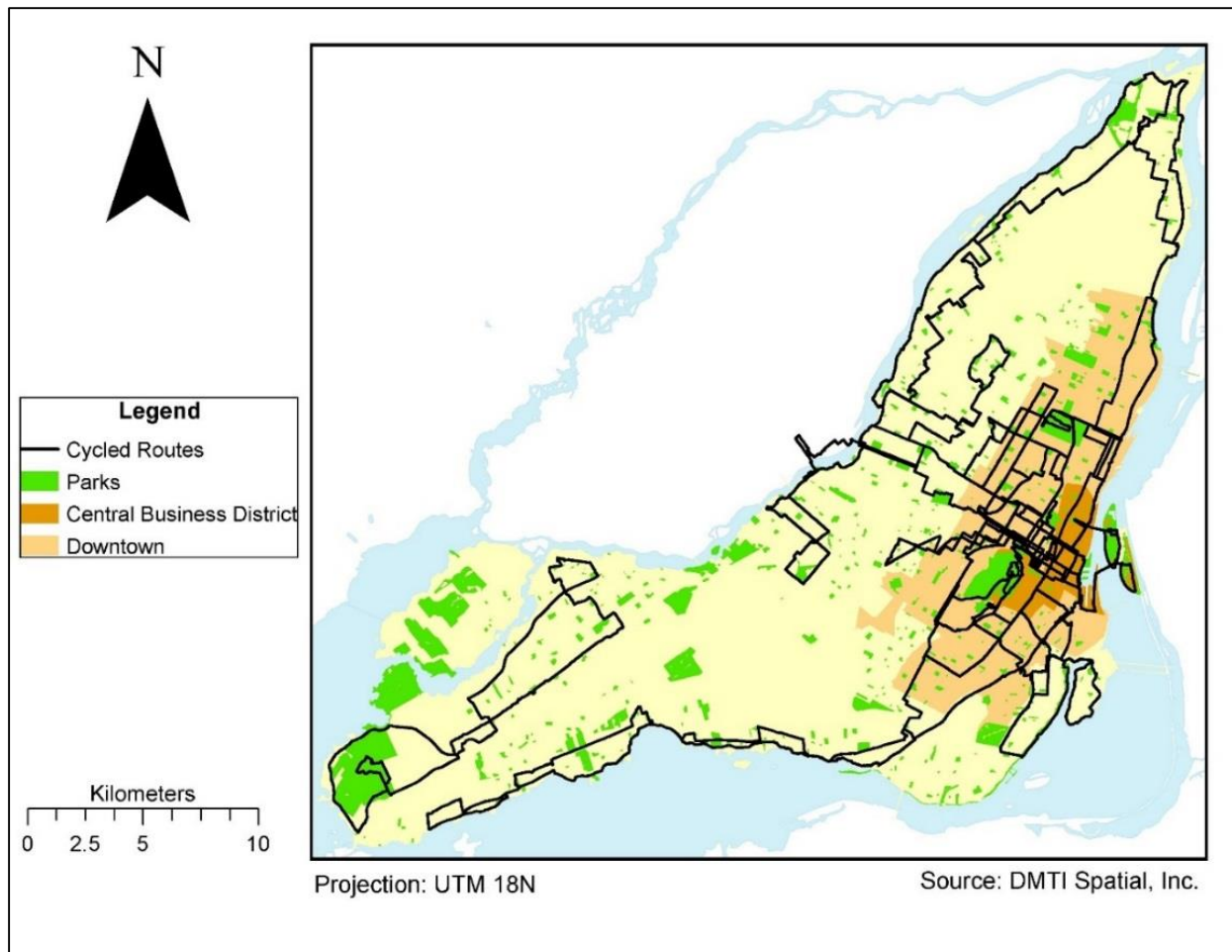
### **3.3. Mobile Data Collection Campaign**

#### *3.3.1. Route Selection*

This portion of the study consisted of two pairs of research assistants each cycling one of 25 pre-defined routes. Each route was a circuit of approximately 25 km in length and was charted with an effort to include as many designated cycling facilities within the study area as possible, across a diverse array of micro-environments. Each route was carefully scrutinized using Google Maps and field visits to ensure that the intended course corresponded with the proper directionality of the streets and that all paths were safe and viable for cycling. One common constraint was the difficulty in finding feasible and cycling-friendly crossings when routes intersected limited access rights-of-way, such as highways and railroad tracks. Prior to finalizing the routes, test runs were conducted in potentially problematic areas to minimize any possible difficulty that the research assistants would have in navigating these areas during the course of the study. During these trial runs, air pollution data were recorded and uploaded so that the research assistants would be familiar with the correct procedures for the actual study.













The final routes assignments were drafted using the online resources provided by Garmin, which were subsequently uploaded onto the GPS devices along with publically available downloadable map files from OpenStreetMap.org. Together, this provided the research assistants with audio-visual turn-by-turn navigation in order to ensure the accurate repeatability of the intended routes.














In the final incarnation of the planned cycling network, fifteen routes began at a single location in downtown Montreal and ten began in five different locations in surrounding towns and boroughs on the island. More detailed information about each route is provided in Table 3.1, including the number of trips on each route as well as the number of files associated with UFP, BC, and GPS. In total, over 2,000 km of were measured. Excluding repeated measures, 500 km of unique roadways were covered, including over 325 km of cycling facilities (Figure 3.2).



*Figure 3.2: The extent of the cycled network, shown with parks, the CBD, and what is defined as the downtown region*

Table 3.1: Cycling Routes Detailed Descriptions

Route	Name	Origin	Count				Average Duration (hrs)	Average Distance (km)	Location
			Trips	UFP Files	BC Files	GPS Files			
1	Maisonneuve O/ CDN–NDG	Downtown	4	7	5	5	1.7	26.1	
2	Lachine Canal/ CDN–NDG	Downtown	4	8	1	8	1.8	26.0	
3	LaSalle/ Sud-Ouest	Downtown	4	8	4	7	1.8	27.2	
4	Lachine/ Dorval	Dorval	2	4	4	3	1.4	25.5	
5	Dollard/ Pierrefonds	Kirkland	1	2	2	2	1.5	24.5	
6	Saint-Laurent/ Ahuntsic	Ahuntsic	2	4	4	4	1.8	26.4	
7	Westmount/ Verdun	Downtown	4	8	6	8	1.9	28.3	
8	Rosemont/ Ahuntsic	Downtown	4	8	6	7	1.7	25.3	
9	Pointe-Claire/ Beaconsfield	Dorval	2	4	2	4	1.6	23.7	
10	Sainte-Anne/ Senneville	Kirkland	1	2	1	2	1.8	26.1	
11	St-Zotique/ Rachel	Downtown	4	8	6	8	1.5	23.3	
12	Vieux Port/ Notre-Dame/ Viau	Downtown	4	7	5	6	1.6	25.1	

Route	Name	Origin	Count				Average Duration (hrs)	Average Distance (km)	Location
			Trips	UFP Files	BC Files	GPS Files			
13	Bellchasse/ Notre-Dame/ Chambly	Downtown	6	11	5	12	1.6	24.6	
14	Île Ste-Hélène/ Île Notre-Dame	Downtown	4	7	7	6	1.4	24.4	
15	Laurier/ Hochelega	Downtown	4	8	6	8	1.7	26.2	
16	St-Leonard/ Villeray	Downtown	4	8	5	6	1.7	26.5	
17	Montréal-Nord	Rivière-des-Prairies	2	4	3	4	1.7	25.6	
18	Montréal-Est/ Mercier	Pointe-aux-Trembles	2	4	4	4	1.8	26.6	
19	Pointe-aux-Trembles	Pointe-aux-Trembles	2	4	0	3	1.6	25.1	
20	Rivière-des-Prairies	Rivière-des-Prairies	2	4	1	2	1.5	23.1	
21	St-Leonard/ Montréal-Nord	Ahunatic	2	4	2	3	1.7	23.5	
22	Ville de Mont-Royal/ Outremont	Downtown	4	8	4	7	2.0	29.3	
23	Île des Sœurs	Downtown	4	8	6	7	1.3	20.3	
24	Rosemont	Downtown	4	7	5	8	1.3	23.4	
25	Parc Mont-Royal/ Côte-des-Neiges	Downtown	4	7	5	6	1.9	28.3	



### 3.3.2. Project Bicycle

Four project bicycles were used, each equipped with a number of instruments. All four bicycles carried a CPC to measure UFP and three bicycles also carried a microaethelometer to measure BC in a pannier above the rear wheel. The instruments were connected to a hose that ran along the frame of the bicycle to the handlebar, near the respiration zone of the cyclist. All four bicycles also carried a GPS unit in order to relate air quality data with its measured coordinate and to help navigate the route to be measured. All instrument clocks were synchronized with a central computer prior to each trip and measurements were recorded at a frequency of 1 Hz. In total, over 213 hours of real-time measurements were recorded.

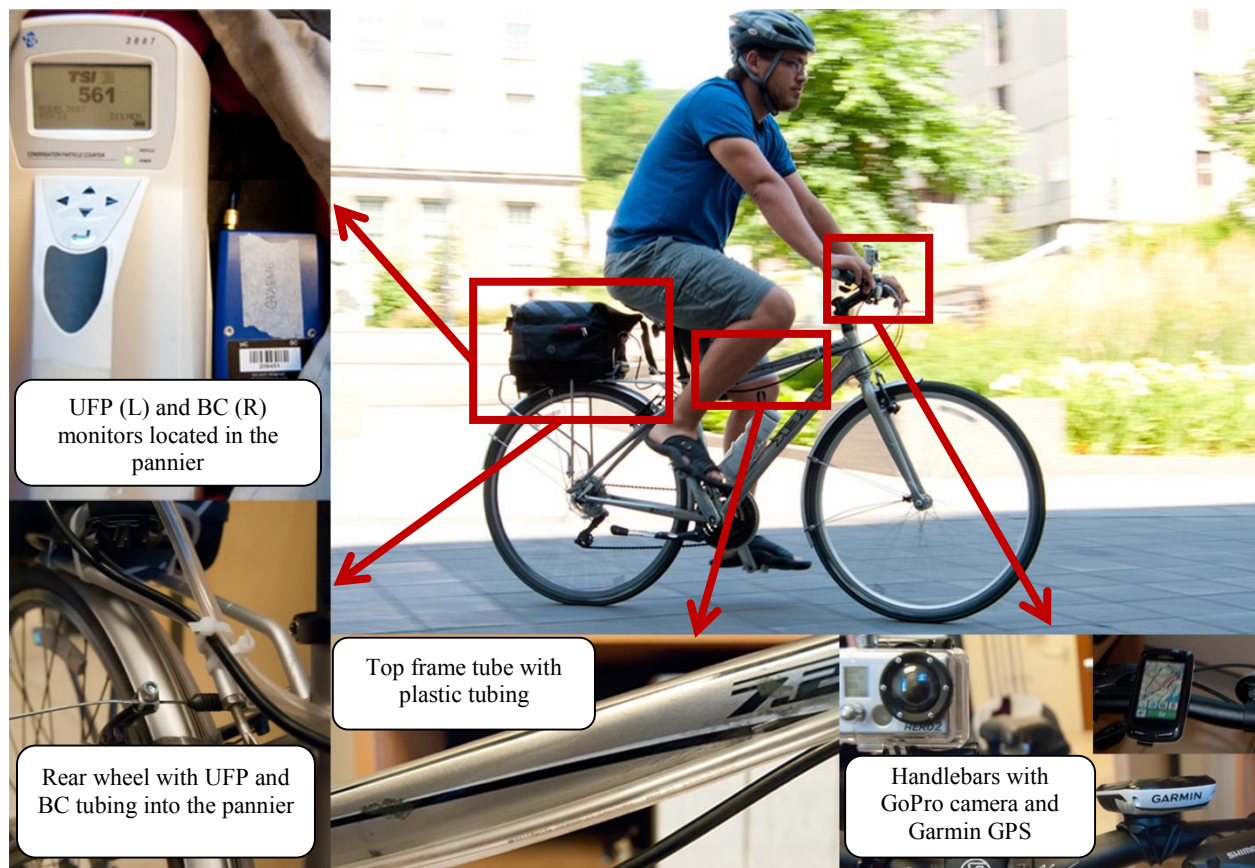


Figure 3.3: Project bicycle set-up used for the mobile data collection campaign.

Instruments were labelled by the first initial of the research assistant primarily operating the device, and were therefore referred to as B (Bernard), G (Graeme), J (Julien), and N (Noel). Each instrument remained associated with a single bicycle and research assistant for the duration

of the study as we found no evidence of systematic errors or drift associated with the instruments during the initial testing.

### *3.3.3. Data Collection Procedure*

The four primary cyclists were split into two groups, A and B, which remained constant for the duration of the study. Group A consisted of instruments G and J while Group B contained instruments B and N. Trips were defined as a pair of research assistants completing a single route during a single time period. Each route was measured during two time periods: in the morning (AM), beginning at approximately 08:00, and the afternoon (PM), at approximately 14:30. Each group measured the downtown routes with two trips: one in each time period. Peripheral routes were each only cycled by one group conducting two trips again, once per time period.

Measurements took place on 23 weekdays over a six week period in the months of June and July of 2012. Trips were scheduled to be conducted five days per week, every other week in this time. Trips originating downtown were typically measured twice per day on at least two different days. In the event of inclement weather, these trips were re-scheduled for the planned off-week. Trips originating in the peripheral regions were measured twice on a single day, excepting two peripheral routes (5 and 10), which were measured only once, in the afternoon, due to inclement weather, and could not be re-scheduled. More detailed information about the nature of each route can again be found in

Table 3.1.

Upon the completion of each trip, all UFP and BC data were uploaded onto a server and subsequently cleared from the memory of the machine. All files were saved with a standardized naming convention which included its route (R), year (Y), month (M), day (D), time period (P), group (G), instrument identification (I), and the data type (T). Table 3.2 lists the possible values to be used in the following naming convention: *RR\_YY\_MM\_DD\_PP\_G\_I\_TT*.

*Table 3.2: Possible Values for the Naming Convention*

Information	Possible Values
Route	01 to 25
Year	12
Month	06 or 07
Day	01 to 31
Time Period	AM or PM
Group	A or B
Instrument	B, G, J, or N
Data Type	UF, BC, or GP

The overall project methodology for the mobile data collection campaign and how the results were processed is depicted by the flowchart in Figure 3.4. Some aspects of the graphic are elaborated in the following chapters.

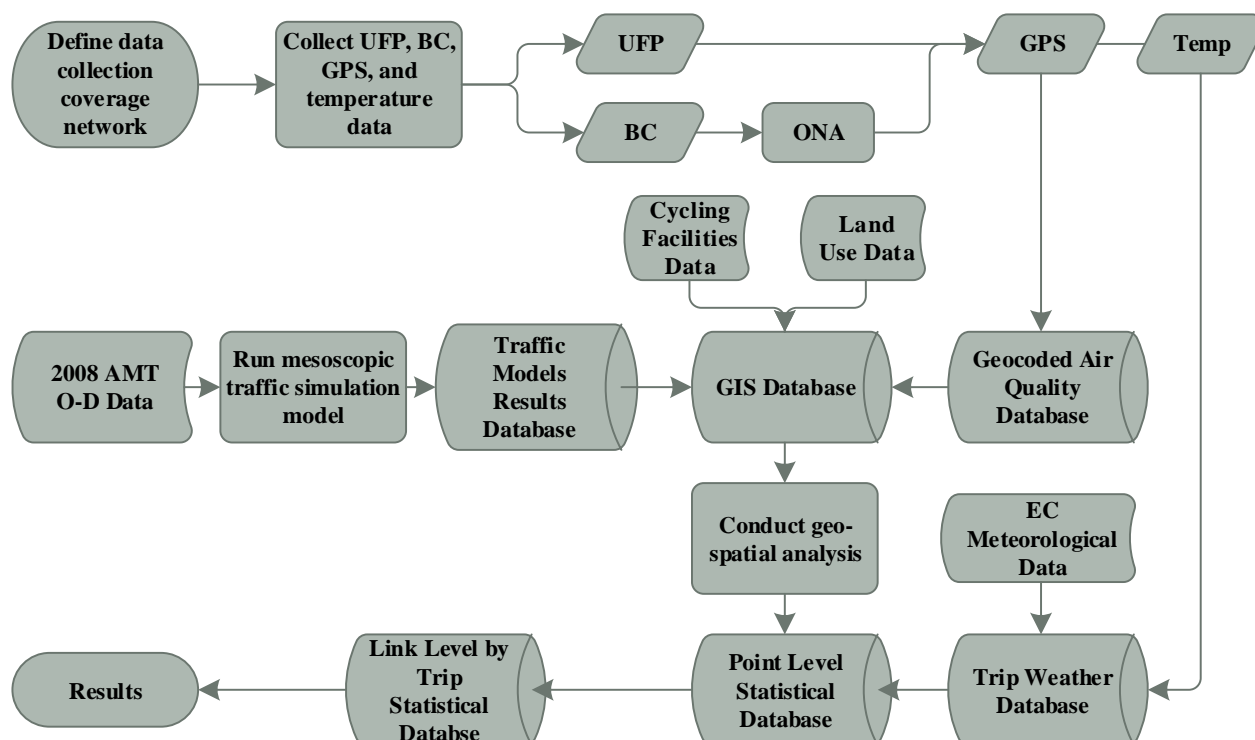


Figure 3.4: Project Flowchart for the Mobile Measurement Data Collection and Processing

### 3.4. Fixed Site Data Collection Campaign

#### 3.4.1. Location Selection

UFP data were collected at 73 sites along a range of roadways in Montreal. Sites were selected to cover a large portion of Montreal Island in an effort to maximize variations in the set of determinant variables available for analysis. In particular, these sites included 45 locations in the downtown core, 25 locations outside the downtown core (on the periphery or in the suburbs), and 3 points located along bridges connecting the Island of Montreal with the rest of the region. The 70 points (excluding the bridges) consist of corridors which were defined by either five or ten measurement locations, and are listed in Table 3.3.

Figure 3.5 shows the 73 monitoring locations overlaying a map of ambient  $\text{NO}_2$  levels in Montreal (Crouse, Goldberg, and Ross 2009). This figure illustrates that the selected sites cover a range of traffic conditions (reflected by differences in ambient  $\text{NO}_2$ ) with the exception of potential hot spots located around highway interchanges where monitoring becomes difficult owing to safety concerns.

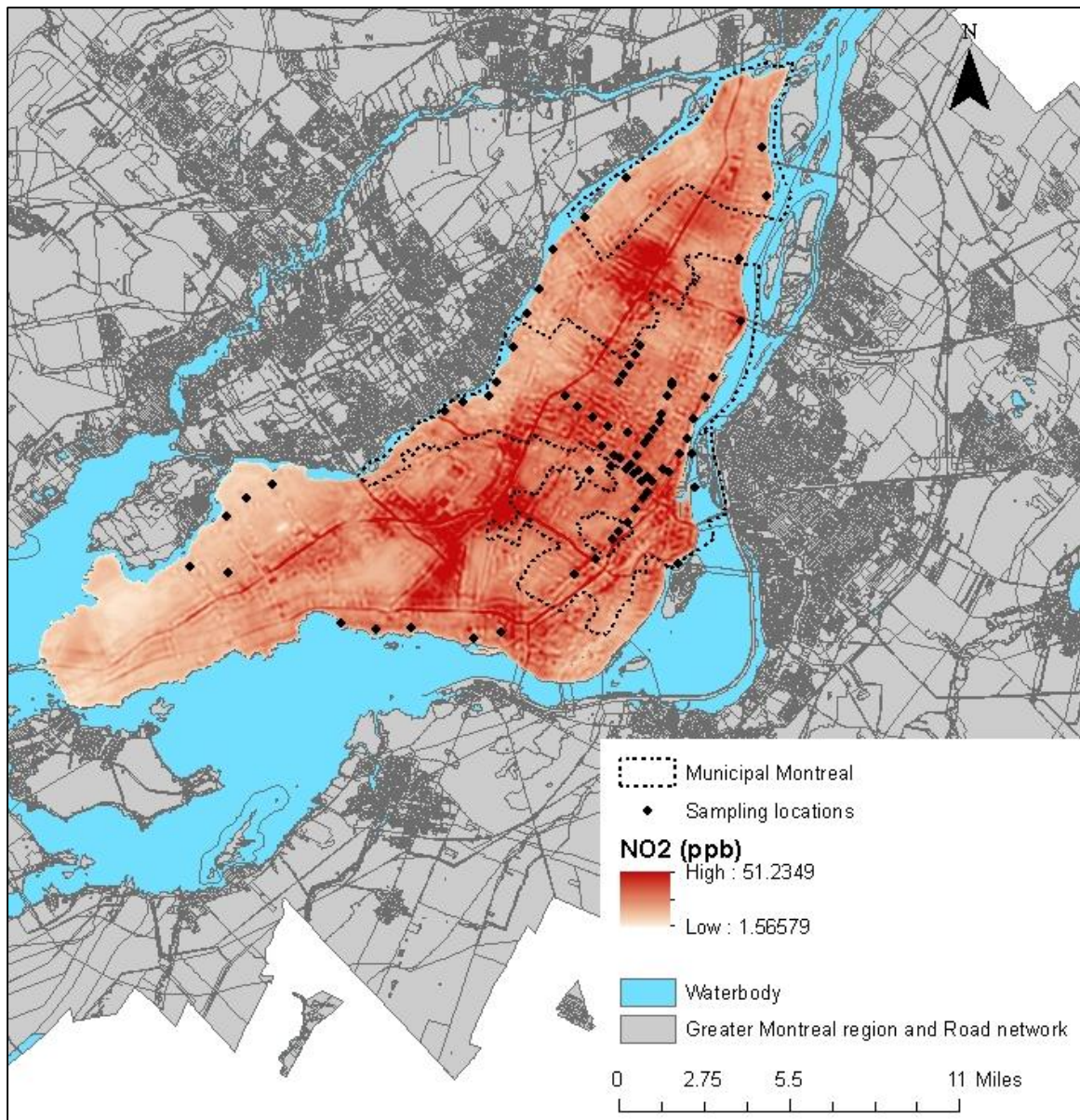


Figure 3.5: Fixed Monitoring Locations shown atop ambient  $\text{NO}_2$  levels in Montreal



Table 3.3: Fixed Site Monitoring Locations

Corridor	ID	Downtown	Measured Street	Cross-Streets	
Maisonneuve (Western)	1	1	de Maisonneuve O	Lambert Closse	Atwater
	2	1	de Maisonneuve O	Oliver	Clarke
	3	1	de Maisonneuve O	Metcalfe	Melville
	4	1	de Maisonneuve O	Northcliffe	Décarie
	5	1	de Maisonneuve O	Beaconsfield	Grand
Maisonneuve (Eastern)	6	1	de Maisonneuve E	Berri	Savoie
	7	1	Ontario	Saint-Urbain	Jeanne-Mance
	8	1	de Maisonneuve O	Union	University
	9	1	de Maisonneuve O	Metcalfe	Peel
	10	1	de Maisonneuve O	Mackay	Guy
Parc/ Côte-Sainte-Catherine	11	1	Hutchison	Milton	Prince Arthur
	12	1	du Parc	des Pins	Duluth
	13	1	du Parc	Duluth	du Mont-Royal
	14	1	de la Côte-Sainte-Catherine	Villeneuve	St-Joseph
	15	1	de la Côte-Sainte-Catherine	Mceachran	Davaar
Notre-Dame (Western)	16	1	René-Lévesque	Berri	Labelle
	17	1	René-Lévesque	Papineau	Cartier
	18	1	Notre-Dame	Frontenac	d'Iberville
	19	1	Notre-Dame	Alphonse D Roy	Davidson
	20	1	Notre-Dame	Pie-IX	de la Salle
Notre-Dame (Eastern)	21	0	Victoria	47e	45e
	22	0	Victoria	15e	14e
	23	0	Notre-Dame	David	Joseph-Versailles
	24	0	Notre-Dame	Boucherville	Hector-Barsalou
	25	0	Sarto-Fournier	Ville-Marie	Vimont
Saint-Urbain	26	1	Saint-Urbain	Sherbrooke	Milton
	27	1	Saint-Urbain	des Pins	Saint Cuthbert
	28	1	Saint-Urbain	du Mont-Royal	Villeneuve
	29	1	Saint-Urbain	Saint Joseph	Laurier
	30	1	Saint-Urbain	Saint Viateur	Bernard
Rachel (Western)	31	1	Rachel O	Saint-Urbain	Clark
	32	1	Rachel E	Drolet	Saint-Denis
	33	1	Rachel E	de la Roche	de Brébeuf
	34	1	Rachel E	Marquette	Papineau
	35	1	Rachel E	Lorimier	des Érables
Rachel (Eastern)	36	1	Rachel E	Frontenac	d'Iberville
	37	1	Rachel E	Montgomery	Molson
	38	1	Rachel E	Joliet	de Chambly
	39	1	Rachel E	Jeanne-d'Arc	Pie-IX
	40	1	Sherbrooke	Pie-IX	Viau
Bridges	41	1	Pont Jacques Cartier	.	.
	42	1	Pont de la Concorde	.	.
	43	1	Pont Île-des-Sœurs	.	.
Boyer	44	1	de Brébeuf	Saint Joseph	Laurier
	45	1	Boyer	Rosemont	Bellechasse
	46	1	Boyer	Saint Zotique	Bélanger
	47	1	Boyer	Everett	Villeray
	48	1	Christophe-Colomb	Jarry	Mistral

Corridor	ID	Downtown	Measured Street	Cross-Streets	
Lakeshore/ Victoria	49	0	Lakeshore	Thrush	Neptune
	50	0	Lakeshore	Claude	Allard
	51	0	Lakeshore	Handfield	George V
	52	0	Victoria	28e	21e
	53	0	Victoria	4e	5e
Saint Zotique	54	1	Saint Zotique	10e	Saint-Michel
	55	1	Saint Zotique	15e	16e
	56	1	Saint Zotique	21e	Pie-IX
	57	1	Saint Zotique	30e	31e
	58	1	Saint Zotique	Viau	38e
Pierrefonds	59	0	Pierrefonds	des Sources	Athena
	60	0	Pierrefonds	Fredmir	Belleville
	61	0	Pierrefonds	Saint-Jean	Graham
	62	0	Pierrefonds	Saint-Charles	Blaignier
	63	0	de Salaberry	Sommerset	Walwoth
Gouin (Western)	64	0	Gouin E	Papineau	Seguin
	65	0	Gouin E	Lajeuneese	Berri
	66	0	Gouin O	Waverly	de l'Esplanade
	67	0	Gouin O	de Salaberry	Poincare
	68	0	Gouin O	Saint Castin	Taylor
Gouin (Eastern)	69	0	Gouin E	Baillargeon	41e
	70	0	Gouin E	4e	5e
	71	0	Gouin E	Lanthier	Lacordaire
	72	0	Gouin E	Saint Julien	de l'Hôtel de Ville
	73	0	Gouin E	Audoin	Leblanc

### 3.4.2. Data Collection Procedure

Two pairs of research assistants collected simultaneous UFP and traffic information at the 73 sites listed in Table 3.3. Data were collected on 32 weekdays over a six week period in June and July of 2012. Traffic data were collected manually during each air pollution monitoring session and recorded the number of cars, trucks, SUVs, buses, motorcycles, and bicyclists at each location. From this the total traffic counts and the ratio of trucks to total traffic could be computed. Real-time UFP data were collected using the aforementioned instrumentation (Section 3.2.1) at one-second sampling intervals using instruments carried in backpacks with sampling tubes placed in technicians' breathing zones.

All measurements were recorded over 10-20 minute periods on sidewalks at midblock. In a limited number of instances, multiple instruments were available for recording air pollution concentrations. In these cases, readings were taken on both sides of the street, in order to investigate what may affect the difference in concentrations from one side to the other. This resulted in 32 locations measured in this fashion a single time and an additional eight locations

each measured twice. In total, these two-sided measurements were conducted at 40 sites on 50 occasions.

Data were collected at each location during peak morning (08:00 – 10:00) and afternoon (15:00 – 17:00 PM) periods as well as during mid-day (11:00 – 14:00). Morning and afternoon measurements were typically conducted on the same day as one another and in ten minute intervals, while mid-day measurements were collected once during the day in twenty minute intervals. Each location was monitored between one and six separate occasions, with an average of three measurements per locations. The 25 locations identified as outside downtown, noted in Table 3.3, were measured on a single day concurrent with the mobile measurements in nearby locations. Sites along each corridor were measured sequentially in their grouping of five sites, as indicated in Table 3.3.

In total, 200 observations were recorded at the 73 locations. Measurements conducted on both sides of the street were completed during the mid-day period to allow for the availability of additional instruments.

### **3.5. Conclusion**

These two exercises served different, yet complementary purposes. The mobile measurements represented a departure from conventional air quality monitoring campaigns while the stationary measurements served as a baseline for comparison. Essentially, the stationary campaign provided more detail at a select number of sites in order to validate the assumptions necessary to utilize the more experimental mobile campaign. Having done so however, each campaign can stand on its own, using its respective strengths to draw unique conclusions.



## **CHAPTER 4 — MOBILE DATA PROCESSING METHODOLOGY**

### **4.1. Introduction**

Upon obtaining air quality and location data, a number of processes were necessary in order to interpret the results. Although the specific data processing methodologies differ somewhat depending on the desired output, they all share a set of essential procedures. Furthermore, air quality data were related to several built environment characteristics, and the procedures by which this was performed are outlined in this section.

The chapter begins with a description of the algorithm used in order to post-process the mobile BC results in Section 4.2. Following this, Section 4.3 details the process by which the air quality measurements were associated with their proper location. Moreover, the location data were used to relate the measurements with specific streets and cycling facilities. Section 4.4 discusses the way in which traffic characteristics were collected, so that these could be attributed to the streets along which the air pollution measurements were recorded. Section 4.5 explains how various built environment characteristics were obtained and modified so that they could be related to the air pollution measurements. Finally, Section 4.6 discusses the relevance of meteorological data and how they were obtained for the purposes of this exercise.

### **4.2. Black Carbon Post-Processing**

All BC data were processed prior to computing descriptive statistics, owing to the fact that the microaethalometer sometimes outputs negative observations when the difference in light attenuation between two consecutive readings is negligible. In particular, an optical noise-reduction averaging algorithm was used to correct the readings (Hagler 2011). This algorithm reads the difference in light attenuation between consecutive measurements and eliminates peaks in BC concentrations associated with a light attenuation differential below 0.05. The algorithm then averages BC data across time intervals defined by the attenuation interval. An example of this noise-reduction process taken from half of our sample in the mobile campaign is shown in Figure 4.1. Note that as the slope of the light attenuation increases, the ONA algorithm averages the data over shorter time steps. Furthermore, the true spike in BC is detected by the algorithm, as indicated by the sharp change in light attenuation, while the noise is mostly averaged.

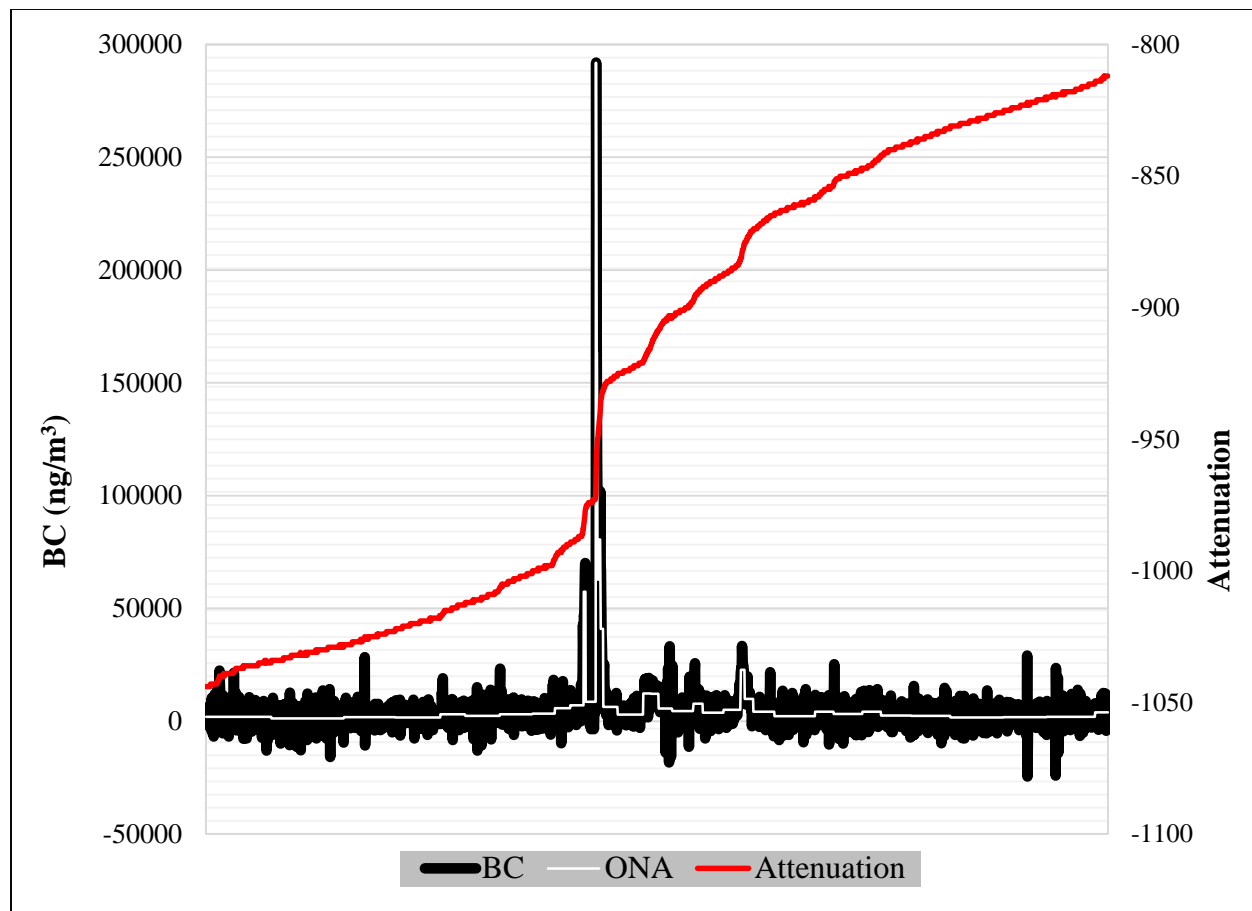


*Figure 4.1: Illustration of the ONA Algorithm Based on Light Attenuation*

This averaging process replaces the 1 Hz values in the dataset with an associated value averaged over a variable duration. The distribution of these durations is depicted in Figure 4.2, which shows the highest frequency for very short time intervals, but with a rather long tail of lengthier time intervals. The median averaging duration was 1.5 minutes, but varies from as little as one second (no averaging) up to a maximum of 1.25 hours. Still, over 90% of the data were averaged over less than five minutes, making such large durations quite exceptional.

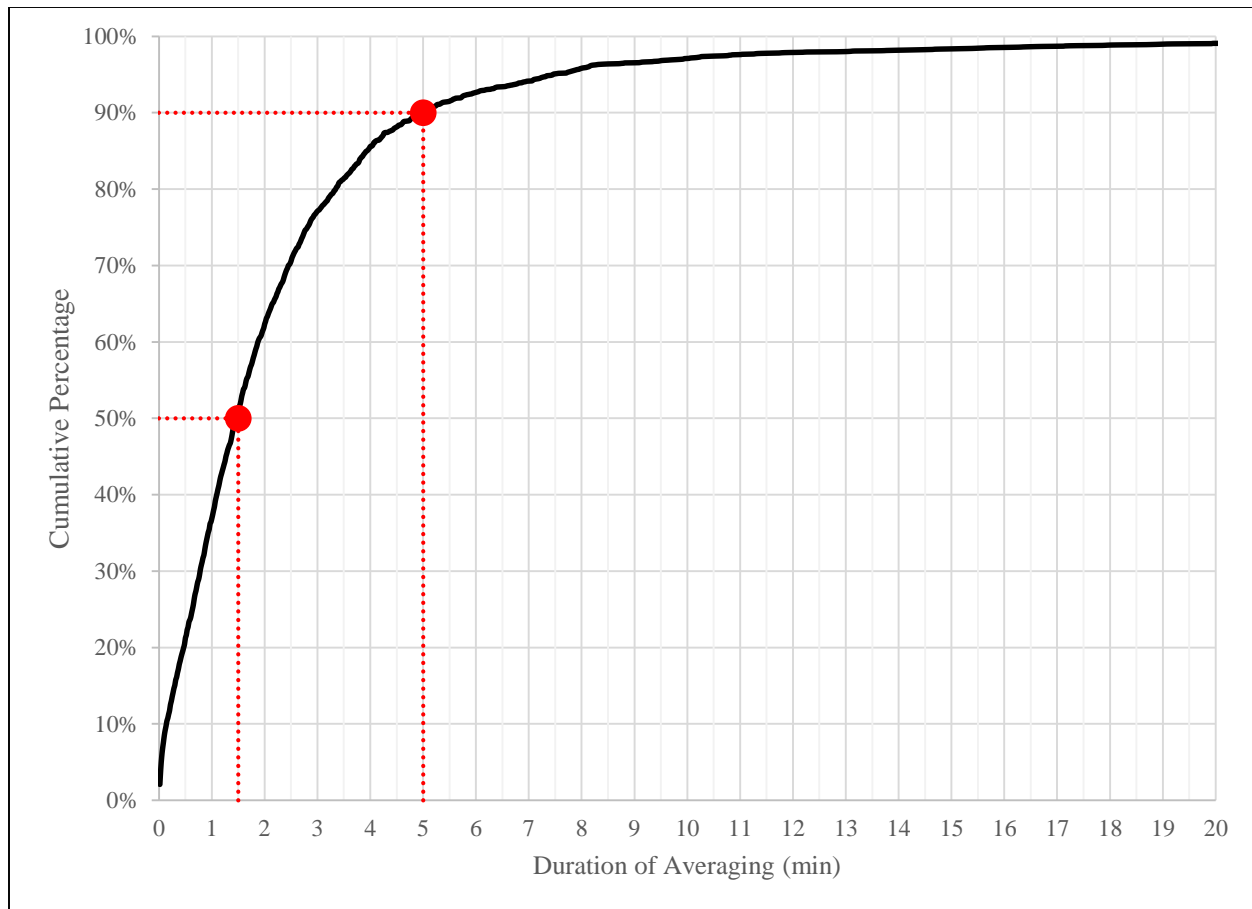


*Figure 4.2: Cumulative Distribution of ONA Averaging Duration, Demarcating the 50<sup>th</sup> and 90<sup>th</sup> percentiles*

### 4.3. Combing Air Pollution Measurements with Location Data

All air quality data were merged with their respective GPS coordinates using the synchronized timestamps provided by each instrument during a given trip. This resulted in a dataset for each instrument, which was subsequently compiled into a single database. Data were excluded if they did not contain at least one air quality measurement or if an air quality measurement had no associated coordinate. For instances of GPS malfunction, the partner's coordinates were used, under the assumption that their proximity is sufficiently close to one another that the air quality data will reflect the same conditions. In total, this merged dataset contained 768,105 records from 157 air pollution instrument files, representing 80 trips.

Using the coordinates provided by the GPS units, the database was geocoded using ArcCatalog 10.1, a program within the ArcGIS suite (ESRI). The resulting shapefile contained

those 768,105 records in point format, along with metadata such as the route, time, instrument, and most importantly, the air pollution data. All geospatial analysis was conducted with ArcMap 10.1 (ESRI). Using a GIS representation of the centerlines of the road network in Quebec (DMTI Spatial, Inc.) and the routes drafted on Garmin Connect converted to GIS files, it was now possible to relate the individual points to their associated road segment. In the context of transportation simulations, road segments between intersections are alternatively referred to as links between nodes. In order to obtain an accurate account of which points were measured along which link, point and link level data were first analyzed at the route level. Through a process of both automation and visual inspection, vehicular roadways which were cycled either on or alongside were demarcated. In the event that there was no street which could have been reasonably associated with a point, the nearest streets was automatically selected. In some cases, the research assistants were forced to divert from the planned route due to construction. Such detours were also included in the possible link assignments. These links were then spatially joined to the points so that each point could now be associated with the nearest indicated vehicular roadway for which the route was cycled. This process ensured that the nearest roadway would only be considered if it was along the direction of the measurements—that is to say if a cross-street which was not measured was nearer to the measurement point, it would be ignored in favor of the parallel street. Figure 4.3 illustrates how point-level data were related to the road links.

In the process of creating the spatial join, a distance field was automatically generated, which reports the perpendicular distance between the point and the link. Additionally, other attributes were generated which related each measurement to the distance from the nearest highway and the nearest major road. These distances will play an important role in further analysis.

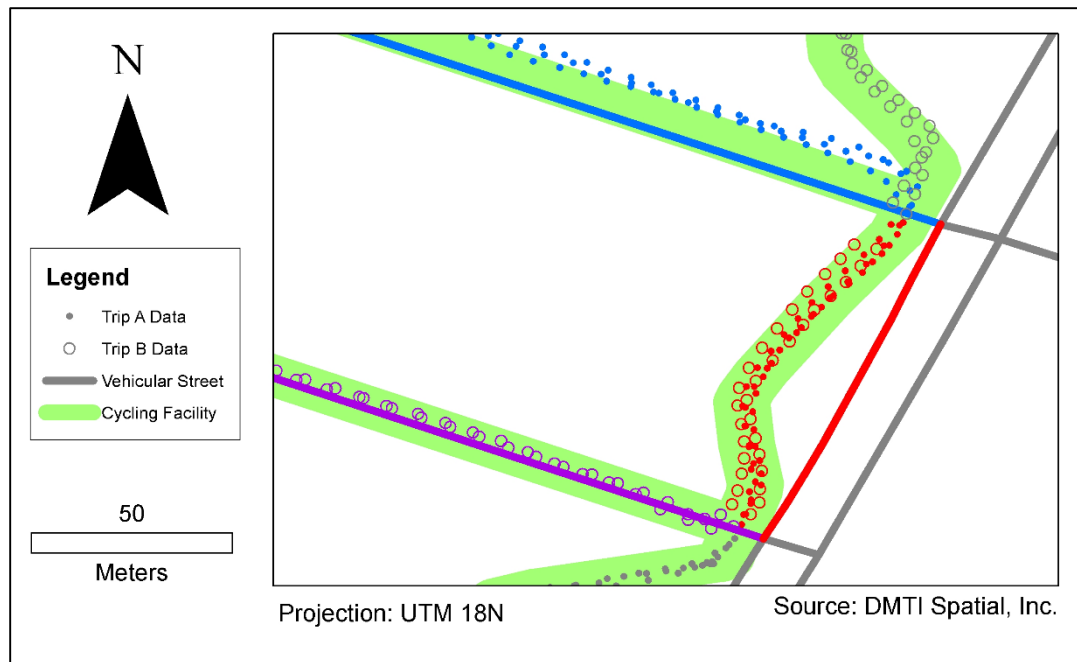


*Figure 4.3 Data were averaged by each trip on each link; for example the red solid circles and hollow circles were both averaged onto the red link, but as two independent observations. All point data were also assigned the properties of the cycling facility (green) that they were cycled on.*

#### 4.4. Traffic Data

The road network GIS data were also used to produce vehicular volumes, which were obtained from a mesoscopic traffic simulation model previously developed by the research team using the software, VISUM (PTV Group) (Sider, Alam, et al. 2013). The model applies a stochastic user equilibrium solution using the 2008 *Agence métropolitaine de transport* (AMT) Origin-Destination (O-D) survey to 127,217 roadway links in the Greater Montreal Region. Road classifications were provided with the road network GIS data, and from these, number of lanes, hourly vehicular capacities, and speed limits were estimated, then further refined upon calibration of the model. Simulations were conducted for each hour in the day, using the output from the previous hour as input for the next hour. Ultimately, the model generated outputs at the link level for vehicular volumes and vehicular speed for each hour in the day.

The meso-simulation created two records for every link, one for each direction. In the case of one-way streets, the capacity of the prohibited direction was set to zero. The dissolve feature in ArcGIS was used to merge these two records back into a single link. In doing so, the volumes in

each direction were summed over each hour and the minimum vehicular speed within each hour was preserved, in order to capture the effect of congestion.

As described in Section 4.3, the air pollution data were each related to a vehicular link, and were therefore able to be related to the simulated traffic properties of that link. These properties include the traffic volume, traffic speed, road hierarchy, hourly vehicular capacity, the number of lanes, and the speed limit.

In an effort to validate the results of this model, the results from the segments which corresponded to the midblock locations of the fixed site monitoring counts were compared. The model values for each time period and the 214 manual traffic counts from the fixed site data collection campaign were normalized to the hour level to test the correlation. We observe a correlation of 0.78 ( $p < 0.0001$ ) between measured and modeled values, which is depicted in Figure 4.4. The model shows an under-prediction, likely due to the fact that it is based on the O-D survey, which assesses household travel patterns while neglecting commercial traffic. Yet the trend is more pertinent than the magnitude in explaining the variance in air pollution, so this relatively high correlation is considered acceptable.

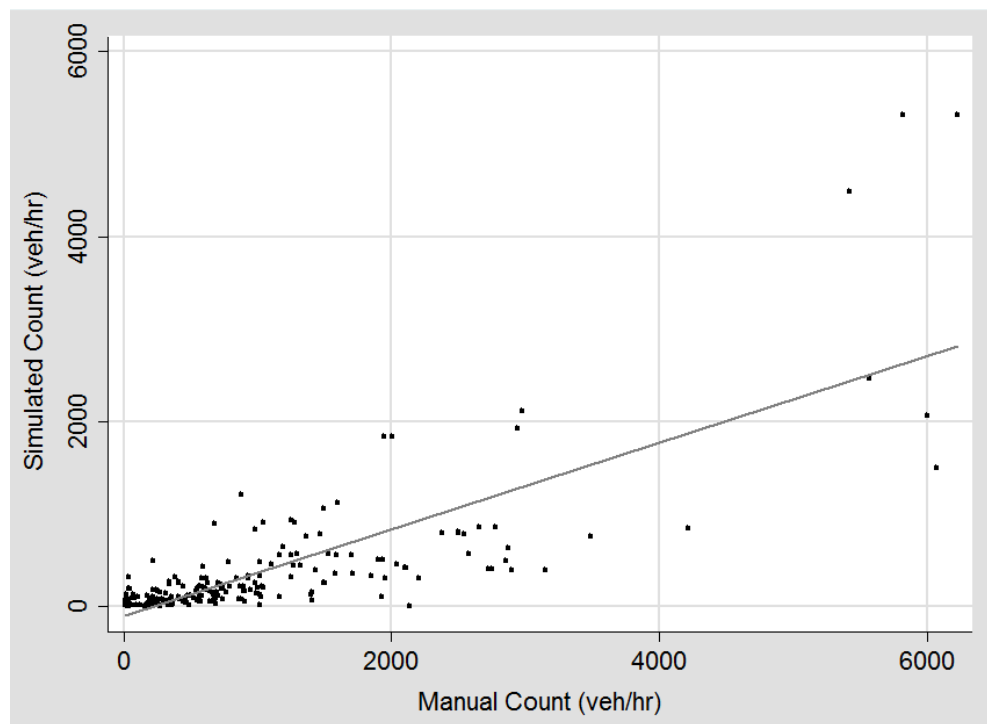


Figure 4.4: Validation of the Simulated Counts against the Manual Counts results in a correlation of  $r=0.78$  ( $p < 0.0001$ ;  $n=214$ )

Traffic data were parsed in a number of different ways, which are later tested for efficacy in explaining air pollution. All aggregations took the sum of the volumes and the minimum vehicular speed on each link. Firstly, the hourly data were related to air quality measurements recorded in that hour. For example, a datum recorded at 09:23 would be related with the attributes of the 09:00 – 10:00 period. Next, traffic data were aggregated at the time period level. In this case, the hours of 07:00 – 10:00 were combined for the AM period while the PM period consisted of 14:00 – 17:00. Following this, these two periods were combined into a value referred to as the total peak period. Finally, the daily values were combined, again meaning the 24 hour sum of volumes and the 24 hour minimum speed.

In addition to the raw volumes and speeds, attributes were created in order to capture effects that may be related to traffic congestion. Not only would congestion imply a substantial number of vehicles present in the vicinity of the cyclist, but idling and low-speed vehicles emit a higher rate of air pollution per unit distance than the same vehicles at cruising speeds. The modeled volume over the estimated capacity, or  $v/c$ , was the first attribute generated to represent congestion. The second attribute was the ratio of the difference between the minimum simulated speed and the speed limit, over the speed limit. That is to say, as the conditions approach free flow speed, the congestion metric will tend towards zero, and as the conditions approached a standstill, the metric would tend towards one.

## **4.5. Built Environment Data**

### *4.5.1. Cycling Infrastructure*

A 2011 GIS representation of the designated cycling network was made available by the City of Montreal. The file contained the designations listed in Table 4.1, along with the implied category of no designated facility. Together, these labels were amalgamated into broader categories so that each one was functionally distinct with respect to air pollution exposure. Table 4.2 shows examples taken from Google StreetView for each designated facility type and how they are reclassified for this analysis.

Class 1, or in-street facilities includes all facility types with no physical separation between the cyclists and motorized traffic. This category consists of roads where there is no cycling designation, roads considered designated cycling routes, where painted sharrows indicate shared streets, and roads which consist of a painted bicycle lane. Class 2 is comprised of cycling facilities

that physically restrict midblock interaction between cyclists and motorized vehicles. Such physical restrictions include bollards, a concrete curb or median, parked cars, or a grass median. Finally, Class 3 contains all multi-use trails, typically found traversing city parks.

*Table 4.1: Cycling Facility Classifications*

City Designation		Functional Classification	
0	(No Designation)	1	In-Street Cycling
1	Shared Street		
2	Bicycle Lane & Shared Street		
3	Bicycle Lane		
4	On-Street Cycle Track	2	Separated Cycling
5	Off-Street Cycle Track		
6	Sidewalk-Level Cycle Track		
7	Multi-Use Trail	3	Trail Cycling

*Table 4.2: Photo Examples of the Physical Configuration of Each Designated Facility Type (Google StreetView)*

(1) <b>In-Street</b>			
(2) <b>Separated</b>			
(3) <b>Trail</b>			

Cycling facilities which were measured in the course of this study were indicated as such. Points were then spatially joined to these facilities along with their attributes. If the distance to the cycling facility was greater than 25 m then the point was assumed to be measured on a roadway



with no affiliated cycling facility, and thus was considered Type 0 and Class 1. In total, approximately 350 of the 425 km of Montreal's designated cycling network were covered during the mobile data collection exercise (Figure 4.5).

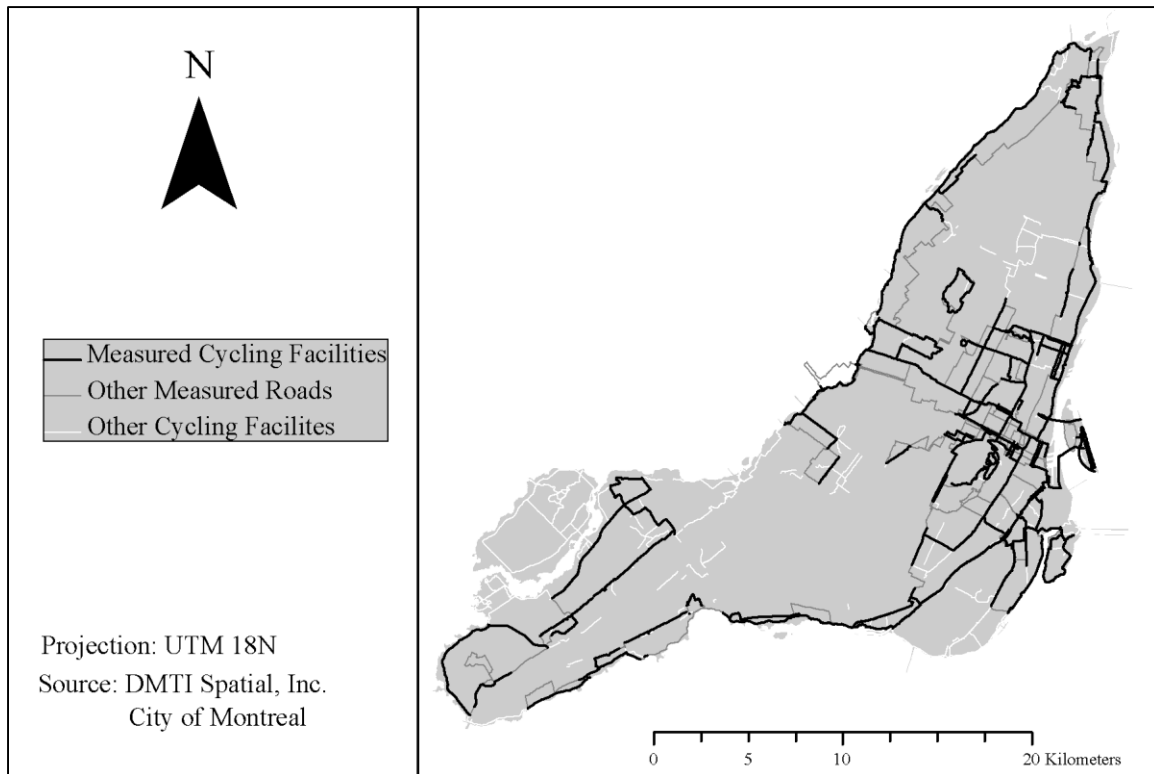


*Figure 4.5: Cycling Network Covered in the Mobile Data Collection Campaign*

#### *4.5.2. Urban Canyon Effect*

The urban canyon effect refers to the air circulation patterns within the space defined by opposite building faces, as depicted in Figure 4.6. Background pollution enters the canyon from the leeward side and is deflected by the buildings on the windward side. The incoming pollution as well as the pollution generated within the canyon due to vehicular traffic tend to accumulate as air is trapped in a cycle between the building faces.

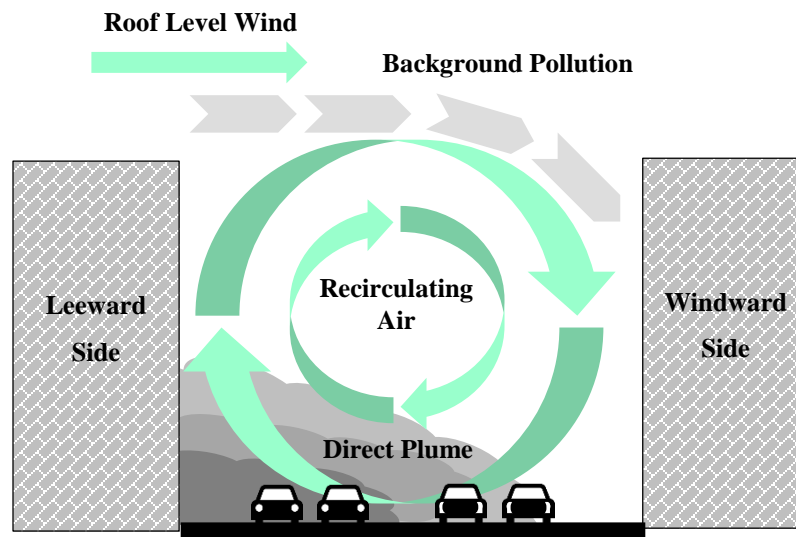


Figure 4.6: Schematic Diagram of the Urban Canyon Effect

In order to test for this effect, GIS data representing the building footprints within the Montreal Census Metropolitan Area (CMA) was acquired (DMIT Spatial, Inc.). Buffers of 25 and 50 m were generated around each roadway link for which there was an air pollution measurement. The building regions were then clipped to the buffer edges. From this, a dummy variable was created for a building falling within 25 m and within 50 m. An ordinal variable was generated from this where 0 represented the roadway link containing a building within 25 m, 1 represented 50 m, and 2 represented no building detected. Additionally, the shape areas were calculated in order to determine the percent of buffer area occupied by buildings at both 25 and 50 m.

#### 4.5.3. Other Land Use Data

Other land use data were acquired using straightforward GIS analysis techniques. Population GIS data were available at the census tract level, so the population density was calculated by dividing the total population in each tract by the shape area. Population may be indirectly associated with air pollution insofar as higher populations will be associated with higher levels of transportation activity, energy consumption, and other sources of pollution such as residential cooking fumes. Air pollution measurements were assigned the population density of the census tract in which they were recorded.

Point-level GIS data for restaurant locations were available for the study area as well. Research has indicated that these cooking fumes contribute to increased UFP levels (Abernethy et

al. 2013). From these data, two metrics were developed. First, a spatial join was used between air quality point-level data and the restaurant point-level data in order to ascertain a distance from the measurement point to the nearest restaurant. Secondly, 100 m buffers were created from the air quality point-level data and the number of restaurants falling within this buffer zone were related to each measurement.

Finally, this study makes use of a GIS representation of the land use zoning designations within the study area. In particular, “Parks and Recreational” and “Industrial and Resource” were expected to decrease and increase pollution respectively. Measurements that fell within one of these zoning categories were each assigned a dummy value indicating their presence therein.

#### **4.6. Meteorological Data**

Meteorological conditions are known to play an important role in air pollution levels. The ambient temperature may affect the chemical behavior of air pollution while wind speed, turbulence, and the atmospheric mixing height will tend to affect the physical dispersion of air pollution. With regard to mixing height, this is determined by the height of the atmospheric temperature inversion. In general, tropospheric air closer to the Earth’s surface is warmer than that above it, with temperature declining as altitude increases. However, at a certain height the air temperature will begin to increase with increasing altitude, thus trapping the pollution below this altitude because the cooler air below is unable to rise past the warmer air above. The altitude of the inversion is known as the mixing height. As this height decreases, the total mixing volume will decrease, thus increasing the overall pollution concentration. A warmer surface will generally result in a higher mixing height.

The physical dispersion of air pollution is also determined by the atmospheric turbulence, which is defined in terms of stability classes. Increased solar radiation and wind speed will increase the turbulence, thus increasing the mixing of air pollution in the atmosphere. This mixing will reduce air pollution concentrations at the breathing height of the population.

In order to account for these meteorological conditions, real-time temperature data were recorded by the GPS unit while wind speed, relative humidity, and general weather conditions were obtained at the hourly level from the nearer of two Environment Canada (EC) meteorological stations on the Island of Montreal. One weather station was located at Dorval Airport while the

other is situated at the corner of Rue McTavish and Rue Sherbooke. The positions are approximately 20 km and less than one kilometer away from the downtown origin of the mobile measurement campaign at McGill University, respectively.

#### **4.7. Conclusion**

These methods have laid the groundwork for all further analysis of data obtained from the mobile measurement campaign. The algorithm used to process the BC data helps ensure that the concentration levels ultimately related to the various characteristics are indicative of the actual field conditions. By geocoding these pollution data, one is able to relate them to a wide array of geospatial attributes. The well-known effect of meteorological conditions on air pollution concentration will allow the data to be controlled for these influences so that the more subtle land use effects may be better understood. Relating the attributes to the air pollution measurements and combining all the records into a single database ultimately allows for considerable efficiency for conducting the statistical analysis.

## **CHAPTER 5 — USING FIXED SITE MONITORING TO UNDERSTAND THE EFFECTS OF BUILT ENVIRONMENT ON AIR POLLUTION CONCENTRATIONS AND DISPERSION**

### **5.1. Introduction**

In addition to the more extensive mobile data collection efforts, to be discussed in much greater detail in the following chapters, a fixed site monitoring campaign was conducted in order to provide context for the results to follow. Manual traffic counts allow the mesoscopic simulation to be validated and stationary air pollution measurements corroborate mobile measurements. Furthermore, the limited spatial extent allows for a more in-depth account of some land use and road characteristics that would be infeasible to detail at the substantially larger scale of the mobile campaign. For instance, by recording the composition of traffic by vehicle type, the impact of trucks on air pollution is able to be observed. Also possible were more detailed measurements which allowed for a more nuanced analysis of the urban canyon effect by measuring concentrations on both sides of the street.

Within the fixed site monitoring analysis, two different effects were investigated. The first and primary objective was to establish the general relationship between UFP concentrations and site characteristics such as traffic, road geometry, and the surrounding built environment. However, in addition to this, a more limited investigation was conducted in order to determine how these affects may contribute to UFP mixing within the street canyon.

Section 5.2 provides a summary of the methodology previously described in Section 3.4. It continues by providing a more thorough account of the data processing component of the methodology, including which variables were procured and how they were analyzed. Section 5.3 discusses the results of this investigation, and is split into three subsections. The first treats all measurements as independent observations, the second analyzes the measurements when they are averaged at each location, and the final explores the factors that cause UFP levels to vary on different sides of the same street. Section 5.4 summarizes and compares the results of the previous section, and concludes the discussion on the fixed site monitoring campaign.

## 5.2. Methodology

### 5.2.1. *Developing Explanatory Variables for Overall UFP Levels*

The specifics of the fixed site data collection exercise can be found in Section 3.4. To summarize briefly, research assistants were sent to midblock sidewalks at 73 predefined locations in order to measure UFP, traffic volumes, and traffic composition by vehicle type. The presence of trucks in particular were of interest, so the ratio of trucks within the total traffic composition was also computed from these data. In total, 200 observations were recorded. Sampling was conducted for 10 minutes in the morning period (81 observations) and 10 minutes in the afternoon (63 observations), typically on the same day. Mid-day sampling was conducted for 20 minutes, with each site monitored no more than once per day (56 observations). Air pollution data were entered into the dataset as the mean of the sampling period at each location on each occasion. If multiple instruments were used for the occasion, the average result was taken as the observational value. At least one UFP measurement is available for each of the 73 locations, with three measurements on average, and up to a maximum of six.

Road geometry and built environment data surrounding each air monitoring location were compiled primarily using field measurements and GIS databases, while a combination of Google StreetView and orthophotographs were used for verification purposes and in the event of incomplete data. Geospatial processing was conducted in ArcMap 10.1 (ESRI) using buffering and spatial join functions. Compiled variables included characteristics of each road segment where monitoring was conducted as well as land use and built environment factors within a buffer around monitoring points. The variables include total road width, whether buildings are present on both sides of the street, and whether buildings on both sides of the street generally have a contiguous façade. The latter two were combined into a dummy variable for the urban canyon effect so that blocks with generally contiguous buildings on both sides of the street were said to have a value of one. Further the presence of areas zoned for “Industrial and Resource” uses are indicated when they are within 150 m of monitoring location.

With respect to meteorological conditions, data were again acquired from the Environment Canada Historical Climate database. Temperature, relative humidity, and wind speed were entered as the three hour average in the given time period of the measurement. That is, the morning period averaged from 07:00 – 10:00, mid-day from 11:00 – 14:00, and afternoon from 14:00 – 17:00.

General weather descriptions were also recorded, as they are necessary in determining the atmospheric stability class. Weather descriptions were coded into the database in the following format: [1] Clear; [2] Mainly Clear; [3] Mostly Cloudy; [4] Cloudy; [5] Rain Showers.

Table 5.1 outlines how stability classes were calculated. Solar radiation itself is a function of the cloud cover and the solar elevation. Cloud cover was considered as a dummy variable using the meteorological data variable previously described. *Clear* and *Mainly Clear* weather were considered to have no cloud cover while *Mostly Cloudy*, *Cloudy*, and *Rain Showers* were considered to have cloud cover. The solar elevation was estimated by linearly interpolating the average altitude of the sun during the three measurement time periods (morning, mid-day, and afternoon) between three days within the study. Study days before the summer solstice were interpolated between the elevations on the first day of the study and the solstice, while those occurring after were interpolated between the elevations on the solstice and on the last day of the study. Given that the monitoring spanned across only 61 days, such an approximation is a reasonable assumption.

*Table 5.1: Stability Class Calculation Table [shown with data entry codes] (Adapted from Pasquill 1961)*

Wind Speed (m/s)	Solar Radiation		
	[0] Slight	[1] Moderate	[2] Strong
[0] <2	B	A-B	A
[1] 2-3	C	B	A-B
[2] 3-4	C	B-C	B
[3] 4-6	D	C-D	C
[4] >6	D	D	C

*Table 5.2: Stability Class Descriptions [shown with data entry codes] (Adapted from Pasquill 1961)*

Stability Class	Description
[1] A	Very Unstable
[2] B	Unstable
[3] C	Slightly Unstable
[4] D	Neutral

Since all measurements were conducted during the day, nighttime values were omitted from Table 5.1. The other component of stability class is the wind speed, shown in the table along

with the numerical coding of each wind speed class. A description of the properties these values correspond to is shown in Table 5.2. For stability classes between two values, the average of the data entry value was used. For instance, a stability class of A-B was assigned a value of 1.5.

### 5.2.2. *Two-Sided Measurements*

Along with the measurements described previously, an additional effort was made to measure the difference in air pollution on either side of the street. Due to the additional instruments required for this investigation, it could only be conducted on 50 occasions during the mid-day period. It was hypothesized that a combination of meteorological and built environment factors would cause the air pollution to be higher on one side of the street than the other. In order to explain this effect, the absolute difference between the UFP concentrations on either side of the street was calculated.

Wind direction was thought to be a likely contender to explain the difference in pollution from one side of the street to the other, however it was not immediately apparent how to classify this principle into a single explanatory variable. In order to do this, the orientation of each study block was measured with respect to True North using Google Earth. All measurement angles were normalized to their corresponding angle of less than  $180^\circ$ . That is to say, as far as the street orientation is concerned, an angle of  $225^\circ$  is identical to  $45^\circ$ , so the latter was used as the standard. From Environment Canada, the prevailing wind direction was recorded using the nearer of two weather monitoring stations on the island. Again, these angles were normalized to their equivalent value less than  $180^\circ$ . Note that this is possible because it is not the direction of the effect which is being tested, but rather just the absolute difference between the two sides of the street. In this sense, a Northerly wind would be expected to have the same effect as a Southerly wind, with respect to a given street orientation.

Since both the orientation of the street and the direction of the wind are expressed in equivalent terms, the absolute difference in the angle can be calculated. From this, the sine of resulting angle is taken in order to obtain a value between zero and one that represents the wind orthogonality to the street. To clarify, if the difference in the angles is  $0^\circ$ , the wind is blowing directly parallel to the orientation of the street; therefore the parameter is computed as the sine of  $0^\circ$ , or zero. Conversely, if the difference in angles is  $90^\circ$ , then the wind is blowing directly perpendicular to the street, thus resulting in the sine of  $90^\circ$ , which is one. It would be expected that parallel wind, given a value of zero, would not increase the difference in concentrations between



the two sides, while an orthogonal wind, given a value of one, would blow the air pollution from one side to the other, thus increasing the difference.

In addition to the wind direction, the wind speed was also thought to have an effect. In this case, the wind speed was represented as both a continuous variable in kilometers per hour as well as a dummy variable demarcated by the median value of 7 km/hr. The potential effect of this variable was uncertain: it was speculated that higher wind speeds could either facilitate pollution being blown from one side to the other, but could also increase atmospheric mixing, which would tend to equilibrate the concentrations with respect to different sides of the same street.

In terms of the built environment, it was mostly the dimensions of the urban canyon which were of interest. That is to say, the width of the space between buildings and the characteristics of the buildings themselves. With respect to the canyon width, this was represented by attributes such as the road width and the number of lanes. The buildings were quantified as in the previous section: that is based on their presence on both sides of the street, the average height of the buildings within 25 m, and whether or not they created a mostly contiguous façade when present. These attributes were collected both in the field and through Google StreetView.

## **5.3. Results**

### *5.3.1. Independent Observations*

The first analysis of the fixed site data treats each of the 200 UFP measurements as an independent observation in the linear regression. As we will see, UFP and its explanatory variables can be highly time-variant, thus treating each observation independently provides a beneficial understanding of the relationship between UFP and these factors.

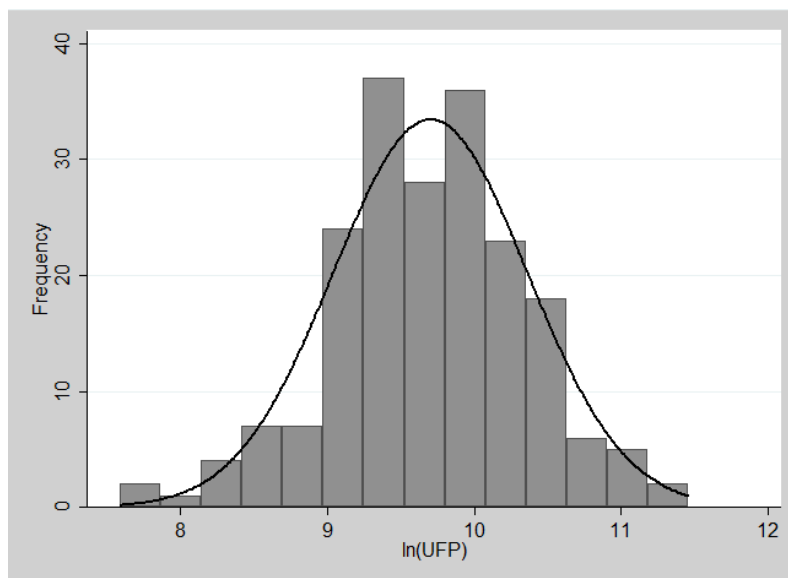


*Figure 5.1: Histogram of  $\ln(\text{UFP})$  for each Observation*

Using this information, a linear regression model was developed. UFP measurements were log-normally distributed, as shown in Figure 5.1, therefore the LN-transform of UFP was taken as the dependent variable. Table 5.3 shows some descriptive statistics for pertinent variables, along with their pairwise correlations with  $\ln(\text{UFP})$ .

From this, we can gauge the effects of meteorology on UFP concentrations. A recurring theme in this chapter and those to follow will be the inverse associations between UFP and both temperature and wind speed. That is, UFP levels increase as temperature and wind speed decrease. Furthermore, increased cloud cover also appears to decrease UFP, however, the solar elevation seems to have no effect. Since solar radiation is a function of only these two factors, cloud cover alone is a sufficient metric.

Stability class also shows a negative correlation. This means that as stability increases, UFP decreases. Put differently, more atmospheric turbulence or instability increases the concentration of UFP in the near-roadway environment. This effect is slightly counter-intuitive. Typically, more atmospheric instability implies better mixing conditions for diluting the overall concentration of pollution. However, these data suggest that such may not be the case in the near-roadway environment. It appears that the increased turbulence mixes pollution from the street so that it equally affects the edges of the road, where these measurements were taken.

Table 5.3: Descriptive Statistics for Select Variables over all Observations

Variable	Units	Mean	S.D.	Min	Max	Correlation ln(UFP)
<b>UFP</b>	#/cm <sup>3</sup>	20145	14010	1977	94798	.
<b>ln(UFP)</b>	.	9.70	0.66	7.59	11.46	.
<b>Temperature</b>	°C	22.92	3.85	13.8	32.7	-0.24 **
<b>Wind Speed</b>	km/hr	7.03	2.40	2	17	-0.13
<b>Wind Speed Class</b>	(ordinal)	0.39	0.67	0	3	-0.22 **
<b>Weather</b>	(ordinal)	2.43	1.02	1	5	-0.26 **
<b>Cloud Cover</b>	(dummy)	0.48	0.50	0	1	-0.32 **
<b>Solar Elevation</b>	°	49.39	10.95	33.5	63.5	N.S.
<b>Solar Radiation</b>	(ordinal)	0.67	0.69	0	2	N.S.
<b>Stability Class</b>	(ordinal)	2.00	0.57	1.5	4.0	-0.16 *
<b>Vehicular Volume</b>	veh/hr	991.32	1152.19	12	6222	0.22 **
<b>Truck Ratio</b>	.	0.04	0.05	0.00	0.50	0.26 **
<b>Road Width</b>	m	9.80	6.67	2.6	28.0	0.19 **
<b>Urban Canyon</b>	(dummy)	0.16	0.37	0	1	0.14 *
<b>Industrial Zoning</b>	(dummy)	0.60	0.49	0	1	0.14

\*\*  $p < 0.01$ ; \*  $p < 0.05$ ; N.S. for  $p > 0.15$

From Table 5.1 we see that stability increases with high wind speed and low solar radiation. Cloud cover decreases solar radiation, so it can therefore be said to increase stability. In this sense, it stands to reason that an increase in wind speed and cloud cover both increase stability, and therefore decrease near-roadway UFP concentrations.

All traffic and BE variables listed in Table 5.3 were positively associated with UFP, which was the expected direction. That is, traffic volume, the ratio of trucks in that volume, road width, the urban canyon dummy variable, and the industrial zoning dummy variable all increased UFP levels. Road width and traffic volume however were highly correlated, so could not both be included in the linear regression, which assumes that all independent variables are in fact independent effects on the dependent variable.

The final regression model from this exercise is shown in Table 5.4. The variables are shown in decreasing order of their standardized beta coefficient, which allows the magnitude of their effects to be compared to one another regardless of their units. This works by normalizing the effects to a variance of one. The model underscores the importance of vehicular volumes and

truck ratios in driving the total UFP concentrations. However, the meteorological effects clearly play a dominant role as well, as depicted by the temperature, cloud cover, and wind speed. The latter two suggest the importance of the stability class in assessing the meteorological impact. The final two variables do not cross the conventional 95% confidence threshold, however due to the relatively small sample size and their intuitive importance, they were left in the final regression. The industrial zoning variable suggests that these areas may be additional sources of UFP to consider in future analysis, while the urban canyon variable suggests that these types of street corridor could exacerbate pollution levels beyond what would otherwise be expected.

*Table 5.4: Linear Regression of  $\ln(\text{UFP})$  for all Fixed Site Observations ( $R^2=0.3044$ ;  $n=200$ )*

Parameter	Units	$\beta$	Coefficient	S.E.	t	P>t
<b>Vehicular Volume</b>	veh·10 <sup>-3</sup> /hr	0.26	0.15	0.04	4.01	0.00
<b>Cloud Cover</b>	(dummy)	-0.25	-0.34	0.08	-4.00	0.00
<b>Temperature</b>	°C	-0.24	-0.04	0.01	-3.99	0.00
<b>Truck Ratio</b>	.	0.18	2.16	0.77	2.80	0.01
<b>Wind Speed Class</b>	(ordinal)	-0.15	-0.15	0.06	-2.38	0.02
<b>Industrial Zoning</b>	(dummy)	0.11	0.15	0.09	1.65	0.10
<b>Urban Canyon</b>	(dummy)	0.10	0.18	0.11	1.60	0.11
<b>Constant</b>	.		10.21	0.27	38.08	0.00

### 5.3.2. Observations Averaged by Site

Although the previous analysis yielded useful interpretations of the underlying causes of UFP levels, its model fit was lower than other studies. This could indicate that modelling multiple observations as independent observations is not an appropriate assumption. In order to test this, the multiple observations at the 73 locations were averaged over each location. Figure 5.2 shows how these values were log-normally distributed, therefore the natural logarithm of the UFP values were used for the regression analysis.

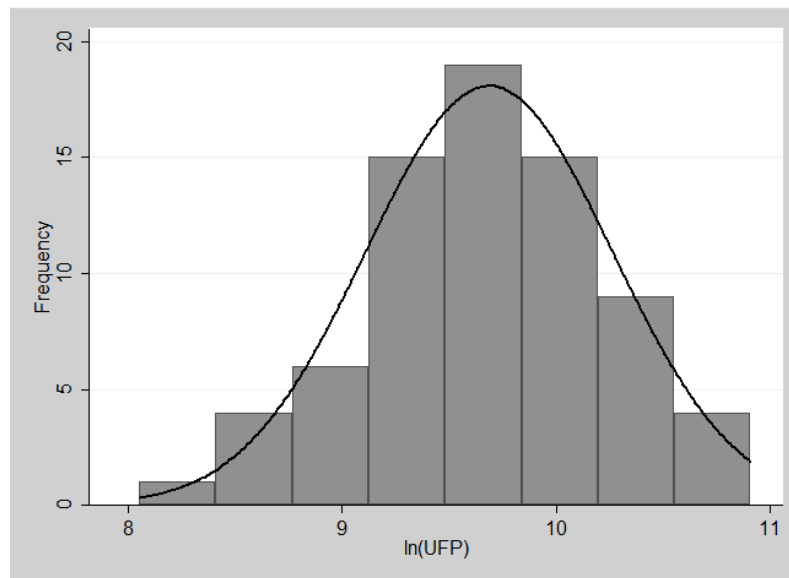


Figure 5.2: Histogram of the  $\ln(\text{UFP})$  Concentration at Each Site

Table 5.5 lists descriptive statistics and the pairwise correlations with  $\ln(\text{UFP})$  for select variables, as they are averaged over the 73 locations. A new dummy variable representing the locations measured in downtown Montreal, representing the 48 sites closest to the study headquarters at the downtown campus of McGill University, defined in Table 3.3.

The final regression developed from this dataset is shown in Table 5.6. The first thing to notice is that its model fit is far superior to that of the previous regression (Table 5.4). Although urban canyons were not able to maintain a significant presence in the model, the downtown Montreal variable is able to coexist with industrial zoning. The former however clearly exerts a strong influence on the model. Time-variant characteristics like meteorology (wind speed and cloud cover) and the truck ratio were able to remain in the model, even after averaging, although it could be argued that the truck ratio itself may be fairly consistent from day to day. Traffic volumes have been replaced by the time-invariant road width, which as mentioned in the previous section, are highly correlated with one another. This suggests that a simpler measure like road width may be adequate for long term models in the event that traffic volumes cannot be easily obtained.

Table 5.5: Descriptive Statistics for Select Variables at Each Site

Variable	Units	Mean	S.D.	Min	Max	Correlation ln(UFP)
Average UFP	#/cm <sup>3</sup>	18813	10753	3141	54650	.
ln(UFP)	.	9.69	0.58	8.05	10.91	.
Downtown Montreal	(dummy)	0.66	0.48	0	1	0.70 **
Temperature	°C	22.9	2.6	17.6	28.7	N.S.
Wind Speed	km/hr	6.68	1.81	2	11	-0.21
Wind Speed Class	(ordinal)	0.37	0.54	0	2	-0.41 **
Weather	(ordinal)	2.52	0.85	1	5	-0.47 **
Cloud Cover	(dummy)	0.51	0.37	0	1	-0.55 **
Stability Class	(ordinal)	2.0	0.4	1.5	3.0	-0.31 **
Vehicular Volume	veh/hr	944.1	1091.4	15	58364	0.26 *
Truck Ratio	.	0.04	0.0	0.00	0.17	0.45 **
Road Width	m	9.6	6.1	2.6	28.0	0.23
Urban Canyon	(dummy)	0.14	0.35	0	1	0.25 *
Industrial Zoning	(dummy)	0.60	0.49	0	1	0.21

\*\* p < 0.01; \* p < 0.05; N.S. for p > 0.15

Table 5.6: Linear Regression for ln(UFP) at Each Site ( $R^2=0.6807$ ;  $n=73$ )

Parameter	Units	$\beta$	Coefficient	S.E.	t	P>t
Downtown Montreal	(dummy)	0.451	0.542	0.107	5.06	0.00
Wind Speed Class	(ordinal)	-0.262	-0.279	0.079	-3.52	0.00
Road Width	m	0.245	0.023	0.008	3.07	0.00
Cloud Cover	(dummy)	-0.199	-0.312	0.137	-2.27	0.03
Truck Ratio	.	0.144	2.272	1.223	1.86	0.07
Industrial Zoning	(dummy)	0.132	0.155	0.093	1.66	0.10
Constant	.	.	8.879	0.127	69.67	0.00

### 5.3.3. Two-Sided Measurements

Finally, we move away from assessing the overall levels of UFP to examining what causes differences in concentrations even across two sides of the same street. It is hypothesized that these differences could be explained in part by the urban canyon effect, depicted by the diagram in Figure 4.6. The urban canyon effect represents an interesting interaction between both meteorology and the built environment.

Due to the log-normal distribution of the absolute difference in UFP concentrations ( $|\Delta\text{UFP}|$ ), a natural log transform was applied to the dependent variable prior to analyses. This distribution is pictured in Figure 5.3. Furthermore, the log transform was intended to offset the presumably greater disparity that is caused simply by the overall higher concentrations present on the street. That is, all else equal, a street with more pollution would be expected to have a higher difference in concentrations between the two sides simply due to sheer magnitude of the concentration.

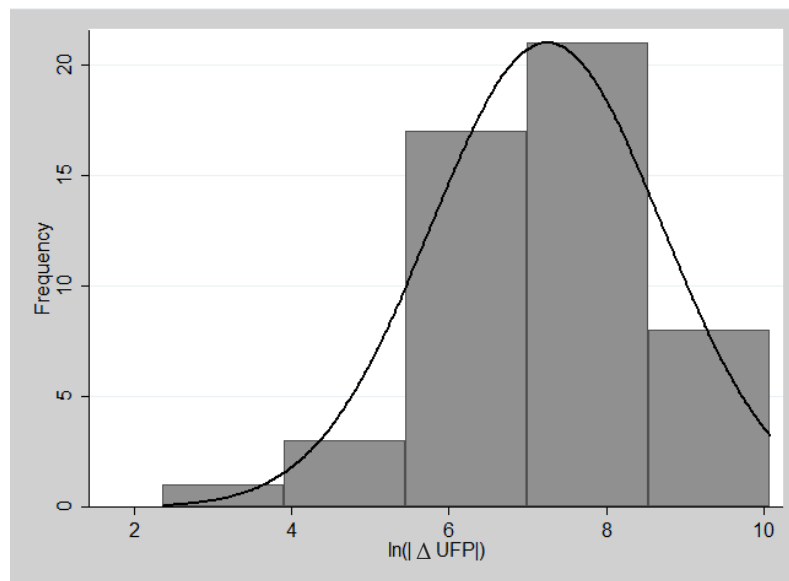


Figure 5.3: Histogram of all observations for  $\ln(|\Delta\text{UFP}|)$  measurements

Table 5.7: Descriptive Statistics for Two-Sided Variables Used in Regression

Variable	Units	Mean	S.D.	Min	Max
$ \Delta\text{UFP} $	#/cm <sup>3</sup>	3,281	4,759	11	23,944
$\ln( \Delta\text{UFP} )$	.	7.24	1.47	2.36	10.08
Wind Orthogonality	.	0.7	0.3	0.0	1.0
Road Width	m	10.7	7.2	2.6	28.0
Wind Speed $\geq 7$ km/hr	(dummy)	0.7	0.5	0	1
Buildings on Both Sides of Street	(dummy)	0.5	0.5	0	1
Truck Ratio	.	0.06	0.03	0.00	0.17

Linear regression analysis was then applied to the dataset, treating all 50 observations independently, and is shown in Table 5.8. This analysis shows that nearly half of the variability in

the difference between concentrations on either side of the street is explained primarily by wind and urban canyon characteristics. The regression suggests that it is indeed lower wind speeds which result in a higher disparity in UFP concentrations. Furthermore, the direction of the wind in relation to the street orientation also appears to have an effect in the expected direction. That is, when the wind is more perpendicular to the street, the pollution is blown from one side to the other.

*Table 5.8: Linear Regression Analysis for  $\ln(|\Delta UFP|)$  ( $R^2=0.4739$ ;  $n=50$ )*

Parameter	Units	$\beta$	Coefficient	S.E.	t	P>t
<b>Road Width</b>	m	0.559	0.113	0.026	4.38	0.00
<b>Wind Speed <math>\geq 7</math> km/hr</b>	(dummy)	-0.324	-0.991	0.343	-2.89	0.01
<b>Wind Orthogonality</b>	.	0.279	1.405	0.555	2.53	0.02
<b>Buildings on Both Sides</b>	(dummy)	0.217	0.631	0.371	1.70	0.10
<b>Truck Ratio</b>	.	0.216	9.463	4.866	1.94	0.06
<b>Constant</b>	.		4.911	0.640	7.67	0.00

With respect to the urban canyon, this effect is represented by road width, which has the strongest effect and the presence of buildings on both sides of the street. Although a smaller road width may have been expected to amplify the urban canyon effect, it appears that the sheer distance from side to side countervails that effect causing an even greater disparity with wider streets. However, the fact that the presence of buildings on both sides positively contributed to the difference suggests that the effect of pollution trapped between building faces was detectable, even in this relatively small investigation.

Finally, the ratio of truck traffic also positively contributed to the difference in UFP. This could simply imply that despite taking the natural log of the difference, higher levels of pollution generated by the increased presence of trucks still contribute to the disparity in UFP levels.

#### 5.4. Discussion and Conclusion

The results presented in this chapter represent the findings of a smaller scale, yet more conventional LUR analysis. From the first two investigations we can see how the way in which data are collected and parsed can strongly influence the results of the model. This point remains important as we continue to the mobile measurement campaign. Of course having fewer, more aggregate measures for UFP, allowed us to achieve a substantially higher  $R^2$  value, however not



all parameters had enough observations and variability in order to remain statistically significant. For instance, the urban canyon variable was not able to remain in the second regression. This highlights the tradeoff we find between smaller aggregated datasets and larger disaggregated ones. With more records, achieving higher model fits becomes more difficult, however they may reveal more insights into the underlying causes of UFP exposure.

These data also reveal some interesting findings with respect to the nature of UFP. Firstly, it is absolutely essential for any model attempting to explain UFP variations to take into account a number of meteorological variables. Temperature was shown to have a relatively strong inverse effect on UFP levels, however certain components of atmospheric stability also proved to have substantial effects. Namely, wind speed and an approximation of cloud cover played a notable role in the models explaining overall UFP concentrations.

The primary purpose of the exercise however was to understand how the traffic and built environment properties influenced exposure. From this we learn that vehicular traffic does indeed have a strong influence, however just as important is the proportion of traffic comprised by trucks. The ability to account for this remains a strength in this smaller scale approach that cannot be rivaled by the vastness of a mobile campaign. Yet we also find that road width can stand as an acceptable proxy for these factors. Finally, we observe that factors such as buildings on both sides of the street and proximity to areas zoned for industrial purposes have noticeable effects on UFP.

In the final investigation of this chapter, the variations in UFP between two sides of the same street are explored. Here we find again that the interaction between meteorology and built environment, presumably by virtue of the urban canyon effect, causes variations even within the same microenvironment. The effects seemed to be driven firstly by the road width, where intuitively, wider streets were more conducive to greater variability between the sides. Though wider streets may countervail the impact of the urban canyon by it allowing air to escape the vortex more easily, the presence of this effect is suggested by the positive coefficient of having buildings on both sides of the street.

Wind speed and direction are the remaining component in this understanding. It appears that higher wind speeds increase the overall mixing, causing the difference between the two sides to decrease. On the other hand, wind orthogonality, despite representing only an average of the regional prevailing wind direction, has a notable effect on the difference in UFP levels with wind

more perpendicular to the street orientation increasing the difference. These findings further emphasize the volatile nature of this pollutant we seek to model and underscores the importance of obtaining data with high spatial resolution.

## **CHAPTER 6 — GENERATING A LAND USE REGRESSION MODEL WITH MOBILE MEASUREMENTS**

### **6.1. Introduction**

Having previously explored some possible causes in the variation of air pollution from the fixed site experiment in Chapter 5, we can now expand these ideas to test the associations found in the larger mobile experiment. This was performed by applying the data collection and processing efforts described in Chapter 3 and Chapter 4, along with additional processing, which is further explained in the following section. Subsequently, Section 6.3 details the results of this exercise. Section 6.4 frames the results of the regressions and other statistical observations in the context of the objectives of the larger study. Finally, Section 6.5 summarizes and concludes the chapter.

### **6.2. Methodology**

The vast majority of the methodology is described in Chapter 3 and Chapter 4. To summarize, research assistants cycled along approximately 500 km of roadways, trails, and cycling facilities carrying air pollution monitoring equipment. The GPS location of the air pollution points were associated with the street that was cycled on or alongside, as shown in Figure 4.3 on page 31. Points that were not on or alongside a motorized roadway were assigned to the nearest one.

The statistical analysis was performed by using the average air pollution values for each trip cycled on each link as an independent observation. In total, 16,962 observations were analyzed including 16,745 records for UFP and 13,218 for BC. Links were measured by a median of 4 trips, though the number of trips reached as high as 53 near the downtown origin. In most cases, the arithmetic mean was used to average the results. For variables that represented distances between a point and a link, the median value was chosen in order to reduce the influence of outlier GPS coordinates. Median values were also used for dummy and ordinal variables, which were subsequently rounded to the nearest integer value. All analysis was conducted with Stata 12 (StataCorp LP).

## 6.3. Results

### 6.3.1. Descriptive analysis

#### 6.3.1.1. Distribution of UFP and BC Levels

Prior to any analysis, a natural log transform was applied to the UFP and BC data to reflect their log-normal distribution (Figure 6.1 and Figure 6.2). Using this database, Pearson correlation coefficients were estimated to preliminarily assess associations between sub-classes of related attributes and the measured air quality data. Following this, simple linear regression models were run in order to evaluate the relationships between the potential explanatory variables and UFP and BC measurements. Descriptive statistics for the UFP and BC concentrations are reported in Table 6.1.

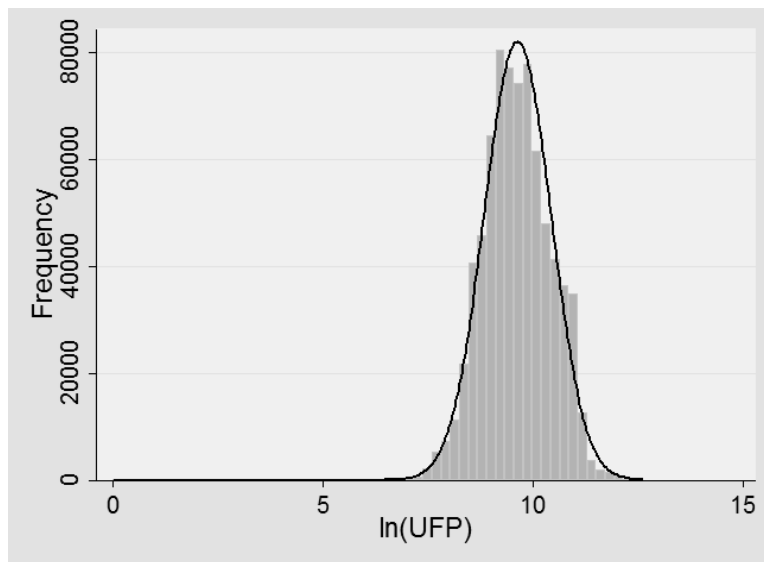


Figure 6.1: Histogram of the  $\ln$ -transformed of all recorded UFP measurements

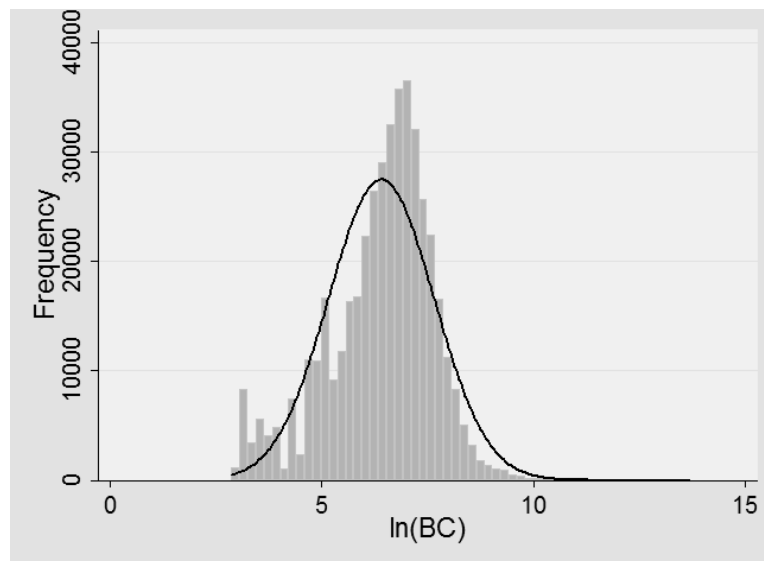


Figure 6.2: Histogram of the ln-transformed of all recorded BC measurements

Table 6.1: Descriptive Statistics for Air Quality Data

Variable	Units	Mean	Min	Max	IQR	
UFP	#/cm <sup>3</sup>	18,954	2,653	75,374	9,712	27,056
BC	ng/m <sup>3</sup>	1,159	68	70,322	343	1,429
ln(UFP)	.	9.64	7.88	11.23	9.18	10.21
ln(BC)	.	6.66	4	11	5.84	7.27

Air quality maps were generated by averaging multiple trips on a single link into a single value and plotting the results on ArcGIS (Figure 6.3 and Figure 6.4). Perhaps the most noticeable observation is that the pollution levels appear to be higher in the downtown region (shaded) than in the periphery. Also apparent from the larger scale map is that pollution levels appear to be lower in park areas (green) than on other streets.

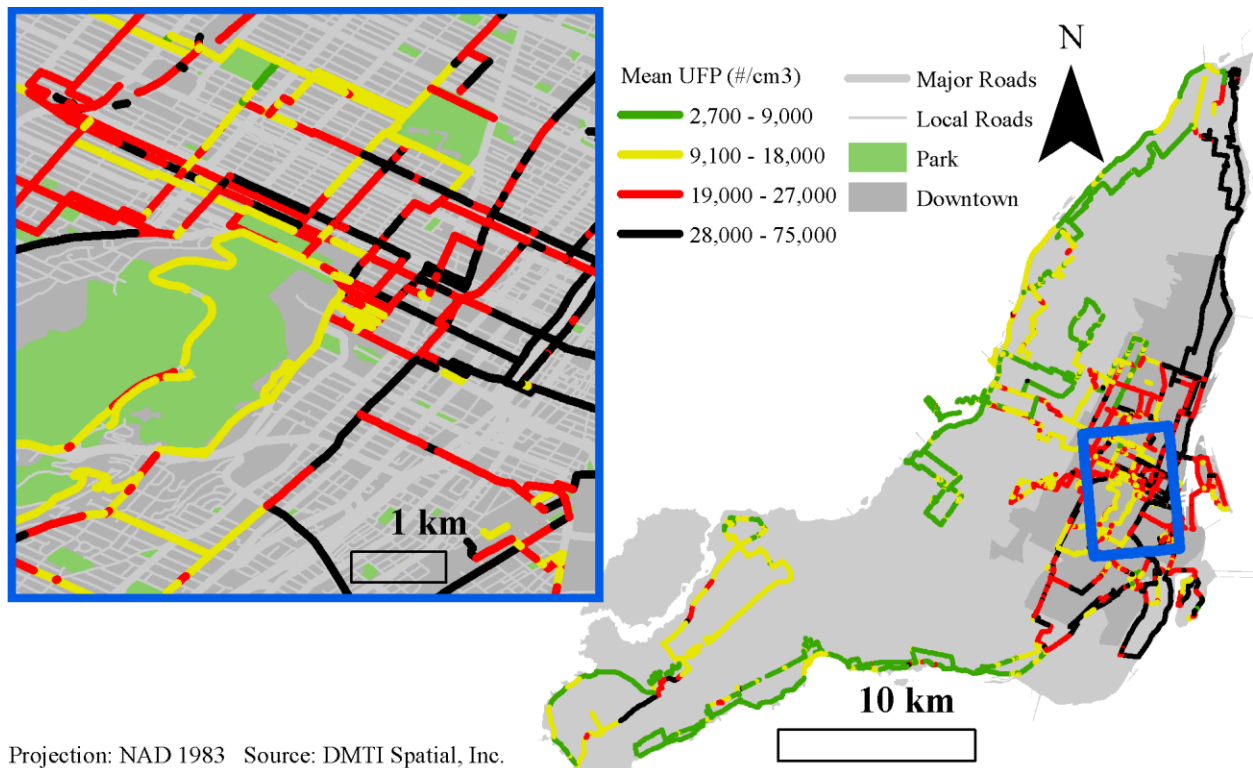


Figure 6.3: Spatial Distribution of UFP

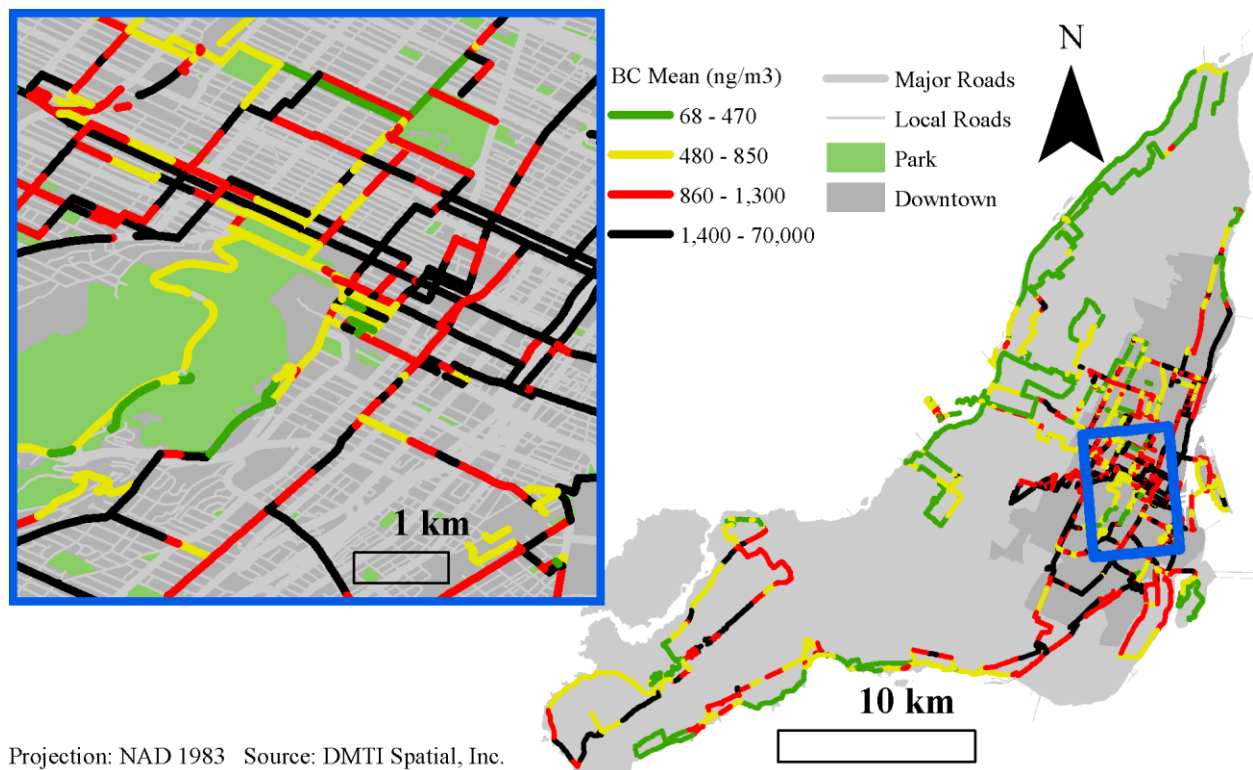


Figure 6.4: Spatial Distribution of BC

### 6.3.1.2. Exploration of Meteorological Effects

The meteorological conditions remained a preeminent indicator for air pollution levels. As such, it warrants additional attention so that it could be controlled for when analyzing the spatial characteristics. Temperature appeared to exert a substantial inverse effect on air pollution levels, in particular for UFP—a result observed by similar studies, including the fixed site data analyzed in Chapter 5. The other two observed meteorological variables also played an important role in pollutant levels, namely wind speed, which had a greater effect on UFP levels, and relative humidity, which had a greater effect on BC levels. These correlations are summarized in Table 6.2.

*Table 6.2: Descriptive Statistics for Meteorological Variables*

Variable	Units	Mean	Min	Max	Correlation ln(UFP)	Correlation ln(BC)
<b>Real-Time Temperature</b>	° C	25	13	40	-0.29*	-0.14*
<b>Temperature <math>\geq 20^{\circ}\text{C}</math></b>	(dummy)	0.84	0	1	-0.35*	-0.04*
<b>Minimum Trip Temperature</b>	° C	21	14	28	-0.39*	-0.24*
<b>Wind Speed</b>	km/hr	14	6	24	-0.30*	-0.23*
<b>Relative Humidity</b>	%	0.55	0.33	0.84	-0.02*	0.28*

\* =  $p < 0.05$

In addition to these conventional meteorological parameters, an effort was made to determine if any effects were present at a specific temperature. Figure 6.5 shows the effect of a dummy variable for temperature at 1°C intervals over the range of observed temperatures during the study period (13.4 – 40.0°C). A noteworthy effect appears to occur for UFP at a temperature of 20°C, at which point the dummy variable has the strongest inverse correlation with UFP levels. However, as shown in the same figure, no such effect was observed for BC. It is possible that this may represent a temperature at which a reaction occurs which transforms UFP to particles of different size.

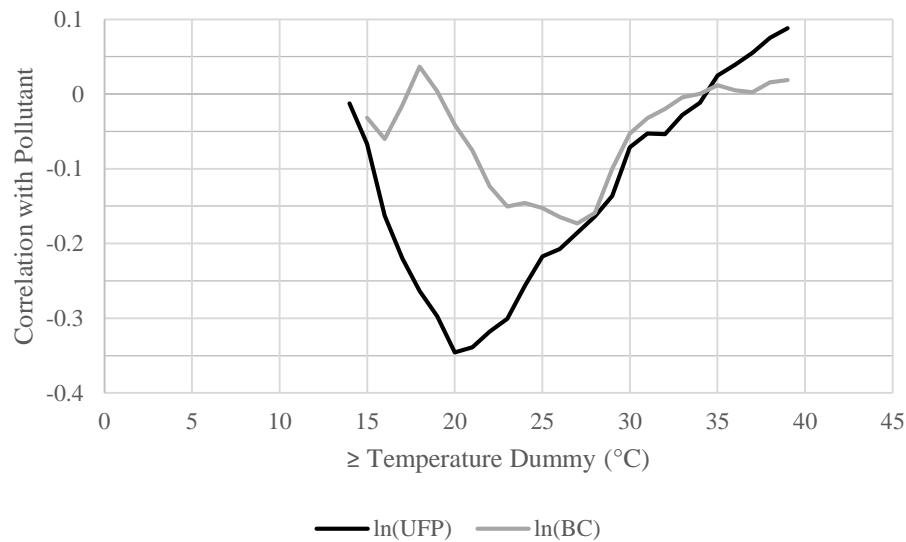


Figure 6.5: Dummy temperature correlations with  $\ln(\text{UFP})$  and  $\ln(\text{BC})$

#### 6.3.1.3. Investigation of Individual Effects

The aforementioned meteorological variables were used in order to better understand the variations in the built environment characteristics, shown in Table 6.3. A linear regression analysis was performed for built environment characteristics with meteorological variables *temp\_c\_min*, *temp\_20c*, *wind\_speed\_kph*, and *rh* for UFP and *temp\_c\_min*, *wind\_speed\_kph*, and *rh* for BC. The normalized beta coefficients for each built environment variable within the respective model are reported.



Table 6.3: Univariate Regression Results for Built Environment Variables

Variable	Mean	Min	Max	Units	$\beta$ UFP	$\beta$ BC	Description
dt_mtl	0.46	0	1	(dummy)	0.308 *	0.214 *	(1) Data were measured in borough or town within or adjacent to Ville-Marie
road_class	4.59	1	5	(ordinal)	-0.055 *	-0.083 *	(1) Expressway; (2) Primary Arterial; (3) Secondary Arterial; (4) Collector; (5) Local
mjrdd	0.37	0	1	(dummy)	0.090 *	0.080 *	(0) Local Road, i.e. road_class [5]; (1) Major Road, i.e. road_class [1-4]
capacity	4507.36	899	207210	veh	-0.004	-0.026 *	Estimated capacity of road based on road class and number of lanes
numlanes	1.78	1	6	count	-0.041 *	-0.030 *	Number of lanes on roadway
speed_limit_kph	44.44	30	100	km/hr	0.061 *	0.071 *	Speed limit of associated roadway
int_25m	0.60	0	1	(dummy)	0.060 *	0.058 *	(1) More than 50% of points are within 25 m of an intersection
link_length_km	110.53	4	3224	m	-0.056 *	-0.051 *	Length of vehicular street with which the measurement was assigned
vol_hr	186.22	0	4631	veh	0.065 *	0.092 *	Mean simulated volume on measured link during the measurement hour
vol_peak	1259.65	0	29498	veh	0.085 *	0.092 *	Mean simulated volume on measured link over the hours covered by the study
vol_period	633.41	0	14749	veh	0.080 *	0.092 *	Mean simulated volume on measured link over the hours in the measurement period
vol_total	2113.90	0	15676	veh	0.095 *	0.083 *	Mean simulated volume on measured link over 24 hours
hwy_vol_total	2408.46	0	9934	veh	-0.031 *	-0.018 *	Mean simulated volume on nearest expressway over 24 hours
mjrdd_vol_total	1671.22	0	7779	veh	0.064 *	0.035 *	Mean simulated volume on the nearest artery or collector over 24 hours
cl_dist_m	16.60	0	533	m	-0.055 *	-0.119 *	Distance from the measured point to the street along which the cyclist was riding
hwy_dist_m	936.28	1	5049	m	-0.210 *	-0.223 *	Distance from the measured point to the nearest highway
hwymjrdd_dist_m	139.76	0	1491	m	-0.116 *	-0.163 *	Distance from the measured point to the nearer of a highway or major road
mjrdd_dist_m	157.10	0	1631	m	-0.089 *	-0.145 *	Distance from the measured point to the nearest major road
vol_dist	197.23	0	49564	veh/m	0.045 *	0.052 *	Interaction term between volume and distance: traffic volume in each time period divided by the centerline distance from the roadway
speed_kph_hr	31.71	0	80	km/hr	-0.131 *	-0.133 *	Minimum Simulated speed on measured link during the measurement hour
speed_kph_peak	31.67	0	80	km/hr	-0.132 *	-0.135 *	Minimum Simulated speed on measured link over the hours covered by the study

Variable	Mean	Min	Max	Units	$\beta$ UFP	$\beta$ BC	Description
speed_kph_period	31.64	0	80	km/hr	-0.132 *	-0.135 *	Minimum Simulated speed on measured link over the hours in the measurement period
congestion_hr	0.28	0	1	(ratio)	0.137 *	0.139 *	Difference between the speed limit and the simulated hourly speed over the speed limit
congestion_peak	0.26	0	1	(ratio)	0.134 *	0.138 *	Difference between the speed limit and the simulated peak speed as over the speed limit
congestion_period	0.28	0	1	(ratio)	0.138 *	0.140 *	Difference between the speed limit and the simulated period speed over the speed limit
vol_cap_hr	0.06	0	1	(ratio)	0.071 *	0.110 *	Ratio of the simulated hourly volume and the estimated capacity
vol_cap_peak	0.08	0	1	(ratio)	0.114 *	0.133 *	Ratio of the simulated peak volume and the estimated capacity
vol_cap_period	0.06	0	1	(ratio)	0.101 *	0.125 *	Ratio of the simulated period volume and the estimated capacity
period	0.51	0	1	(dummy)	0.077 *	0.013 *	Time period of measurement: (0) Morning; (1) Afternoon
bldg_25m	0.60	0	1	(dummy)	0.148 *	0.105 *	(1) Contains a building within 25 m of the link
bldg_25m_perc	0.24	0	4	(ratio)	0.147 *	0.105 *	% of area in a 25 m buffer around each measured point containing building footprints
bldg_50m	0.74	0	1	(dummy)	0.164 *	0.110 *	(1) Contains a building within 50 m of the link
bldg_50m_perc	0.60	0	6	(ratio)	0.202 *	0.159 *	% of area in a 50 m buffer around each measured point containing building footprint
bldg_row	1.34	0	2	(ordinal)	0.168 *	0.116 *	(1) Does not contain a building within 50 m of the link; (2) Contains a building within 50 m of the link but not within 25 m; (3) Contains a building within 25 m of the link
resto_100m	1.06	0	33	(count)	0.157 *	0.111 *	Number of restaurants within a 100m buffer of each measured point
resto_dist_m	314.89	5	2800	m	-0.228 *	-0.179 *	Distance from the measured point to the nearest restaurant
industrial	0.12	0	1	(dummy)	0.042 *	0.044 *	(1) More than 50% of points on link are in an industrial area
park	0.12	0	1	(dummy)	-0.057 *	-0.059 *	(1) More than 50% of points on link are in a park
popdens11_borough	6622.69	123	12348	#/km2	0.114 *	-0.007 *	2011 population density at the borough level
urban_borough	0.60	0	1	(dummy)	0.176 *	0.027 *	(1) Borough has a population density greater than or equal to 5,000/km2

### 6.3.2. Regression analysis

Finally, a multivariate regression analysis was conducted in order to create explanatory models for UFP and BC. Models began with the base meteorological variables from the previous section and subsequently added the strongest variables from the univariate analysis in each sub-category of variables. The UFP linear regression (Table 6.4) and BC linear regression (Table 6.5) show the strongest models, ordered by decreasing impact of the normalized beta coefficient.

Table 6.4: Linear Regression for  $\ln(\text{UFP})$  Mobile Measurements ( $R^2 = 0.3401$ ;  $n = 16,745$ )

Parameter	Units	$\beta$	Coefficient	S.E.	t	P> t
Downtown Montreal	(dummy)	0.228	0.367	0.011	32.03	0.000
Wind Speed	km/hr	-0.224	-0.030	0.001	-33.09	0.000
Temperature $\geq 20^\circ\text{C}$	(dummy)	-0.200	-0.407	0.016	-25.34	0.000
Minimum Trip Temperature	$^\circ\text{C}$	-0.197	-0.037	0.002	-23.4	0.000
Relative Humidity	.	-0.102	-0.618	0.039	-15.77	0.000
Distance from Restaurant	km	-0.092	-0.268	0.000	-12.29	0.000
Distance from Highway	km	-0.086	-0.102	0.000	-12.38	0.000
Major Road	(dummy)	0.075	0.117	0.010	11.73	0.000
Building within 50 m	(dummy)	0.052	0.104	0.014	7.31	0.000
Park & Recreation	(dummy)	-0.032	-0.072	0.015	-4.85	0.000
Vehicular Volume / Distance	veh·10 <sup>-3</sup> /m	0.014	0.015	0.000	2.16	0.031
Industrial & Resource	(dummy)	0.013	0.030	0.015	2.02	0.043
Constant	.	11.331	0.042	267.990	0.00	0.000

Table 6.5: Linear Regression for  $\ln(\text{BC})$  Mobile Measurements ( $R^2 = 0.2009$ ;  $n = 13,217$ )

Variable	Units	$\beta$	Coefficient	S.E.	t	P> t
Relative Humidity	%	0.250	2.507	0.082	30.63	0.000
Distance from Highway	m	-0.159	0.000	0.000	-19.29	0.000
Downtown Montreal	(dummy)	0.140	0.364	0.022	16.43	0.000
Minimum Trip Temperature	$^\circ\text{C}$	-0.131	-0.041	0.003	-14.7	0.000
Wind Speed	km/hr	-0.103	-0.022	0.002	-11.57	0.000
Distance from Nearest Roadway	km	-0.081	-0.003	0.000	-9.47	0.000
Distance from Nearest Major Road	km	-0.052	0.000	0.000	-5.91	0.000
Park & Recreation	(dummy)	-0.044	-0.162	0.031	-5.19	0.000
Building Present Within 50 m	(dummy)	0.042	0.133	0.027	4.96	0.000
Major Road	(dummy)	0.037	0.092	0.021	4.29	0.000
Industrial & Resource	(dummy)	0.030	0.111	0.029	3.8	0.000
Volume-Distance Interaction	veh·10 <sup>-3</sup> /m	0.019	2.990	1.330	2.45	0.014
Constant	.	.	6.212	0.086	72.56	0.000

## 6.4. Discussion

Despite the presence of a number of land use indicators, the ‘Downtown Montreal’ dummy variable still shows stronger associations than all other effects, and suggests that there are still many characteristics of the downtown environment that are not fully captured in this study. Following that, the meteorological variables show strong inverse effects, as expected.

However many interesting conclusions can be drawn from the built environment variables. The fact that the distance to the nearest restaurant shows a strong association suggests that restaurants are in fact significant contributors of UFP in their own right via cooking fumes, independent of their association with other urban characteristics. Furthermore, both the distance to the nearest highway as well as whether the measurement was actually conducted on a major road both coexisted in the model, implying that both the characteristics of the street as well as the location of the street in relation to other high-polluting roads both influence UFP concentrations.

The remaining attributes were not as strong, though their presence allows us to better understand their interactions. Buildings within 50 m are a positive contributor in the model, suggesting that even considering that the building density is higher downtown, the buildings themselves may also play a role in the increased UFP exposure, perhaps through the urban canyon effect. The immediate land use also produced a notable effect in the expected directions insofar as parks provided a negative effect on UFP while industrial areas produced a positive one. Finally, an interaction term between traffic volume and the distance from the roadway produced a positive effect, meaning that more traffic, closer to the street contributes to higher UFP levels.

The strongest linear regression generated for BC can be seen in Table 6.5. There are several notable observations about this regression. As discussed previously, meteorological conditions define the largest portion of the model by way of relative humidity and wind speed. Interestingly though, the next strongest variable is the distance from the nearest highway, soon after followed by distances to the nearest road and the distance to the nearest major road. In this way, BC appears to be far more sensitive to the microscopic effects of the road characteristics. The fact that these variables are able to coexist with such strong impacts highlights the significant role that traffic plays in BC generation. This stands to reason considering that the dominant source for BC is understood to be diesel trucks. Again, the presence of buildings remained a positive factor, perhaps as a rough proxy for an urban canyon effect. Industrial and park areas were both significant and

stronger than in the UFP model. Of note however is that given the built environment characteristics, the temperature variable used in the univariate regressions became insignificant, implying that temperature does not affect BC nearly as strongly as it does UFP.

Detecting pollution distance decay trends proved to be difficult given the highly aggregate methodology utilized in this study. The effects of distance from a particular link appear to be largely masked by the substantial variability in the characteristics of the measured roads. However, this methodology did reveal a clear trend in another regard—namely the exponential decay of extreme values with increasing distance from the roadway, as pictured in Figure 6.6. The maximum pollutant within each 1 m interval from the road centerline was plotted and fit with a power curve, showing that while the average pollutants levels may persist at greater distances from the roadway, spikes in pollutant levels tend to decline precipitously from their source.

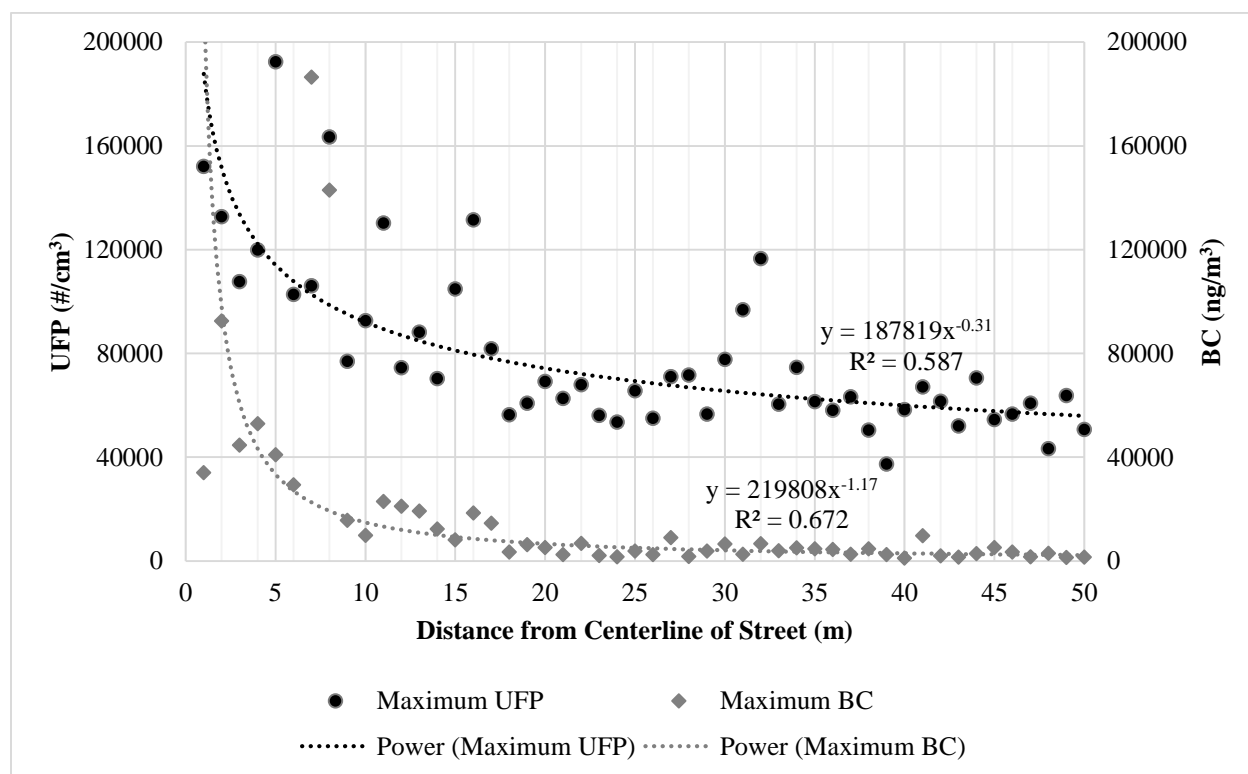


Figure 6.6 Maximum Pollution Decay over Distance in Intervals of 1 m

## 6.5. Conclusion

It is important to note the exceptionally large size of the database from which the statistical analysis was performed. While typical studies in this field may analyze approximately 50 to 200 unique

locations, this database contained over 16,000 records. Such a large dataset is a mixed blessing; with larger datasets one is able to acquire more robust measurements, however they may also introduce an exceptional amount of unexplained variability in the data. Any passing truck or change in local wind direction may cause variation inexplicable by such an aggregate model. This necessarily caused the correlation and regression coefficients found in this study to be generally lower than other studies of a similar nature. In addition, the nature of collecting data over such a broad and varied spatial extent precludes capturing detailed local effects such as more direct measurements of the urban canyon effect, the wind direction relative to the cyclists, and the composition of traffic, especially the proportion of truck traffic.

Ultimately, these findings strengthen our understanding on a number of fronts. First of all, BC appears to be more sensitive to micro-environmental effects than UFP. Its response to indicators such as link level traffic volume and congestion, distance to major roads and highways, and presence in recreational or industrial areas was notably larger than UFP. This implies that it remains closer to its source, and therefore more may be done to mitigate its effects on a carefully planned cycling network. One possible explanation for this is the larger particle size of BC causes it to settle sooner than its lighter counterpart. On the other hand, UFP seemed to be dominated more by regional impacts. It responded far more strongly to weather conditions and borough-level land use characteristics than BC.

More work is needed in order to untangle the interaction between micro and macro determinants of pollution. By working with such an aggregated dataset, it is difficult to detect the subtle ways in which some areas may be more heavily governed by one cause, while other areas may be dominated by another. Yet despite substituting extremely labor intensive field visits required to manually collect traffic, road geometry, and land use data collection with regional, in favor of GIS based methods, the study was still able to detect evidence of both large and small scale effects that support the findings of similar experiments.

## **CHAPTER 7 — UNDERSTANDING THE EFFECTS OF CYCLING FACILITY INFRASTRUCTURE AND ROUTE CHOICE**

### **7.1. Introduction**

This chapter presents one facet of the results collected from the first data collection campaign, whereby air pollution concentrations were collected along approximately 500 km of roads in Montreal by cyclists equipped with global positioning system (GPS) devices and air pollution sampling instruments. It focuses on exploring the relationship between road characteristics, cycling facility characteristics, and concentrations of two pollutants: ultrafine particles (UFP) and black carbon (BC). This investigation attempts to expand on previous findings in order to strengthen our understanding of the role that cycling infrastructure plays in cyclists' exposure to pollution.

Section 7.2 lays out the methodology of this particular exercise. The overarching methodological framework can be found in Chapter 3 and Chapter 4, however the way in which the data has been processed differs subtly from Chapter 6. Section 7.3 covers the descriptive and quantitative results arising from this analysis. Finally, Section 7.4 discusses the overall findings and conclude the chapter.

### **7.2. Methodology**

Again, the majority of the methodological framework for this chapter can be found in Chapter 3 and Chapter 4. The properties of all data points were averaged onto the nearest roadway or trail link per each trip. That is to say, each cycling trip on each link was treated as an independent observation. Properties included the road hierarchy classification and traffic volumes of the nearest motorized roadway and associated cycling facility properties if they fell within 15 m of the point. This process resulted in a total of 17,775 independent observations, including 17,516 for UFP and 13,335 for BC. Each link was covered by an average of four trips. However, some links were covered only once, and links near the downtown origin were covered up to 62 times.

Note that this methodology differs from that of Chapter 6 in that the air pollution measurements are averaged onto all roadways, motorized or not, whereas the previous chapter considers only their relation with the motorized roadway. This discrepancy is due to the subtle

difference in objectives of these two analyses. In the previous analysis, the pollution concentrations were primarily compared to the land use and street characteristics of the microenvironments in which they were cycled. In this chapter however, the focus is more on the actual nature of the specific link that the research assistant has measured. In this way, we still know how far that point was from a motorized street, however it will spatially be associated with the link that was actually measured, regardless of whether it was a vehicular street or a trail.

A number of designated cycling facility types were amalgamated based on similar characteristics. Shared streets, painted lanes, and roadways where no cycling infrastructure was present within 15 m of the point of measurement were classified as “in-street.” “Separated” facilities include cycle tracks, typically a bi-directional within the right-of-way of the street. These were usually separated by a concrete curb, bollards, or parked cars. Also included in this classification were facilities running alongside the roadway, separated by a grass median, thus increasing the distance between the cyclists’ path and the roadway. The third classification considered is comprised of multi-use trails, which are typically located within parks and at substantial distances from the roadway. Some trails are officially designated as cycling facilities, however data points that were nearest to undesignated trails and not within 15 m of a motorized roadway or an officially designated cycling facility were also included in this category.

Finally, in order to distinguish the effects of the cycling facilities from that of traffic volumes of the road, the road hierarchy was considered for each facility type. Local roads were considered as one category and all highways, arterials, and collectors were considered “major” roads. Since these data were related at the point level, categorical and dummy variables were rounded to the nearest integer following the averaging process described earlier. Figure 7.1 presents a snapshot of the data structure. In total, 4,356 links were measured (556 km), including 2,607 links categorized as “in street” (294 km); 1,597 links as “separated” (231 km); and 152 links as “trail” (31 km).



	Trip_Number	Link_ID	UFP	BC	Major_Road	Cycling_Facility_Type	Cycling_Facility_Class	Distance_from_Road	Daily_Volume	Downtown	Period
2910	12	6657470	19196	5253	1	1	2	17.4	1715	1	1
2911	12	6657474	26047	5277	1	1	2	18.8	2281	1	1
2912	12	6657477	22756	2822	1	1	2	57.6	1785	1	1
2913	12	6657504	17626	5467	0	0	1	2.04	1593	1	1
2914	12	6703708	18901	6434	0	0	1	4.29	1707	1	1
2915	12	6704510	18951	2921	1	0	0	5.26	1140	1	1
2916	13	88646	8840	1558	0	0	1	4.84	1373	1	0
2917	13	90872	18504	1695	0	0	1	4.76	1331	1	0
2918	13	90874	22075	1756	0	0	1	5.57	1115	1	0
2919	13	90876	32070	1756	0	0	1	.893	2425	1	0
2920	13	90878	17347	1756	0	0	1	.85	2425	1	0
2921	13	90880	34516	1756	0	0	1	.969	2287	1	0
2922	13	90882	10663	1756	0	0	1	.48	162	1	0
2923	13	90884	13834	6394	0	0	1	.885	162	1	0

Figure 7.1: A screenshot of the database to illustrate how data were related

## 7.3. Results

### 7.3.1. Air Pollution Mapping

UFP (Figure 7.2) and BC (Figure 7.3) levels collected in the morning peak period and averaged over each link are illustrated below. Through visual inspection of the two maps, we observe significant spatial variability in the data collected.

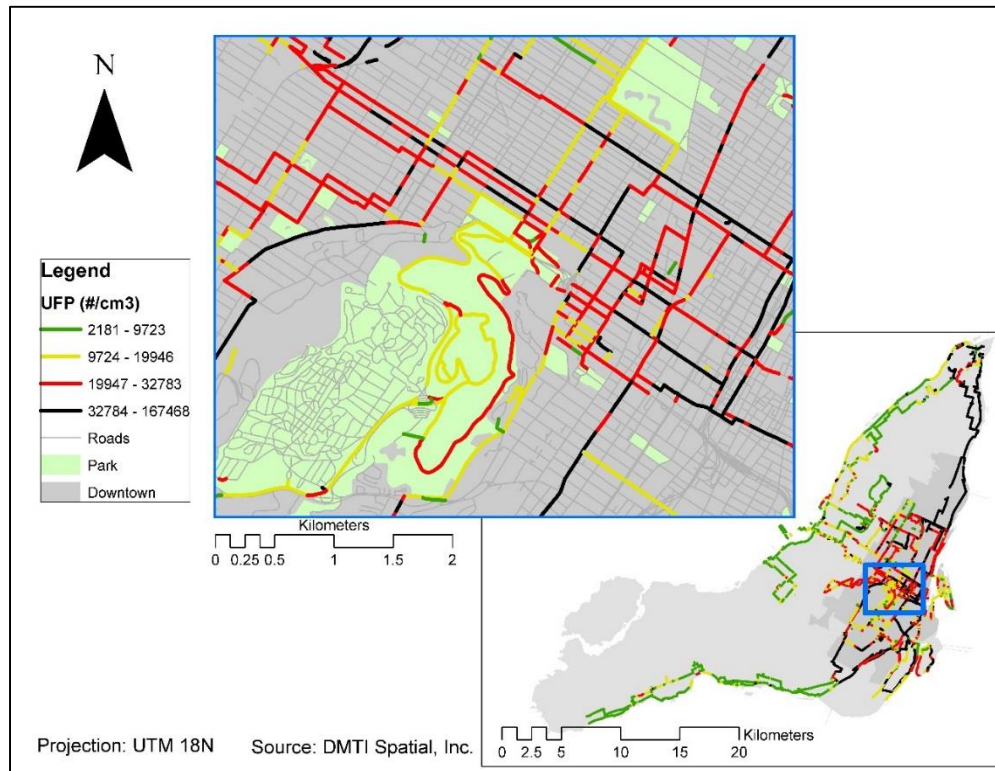


Figure 7.2: UFP concentration maps for the morning period, divided by quartiles; the link results shown are the average of all trips on the link.

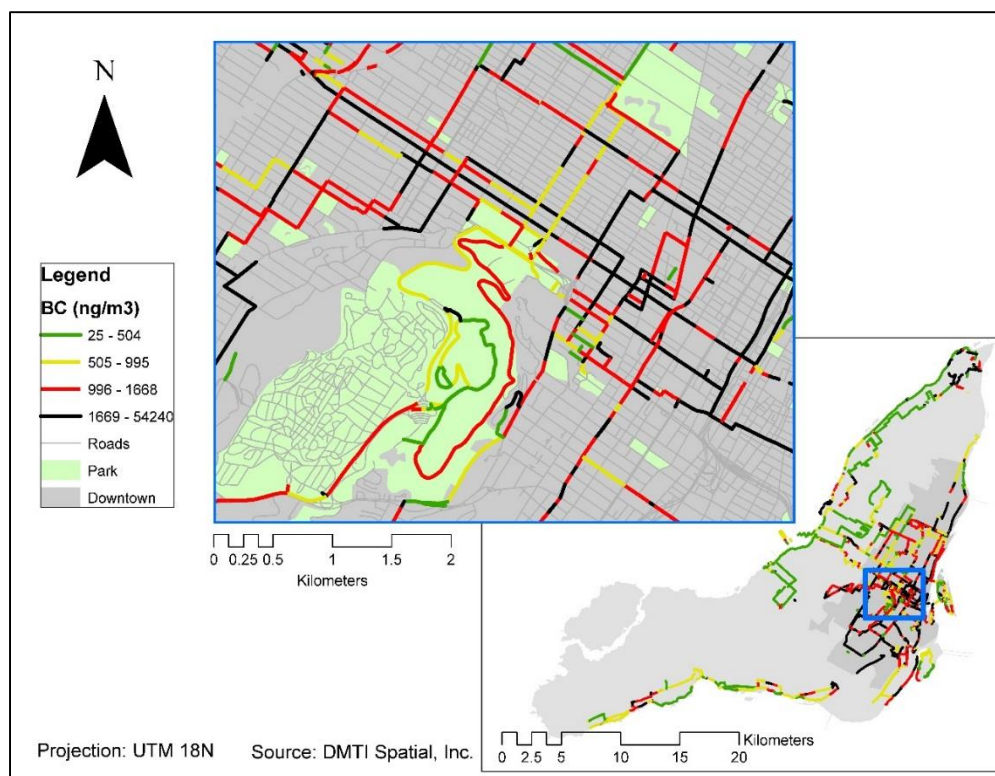


Figure 7.3: BC concentration maps for the morning period, divided by quartiles; the link results shown are the average of all trips on the link.

All-day downtown UFP levels range between 3,511 and 192,340 particles/cm<sup>3</sup> and BC levels range between 18 and 186,528 ng (Table 7.1). For the purposes of this study, “downtown” was defined as the central business borough and all towns and boroughs adjacent to it (Figure 3.2).

Table 7.1: Air Pollution Variability

Attribute	UFP (#/cm <sup>3</sup> )				BC (ng/m <sup>3</sup> )			
	n	Min	Mean	Max	n	Min	Mean	Max
<b>Downtown</b>	11,965	3,511	23,451	192,340	9,271	18	1,481	186,528
<b>Suburbs</b>	5,551	1,411	15,836	112,298	4,064	23	855	92,425
<b>Morning</b>	8,483	2,181	24,948	192,340	6,759	24	1,484	56,351
<b>Afternoon</b>	9,033	1,411	17,382	189,087	6,576	18	1,091	186,528

One thing to note is that morning UFP and BC readings are higher than afternoon readings (Table 7.1). This is due primarily to their inverse relationship to temperature and wind speed, which are both lower in the morning. While there is no health standard for UFP, mean concentrations typically observed in urban areas range between 6,000 and 60,000 particles/cm<sup>3</sup>

(Wang et al. 2011). The concentration map presented in Figure 7.2 clearly shows that the majority of roads in Montreal experience levels within this range.

### 7.3.2. Cycling Facilities Analysis

Air pollution results aggregated per cycling facility type are shown below in Table 7.2. The table shows the average UFP, BC, daily vehicular volume, and the median distance between the GPS points and the centerline of the nearest motorized roadway. Also shown are the relative differences in mean UFP and BC using their respective road hierarchy for “in-street” facilities as their baseline value.

*Table 7.2: Pollution, Traffic, and Distance from Road by Cycling Facility Class*

	In-Street		Separated Track		Trail	
	Major	Local	Major	Local	Major	Local
<b>Cycling Facility Classification</b>	0	1	2	3	4	5
<b>Number of Link-Trips</b>	3,665	7,058	4,017	2,420	254	334
<b>Total Length (km)</b>	103	191	137	94	19	15
<b>Mean UFP (#/cm<sup>3</sup>)</b>	22,551	19,681	23,223	20,733	13,693	15,120
<b>UFP % Change from Baseline</b>	.	.	3%	5%	-41%	-27%
<b>Minimum UFP</b>	1,547	1,411	1,547	1,798	3,171	2,856
<b>Maximum UFP</b>	189,097	192,340	167,468	134,403	70,0619	77,125
<b>Mean BC (ng/m<sup>3</sup>)</b>	1,733	1,133	1,404	1,063	687	638
<b>BC % Change from Baseline</b>	.	.	-19%	-6%	-51%	-40%
<b>Minimum BC</b>	18	18	18	23	18	28
<b>Maximum BC</b>	186,528	54,240	92,424	56,661	9,900	6,183
<b>Daily Traffic Volume (veh)</b>	3,660	1,467	3,848	1,398	4,383	1,313
<b>Median Distance from Road Centerline (m)</b>	4.2	3.4	8.8	8.5	145.1	67.6

A number of observations can be made based on the data presented in Table 7.2. First, despite trails having vehicular volumes approximately equal to or greater than the other two categories, both UFP and BC levels are notably lower than on the other two facility types. Of course the median distances from the motorized roadway centerline are substantially greater than the other facilities, indicating that these pollutants may drastically decay at greater distances from the roadway. Also noteworthy is that between the in-street and separated facilities, the road hierarchy appears to play a stronger role than the actual facility type. In fact, comparing like road

hierarchies, UFP levels are nearly identical between in-street and separated facilities, albeit with the latter slightly elevated. However for BC there appears to be a larger reduction for separated facilities as compared to in-street. This may suggest that BC is more sensitive to the subtle difference in composition and distance from the roadway than UFP, however the greater distances seen for trails seem to dominate the ultimate pollution level. Also of note is that when reductions are present, they appear to be greater on major roads than local ones. This suggests that there may be more to be gained by increasing the separation between cyclists and motorized traffic on these larger streets.

Understanding now the differences in volume and distance of the various facilities, a closer look at pollution levels is revealed by the box plots of UFP (Figure 7.4) and BC (Figure 7.5). Minimum pollution levels for both UFP and BC appear to be unaffected by facility type. Maximum and interquartile UFP levels also appear nearly identical for in-street and separated facilities. However, the differences for BC appear to be more substantial, where not only are the maximum concentrations lower, the interquartile ranges also show conspicuously lower concentrations for separated facilities than in-street. Again though, cycling trails, typically far from the motorized roadway, are clearly lower than their counterparts.

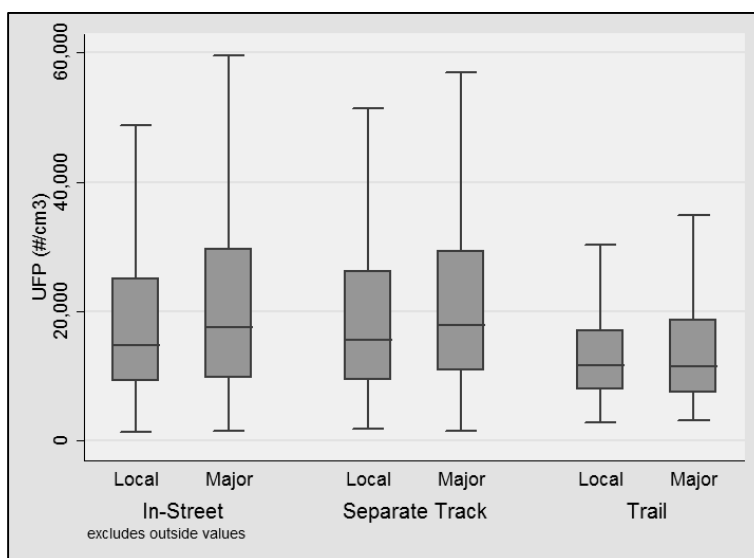


Figure 7.4: Box plot of UFP by cycling facility and road type (omitting extreme values)

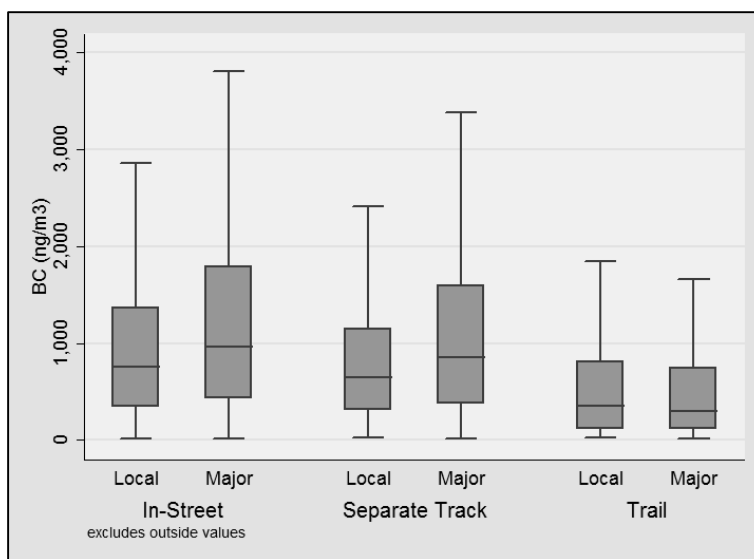


Figure 7.5: Box plot of BC by cycling facility and road type (omitting extreme values)

### 7.3.3. Regression Analysis

Finally, a regression analysis was conducted in order to obtain a more quantitative understanding of the interaction between the cycling facilities and road hierarchy. Dummy variables were included for relations with a major road, separated facility, and trail facility. Previous analysis of this dataset depicted the dominant effects of meteorology, so they were also included in the regression. Meteorological variables include a dummy variable for the real-time temperature being over 20°C, and trip-level variables including the minimum temperature, wind speed, and relative humidity. Table 7.3 presents the variables considered for the regression analysis.

Regressions were performed with the natural logarithm transform of the dependent variables due to their log-normal distribution, and were subsequently sorted by relative effect, as determined by the magnitude of their normalized beta coefficient.

The coefficients presented in Table 7.4 for UFP and Table 7.5 for BC illustrate the effects of meteorology, type of facility, and traffic on measured air pollution levels. The baseline for the facility type dummy variables is a local, in-street facility.

It is important to note at the onset that these regressions are not meant to develop predictive models of UFP and BC in near-road environments. Clearly, land use and other road geometry variables affect the measured concentrations and are not included in the models. The main purpose of these regressions is to capture the simultaneous effects of traffic and bicycle facility design

while adjusting for meteorology, therefore shedding light on the associations between air pollution and bicycle facilities.

*Table 7.3: Descriptive Statistics for Regression Variables Considered*

Variable	Units	Mean	Min	Max
<b>Daily Traffic Volume</b>	Vehicles	2486.18	0.00	15,676
<b>Centerline Distance from Motorized Roadway</b>	m	16.02	0.04	687.57
<b>Major Road</b>	(dummy)	0.45	0	1
<b>Separated Facility</b>	(dummy)	0.36	0	1
<b>Trail Facility</b>	(dummy)	0.03	0	1
<b>Real-Time Temperature <math>\geq 20^{\circ}\text{C}</math></b>	(dummy)	0.85	0	1
<b>Minimum Trip Temperature</b>	$^{\circ}\text{C}$	20.00	13.00	34.00
<b>Trip Wind Speed</b>	km/hr	14.53	5.50	24.50
<b>Trip Relative Humidity</b>	.	0.53	0.29	0.84

The UFP regression in Table 7.4 shows more quantitatively what was earlier described. Cycling on a trail has the largest negative effect on UFP levels, even stronger than cycling on or alongside a major road. The dummy variable for separated facilities was included to show that they produced no additional significant difference for UFP concentrations.

*Table 7.4: Linear Regression for  $\ln(\text{UFP})$  ( $n=17,516$ ;  $R^2=0.223$ )*

Variable	Units	$\beta$	Coefficient	SE	t	$P >  t $
<b>Minimum Temperature</b>	$^{\circ}\text{C}$	-0.258	-0.048	0.002	-28.95	0.000
<b>Wind Speed</b>	km/hr	-0.197	-0.027	0.001	-27.51	0.000
<b>Temperature <math>\geq 20^{\circ}\text{C}</math></b>	(dummy)	-0.156	-0.325	0.017	-18.69	0.000
<b>Relative Humidity</b>	.	-0.127	-0.767	0.041	-18.59	0.000
<b>Trail Facility</b>	(dummy)	-0.098	-0.413	0.028	-14.56	0.000
<b>Major Road</b>	(dummy)	0.060	0.090	0.010	8.60	0.000
<b>Separated Facility</b>	(dummy)	0.005	0.008	0.011	0.71	0.476
<b>Constant</b>	.	.	11.739	0.040	293.60	0.000

Table 7.5, which shows the linear regression for BC, paints a slightly different picture. Here, the effect of trails has shown to be even greater than some meteorological variables, and the effect of separated facilities appears to have a statistically significant effect on lowering BC

concentrations. Again, this suggests that BC may be more sensitive to the distance from the roadway and other micro-environmental factors than UFP.

*Table 7.5: Linear Regression for  $\ln(BC)$  ( $n=13,335$ ;  $R^2=0.153$ )*

Variable	Units	$\beta$	Coefficient	SE	t	P >  t
<b>Relative Humidity</b>	.	0.217	2.190	0.084	26.14	0.000
<b>Minimum Temperature</b>	°C	-0.215	-0.068	0.003	-21.18	0.000
<b>Trail Facility</b>	(dummy)	-0.131	-0.872	0.054	-16.11	0.000
<b>Temperature <math>\geq 20^\circ\text{C}</math></b>	(dummy)	0.109	0.406	0.034	11.80	0.000
<b>Wind Speed</b>	km/hr	-0.099	-0.021	0.002	-10.80	0.000
<b>Major Road</b>	(dummy)	0.097	0.236	0.020	11.64	0.000
<b>Separated Facility</b>	(dummy)	-0.067	-0.171	0.021	-7.96	0.000
<b>Constant</b>	.	.	6.681	0.082	81.74	0.000

Two other factors—the centerline roadway distance and the simulated daily volume—were also considered but ultimately omitted. In the case of the centerline distance, it was moderately co-linear with the trail facility, however the latter had a slightly larger impact. The daily volume could not co-exist in the model with the major road dummy variable, and again, the latter had a slightly larger impact. Yet, this in itself tells us something more. These two variables were considerably difficult to procure, requiring either extensive GIS work or a region-wide mesoscopic simulation, respectively. To obtain the same results with much simpler, available information, this exercise will be easier to both comprehend and repeat.

## 7.4. Conclusion and Discussion

This research exercise has contributed a number of interesting findings. In summary, multi-use trails showed the lowest concentrations for both pollutants. For in-street and separated facilities, riding on or alongside a local street had a larger negative influence on levels for both pollutants; facility type had no effect on UFP but did in fact show a negative effect on BC concentrations. These results are mostly consistent with the mild reductions seen in pollution on separated facilities, and more notable reductions on less-trafficked streets, seen in the existing literature. Yet, in addition to these pollutants in particular, these measurements may serve as a surrogate for an assortment of other harmful pollutants which have been shown to be correlated with UFP and BC.

Therefore, efforts to reduce exposure to these will also likely benefit cyclists' wellbeing with respect to other pollutants as well.

There were a number of limitations in this study. For one, land use characteristics not directly related to cycling facilities were beyond the scope of this investigation, which sought to address specifically the effect of cycling infrastructure. The authors are aware of the importance of these factors, however they have already been addressed in Chapter 6. Furthermore previous research by this group has shown the importance of vehicle composition, in particular trucks, as a determinant of UFP and BC (Hatzopoulou et al. 2013). Other limitations arise when analyzing such a large, aggregate dataset. Due to the high temporal variability and large spatial extent, many effects on pollutant concentrations necessarily went unobserved. For instance, the specific quantity and composition of traffic, as well as unobserved changes in meteorological conditions, can play a large role in instantaneous UFP and BC levels. Although averaging so many observations will inevitably mask this variability, the authors believe that the trends ultimately detected are subsequently more reliable.

Although this research question is in need of more studies in order to draw more robust conclusions, a number of provisional recommendations can be drawn from the results of this particular exercise. With respect to designing comprehensive urban cycling networks, an effort to attract utilitarian cyclists to either less trafficked streets, or better yet, park trails, could help in mitigating their exposure to UFP and BC. This should not be understood as a suggestion to design burdensome, indirect networks for cyclists. On the contrary, the authors suggest that access and convenience for cyclists on local streets be increased. For example, in the study area of Montreal many local streets adjacent and parallel to major streets permit only one-way traffic, often switching directions every few blocks, in order to prevent abusing the side-streets as thoroughfares. However if contra-flow lanes were painted as necessary, or bicycle “salmoning” (riding in the opposite direction permitted to traffic) were sanctioned on these low-volume side-streets, cyclists may be exposed to lower concentrations of pollution. The same could be said of allowing access for cyclists to pass through diverters, which force drivers to turn, usually onto a major street, rather than continuing on a side street.

Finally, it appears that at least for BC, separated facilities do provide mild benefits. It is unclear from this project whether these are due simply to the increased distance or rather the



specific composition of the cycle track. Future research in this area could be to determine whether separation such as a row of parked cars between the travelled way and the cycle track reduce the BC exposure more than the distance alone. Furthermore, this effect was greater on major streets, implying that the presence of separated cycling infrastructure may be more critical for cyclist health on such roads.

## CHAPTER 8 — CONCLUSION

### 8.1. Implications

Broadly speaking, the implications of this research consist of two aspects: the methodological practices of researchers and the practical ramifications following from the interpretation of the results. Both of these points are addressed in this section.

#### *8.1.1. Methodological Implications*

With regard to the methodological framework proposed by this research, many lessons may be constructed. From Chapter 5 it is clear that by averaging measurements and explanatory variables over multiple repetitions, and thus reducing the overall number of records being analyzed, the model fit can improve substantially. While this is true of any averaging process, such a process may mask much of the inherent variability in air pollution concentrations and the causes thereof. The vastly expanded scope engendered by the mobile campaign yields lower model fit values, yet the sheer size of the sample uncovers associations that may not have been detected by more spatially limited efforts.

Overall, both methods have their strengths and weaknesses. The fixed site monitoring was better able to capture variables that required more detailed quantifications, such as the urban canyon effect, the importance of truck traffic, and the difference in UFP levels on either side of the street. The mobile campaign however was able to approximate these variables through large GIS databases, while additionally showing effects for restaurants, distance from highways, and subtle effects of cycling infrastructure.

#### *8.1.2. Consequential Implications*

Recent decades have seen North American cities increasing their development of cycling infrastructure, and the cycling population in these places has responded by more than doubling since 1990 (Pucher, Dill, and Handy 2010; Pucher, Buehler, and Seinen 2011). However this increase in popularity comes with growing concern about the health and safety of cyclists. If municipalities are to continue their no doubt laudable efforts to improve cycling infrastructure and, in turn, cycling mode share, then research must concurrently study the health outcomes of cyclists and establish best practices for this infrastructure development.

The investigations examined in this thesis represent a study in the emerging field of cyclist exposure to air pollution and the role that the cycling infrastructure and other built environment characteristics play in altering that exposure. The regressions developed suggest that by planning cycling networks on smaller streets with less traffic, especially freight traffic, the overall exposure of air pollution to cyclists may be reduced. There is also limited evidence suggesting that creating facilities along the edges of streets does in fact reduce exposure to air pollution, in particular BC. When viable however, the greatest reductions in the microenvironment were seen through park trails, which could be an important element in developing networks in the urban context. Of course efforts to reduce overall pollution, such as by reducing the overall vehicular traffic, will have a positive impact on cyclist health, however it is important to understand how these levels may vary in spatially proximate locations in order to create the most healthful experience for urban cyclists.

## **8.2. Limitations**

Like all research, this was no exception in having a number of limitations. Some arise from the nature of the study itself and others from the logistic feasibilities associated with conducting a spatially expansive data collection campaign such as this.

The LUR model fits obtained in this thesis tend to be lower than more conventional fixed site monitoring campaigns that typically span a number of weeks. One explanation for this however is through the sheer size and variability within the database. Whereas most other studies of this nature are limited to no more than the order of hundreds of records averaged over a number of weeks, the mobile data collection campaign is on the order of tens of thousands of records measured for less than a minute. Furthermore, the sampling on each link occurred over a duration on the order of minutes, whereas more conventional techniques tend to average over a duration on the order of weeks. As such, it should be expected that the model fit would be lower than conventional techniques. The objective of the study however should be kept in mind. This analysis sought to vastly expand the spatial extent of coverage by sacrificing temporal repetition. From this, the intent was to capture the most underlying effects that will affect one's exposure to air pollution on any given street.

The subtext of this problem is that there is simply too much unexplained variability in air pollution measurements when taking a snapshot rather than an in-depth look at each location. Despite having measurements recorded every second during the mobile campaign, the data cannot

be used to its full potential without independent variables at equally high temporal resolution. However, with the exception of temperature data no information was of this resolution. For this reason, brief spikes in air pollution remain unexplained in these models since real-time traffic data would have been infeasible to acquire.

Similarly, the mobile data collection campaign lacked information regarding vehicle composition, which as explained in Chapter 5 proved to be a stronger determinant of air pollution than traffic volumes alone. As explained in Section 4.4, manual traffic counts would have been infeasible to conduct along the 2,000 km of roadways measured in the mobile campaign, and as such, a mesoscopic simulation based on the AMT O-D survey was used. This survey however includes only passenger trips. Large diesel trucks, which are primarily used for freight traffic, are not accounted for. In fact, modelling truck traffic presents unique challenges to researchers due to their exceptional complexity (Roorda et al. 2010). As such, the lack of freight traffic data was a notable limitation in the regression analysis.

Next, the approach to this investigation starts from the assumption that the variability can all be explained by immediate sources of pollution. In truth however, background concentrations may vary from day to day, influenced in part by regional wind patterns and pollution sources. However, these background concentrations were not considered in the analysis. Related to this is the use of the “Downtown Montreal” dummy variable. Despite a number of variables intended to characterize the downtown environment, the presence of unexplained background concentrations in this region remained a substantial explanatory variable in the mobile data models.

Although the fixed site monitoring employed a more conventional air pollution monitoring approach, the sampling periods were considerably shorter than most campaigns. Though much of the observed variability was able to be accounted for in the regression model, UFP concentrations are prone to fluctuate substantially.

Finally, this study was conducted only during the summer months. UFP and BC are both heavily subject to meteorological conditions, so the overall climate in which they are measured could have a large impact on the resulting model. In the same sense, explanatory models may vary from city to city due to climatic and geographic factors.

### **8.3. Future Work**

As mentioned in Chapter 1, this thesis represents a subset of a larger study aimed at determining the acute health outcomes associated with exposure to urban air pollution. As such, these investigations lay the groundwork for future work which will study in greater detail the epidemiological implications of these air pollution concentrations. By strengthening our understanding of what we believe to be the underlying causes of the variations in air pollution, routes can be better planned in order to match an expected level of air pollution.

Finally, much work remains to be done in determining a set of best practices with respect to cycling facility design. Chapter 7 represents a preliminary investigation into the factors that may account for varying levels of UFP and BC, however more research is required before strong conclusions can be drawn. The subject would benefit greatly from more detailed research of specific cycling corridors, especially if a before and after analysis was able to be conducted on a retrofitted bicycle path. Furthermore, a more detailed quantification of cycling facility infrastructure would benefit our understanding of this subject. Due to data limitations, it was infeasible to determine for instance if the cycling facilities were separated by a floating parking lane, and moreover whether parked cars were even present. Such an analysis would have to limit its spatial scope substantially, but could provide better insight into how the actual geometry may affect the cyclists' air pollution exposure. The same can be said of cycle tracks separated by other passive boundaries, such as a tree line or other shrubbery.

### **8.4. Summary**

The research presented in this thesis has duly met the objectives defined in Chapter 1. The thesis presents an innovative framework for collecting air pollution data and using GIS based techniques in order to assess the effects of the built environment and meteorology across an exceptionally large spatial extent. The results of the statistical analysis show comparable results to other land use regression analyses. Although the model fit tends to be lower than that of long term fixed site studies, the exercise shows that even low temporal resolution and high spatial coverage can provide meaningful insight into the causes of variations in air pollution concentrations. Of course, the ephemeral nature of UFP adds to the difficulty in effectively modeling short-term samples, rather than long-term averages. However if we wish to better understand personal exposure to UFP, more

work is needed in explaining the real-time changes in concentration so that they may be more effectively used in epidemiological research.

In addition to the methodological innovations, the results themselves shed additional light on the complex nature of urban air pollution. The association with meteorological factors such as temperature, wind speed, and stability class have been relatively well documented, however this study highlights their central role in explaining much of the temporal variation in both UFP and BC. Yet land use factors were also shown to play a notable role as well. Of particular interest was the distance to restaurant locations—an often overlooked contributor of UFP that appears to merit closer attention in future studies. Traffic volumes and congestion were also shown to be contributors, even when using simulated traffic network data. However, Chapter 5 has shown the importance of not just raw vehicular flows, but of the particular composition thereof. Indeed, the presence of truck traffic appears to disproportionately affect air pollution levels. The mobile LUR accounts for this only indirectly via the distance from highways, which of course are a substantial source of both traffic volumes and freight traffic. Finally, the impact of land use zoning was also a contributor to both the stationary and mobile LURs. In particular, measurements near industrial zones tended to yield higher air pollution concentrations, and to a lesser extent, parks generally appeared to reduce concentrations.

Regarding the effect of cycling infrastructure, the primary finding was that the type of road on which the facility was located was a better predictor of air pollution exposure than the actual design of the facility. However the design, and moreover the distance from the roadway of the facility were not without their impacts. Separated cycle tracks tended to result in bicyclists riding farther from the centerline. A combination of this with the possible passive barriers present on this facility type slightly reduced BC concentrations, even when normalizing by road type. Yet the most substantial impact on air pollution was had by off-street trails, which typically traverse city parks and are located far from busy roadways. Here, a notable drop in UFP and BC levels was observed, and they remained an important factor in the regression analysis. Ultimately, the preliminary recommendations drawn from this analysis in terms of best practices is to facilitate cyclists' use of local streets by alleviating physical and legal interventions designed to curb vehicular traffic for bicyclists.

Issues concerning cycling, land use, the built environment, traffic, air pollution, and health create a complex web of interactions. However, in order to understand the essence of these relationships a compendium of research is required. Any study sufficiently in-depth to provide meaningful answers will necessarily cover only a fraction of this web. The research described in this thesis sits at a single junction of this intricate framework. Its findings build upon the immense body of knowledge that precede it, and will hopefully serve to support further investigations seeking to untangle these interactions. Ultimately, such detailed understanding is essential in order for society to create environmentally sustainable and globally healthful urban environments.

## REFERENCES

- Abernethy, Rebecca C, Ryan W Allen, Ian G Mckendry, and Michael Brauer. 2013. "A Land Use Regression Model for Ultra Fine Particles in Vancouver, Canada." *Environmental Science & Technology* 47 (10): 5217–5225.
- Baldauf, R., E. Thoma, A. Khlystov, V. Isakov, G. Bowker, T. Long, and R. Snow. 2008. "Impacts of Noise Barriers on near-Road Air Quality." *Atmospheric Environment* 42 (32) (October): 7502–7507. doi:10.1016/j.atmosenv.2008.05.051.
- Berghmans, P, N Bleux, L Int Panis, V K Mishra, R Torfs, and M Van Poppel. 2009. "Exposure Assessment of a Cyclist to PM10 and Ultrafine Particles." *The Science of the Total Environment* 407 (4) (February 1): 1286–98. doi:10.1016/j.scitotenv.2008.10.041.
- Boogaard, Hanna, Frank Borgman, Jaap Kamminga, and Gerard Hoek. 2009. "Exposure to Ultrafine and Fine Particles and Noise during Cycling and Driving in 11 Dutch Cities." *Atmospheric Environment* 43 (27) (September): 4234–4242. doi:10.1016/j.atmosenv.2009.05.035.
- Briggs, David J., Susan Collins, Paul Elliott, Paul Fischer, Simon Kingham, Erik Lebret, Karel Pryl, Hans Van Reeuwijk, Kirsty Smallbone, and Andre Van Der Veen. 1997. "Mapping Urban Air Pollution Using GIS: A Regression-Based Approach." *International Journal of Geographical Information Science* 11 (7) (October): 699–718. doi:10.1080/136588197242158.
- Briggs, David J., C de Hoogh, J Gulliver, J Wills, P Elliott, S Kingham, and K Smallbone. 2000. "A Regression-Based Method for Mapping Traffic-Related Air Pollution: Application and Testing in Four Contrasting Urban Environments." *The Science of the Total Environment* 253 (1-3) (May 15): 151–67.
- Briggs, David J., Kees de Hoogh, Chloe Morris, and John Gulliver. 2008. "Effects of Travel Mode on Exposures to Particulate Air Pollution." *Environment International* 34 (1) (January): 12–22. doi:10.1016/j.envint.2007.06.011.
- Brook, Robert D, Barry Franklin, Wayne Cascio, Yuling Hong, George Howard, Michael Lipsett, Russell Luepker, et al. 2004. "Air Pollution and Cardiovascular Disease: A Statement for Healthcare Professionals from the Expert Panel on Population and Prevention Science of the American Heart Association." *Circulation* 109 (21) (June 1): 2655–71. doi:10.1161/01.CIR.0000128587.30041.C8.
- Brunekreef, Bert, and Stephen T Holgate. 2002. "Air Pollution and Health." *Lancet* 360 (9341) (October 19): 1233–42. doi:10.1016/S0140-6736(02)11274-8.



- Buccolieri, Riccardo, Christof Gromke, Silvana Di Sabatino, and Bodo Ruck. 2009. "Aerodynamic Effects of Trees on Pollutant Concentration in Street Canyons." *The Science of the Total Environment* 407 (19) (September 15): 5247–56. doi:10.1016/j.scitotenv.2009.06.016.
- Calderón-Garcidueñas, Lilian, Anna C Solt, Carlos Henríquez-Roldán, Ricardo Torres-Jardón, Bryan Nuse, Lou Herritt, Rafael Villarreal-Calderón, et al. 2008. "Long-Term Air Pollution Exposure Is Associated with Neuroinflammation, an Altered Innate Immune Response, Disruption of the Blood-Brain Barrier, Ultrafine Particulate Deposition, and Accumulation of Amyloid Beta-42 and Alpha-Synuclein in Children and Young Adults." *Toxicologic Pathology* 36 (March): 289–310. doi:10.1177/0192623307313011.
- Card, Jeffrey W, Darryl C Zeldin, James C Bonner, and Earle R Nestmann. 2008. "Pulmonary Applications and Toxicity of Engineered Nanoparticles." *American Journal of Physiology-Lung Cellular and Molecular Physiology* 295 (3): 400–411. doi:10.1152/ajplung.00041.2008.
- Chen, Hong, Mark S Goldberg, and Paul J Villeneuve. 2008. "A Systematic Review of Relation between Long-Term Exposure to Ambient Air Pollution and Chronic Disease." *Reviews on Environmental Health* 23 (4): 243–297.
- Collins, Sue, Kirsty Smallbone, and David J. Briggs. 1995. "A GIS Approach to Modelling Small Area Variations in Air Pollution within a Complex Urban Environment." In *Innovations in GIS 2*, 245–253. Taylor & Francis.
- Crouse, Dan L., Mark S. Goldberg, and Nancy a. Ross. 2009. "A Prediction-Based Approach to Modelling Temporal and Spatial Variability of Traffic-Related Air Pollution in Montreal, Canada." *Atmospheric Environment* 43 (32) (October): 5075–5084. doi:10.1016/j.atmosenv.2009.06.040.
- De Nazelle, Audrey, Scott Fruin, Dane Westerdahl, David Martinez, Anna Ripoll, Nadine Kubesch, and Mark Nieuwenhuijsen. 2012. "A Travel Mode Comparison of Commuters' Exposures to Air Pollutants in Barcelona." *Atmospheric Environment* 59 (November): 151–159. doi:10.1016/j.atmosenv.2012.05.013.
- De Nazelle, Audrey, and Daniel a. Rodríguez. 2009. "Tradeoffs in Incremental Changes towards Pedestrian-Friendly Environments: Physical Activity and Pollution Exposure." *Transportation Research Part D: Transport and Environment* 14 (4) (June): 255–263. doi:10.1016/j.trd.2009.02.002.
- Dockery, D W. 2001. "Epidemiologic Evidence of Cardiovascular Effects of Particulate Air Pollution." *Environmental Health Perspectives* 109 Suppl (March) (August): 483–6.
- Dons, Evi, Luc Int Panis, Martine Van Poppel, Jan Theunis, and Geert Wets. 2012. "Personal Exposure to Black Carbon in Transport Microenvironments." *Atmospheric Environment* 55 (August): 392–398. doi:10.1016/j.atmosenv.2012.03.020.

- Dons, Evi, Martine Van Poppel, Bruno Kochan, Geert Wets, and Luc Int Panis. 2013. "Modeling Temporal and Spatial Variability of Traffic-Related Air Pollution: Hourly Land Use Regression Models for Black Carbon." *Atmospheric Environment* 74 (August): 237–246. doi:10.1016/j.atmosenv.2013.03.050.
- Farrell, William, S Weichenthal, M Goldberg, and Marianne Hatzopoulou. 2013. "Measuring Cyclists' Exposure to Transportation Emissions Across Urban Cycling Facilities." In *Proceedings 92nd Annual Meeting of the Transportation Research Board*. Vol. 6970.
- Farrell, William, Scott Weichenthal, Mark Goldberg, and Marianne Hatzopoulou. 2014a. "A Statistical Model Explaining Air Pollution Exposure of Cyclists in Urban Environments." In *Proceedings 93rd Annual Meeting of the Transportation Research Board*. Vol. 214.
- . 2014b. "Evaluating Air Pollution Exposures across Cycling Infrastructure Types : Implications for Facility Design". *Proceedings 2nd Meeting of the World Symposium on Transport and Land Use Research*.
- Frank, Lawrence Douglas, Jacqueline Kerr, James F Sallis, Rebecca Miles, and Jim Chapman. 2008. "A Hierarchy of Sociodemographic and Environmental Correlates of Walking and Obesity." *Preventive Medicine* 47 (2) (August): 172–8. doi:10.1016/j.ypmed.2008.04.004.
- Frank, Lawrence Douglas, Brian E Saelens, Ken E Powell, and James E Chapman. 2007. "Stepping towards Causation: Do Built Environments or Neighborhood and Travel Preferences Explain Physical Activity, Driving, and Obesity?" *Social Science & Medicine* (1982) 65 (9) (November): 1898–914. doi:10.1016/j.socscimed.2007.05.053.
- Gilbert, Nicolas L, Mark S Goldberg, Bernardo Beckerman, Jeffrey R Brook, and Michael Jerrett. 2005. "Assessing Spatial Variability of Ambient Nitrogen Dioxide in Montréal, Canada, with a Land-Use Regression Model." *Journal of the Air & Waste Management Association* (1995) 55 (8) (August): 1059–63.
- Greaves, Stephen, Tharit Issarayangyun, and Qian Liu. 2008. "Exploring Variability in Pedestrian Exposure to Fine Particulates (PM<sub>2.5</sub>) along a Busy Road." *Atmospheric Environment* 42 (8) (March): 1665–1676. doi:10.1016/j.atmosenv.2007.11.043.
- Hagler, Gayle S.W. 2011. "Post-Processing Method to Reduce Noise While Preserving High Time Resolution in Aethalometer Real-Time Black Carbon Data." *Aerosol and Air Quality Research* 11 (5): 539–546. doi:10.4209/aaqr.2011.05.0055.
- Hatzopoulou, Marianne, Scott Weichenthal, Hussam Dugum, Graeme Pickett, Luis Miranda-Moreno, Ryan Kulka, Ross Andersen, and Mark Goldberg. 2013. "The Impact of Traffic Volume, Composition, and Road Geometry on Personal Air Pollution Exposures among Cyclists in Montreal, Canada." *Journal of Exposure Science & Environmental Epidemiology* 23 (1): 46–51. doi:10.1038/jes.2012.85.

- Health Effects Institute. 2010. "Traffic-Related Air Pollution: A Critical Review of the Literature on Emissions , Exposure , and Health Effects A Special Report of the HEI Panel on the Health Effects of Traffic-Related Air Pollution Executive Summary." *Special Report 17*.
- Henderson, Sarah B. 2007. "Application of Land Use Regression to Estimate Long-Term Concentrations of Traffic-Related Nitrogen Oxides and Fine Particulate Matter." *Environmental Science & Technology* 41 (7): 2422–2428.
- Highwood, Eleanor J, and Robert P Kinnersley. 2006. "When Smoke Gets in Our Eyes: The Multiple Impacts of Atmospheric Black Carbon on Climate, Air Quality and Health." *Environment International* 32 (4) (May): 560–6. doi:10.1016/j.envint.2005.12.003.
- Hoek, Gerard, Rob Beelen, Kees de Hoogh, Danielle Vienneau, John Gulliver, Paul Fischer, and David J. Briggs. 2008. "A Review of Land-Use Regression Models to Assess Spatial Variation of Outdoor Air Pollution." *Atmospheric Environment* 42 (33) (October): 7561–7578. doi:10.1016/j.atmosenv.2008.05.057.
- Hoek, Gerard, Rob Beelen, Gerard Kos, Marieke Dijkema, Saskia C van der Zee, Paul H Fischer, and Bert Brunekreef. 2011. "Land Use Regression Model for Ultrafine Particles in Amsterdam." *Environmental Science & Technology* 45 (2) (January 15): 622–8. doi:10.1021/es1023042.
- Int Panis, Luc, Bas de Geus, Grégory Vandenbulcke, Hanny Willems, Bart Degraeuwe, Nico Bleux, Vinit Mishra, Isabelle Thomas, and Romain Meeusen. 2010. "Exposure to Particulate Matter in Traffic: A Comparison of Cyclists and Car Passengers." *Atmospheric Environment* 44 (19) (June): 2263–2270. doi:10.1016/j.atmosenv.2010.04.028.
- Jacobs, Lotte, Tim S Nawrot, Bas de Geus, Romain Meeusen, Bart Degraeuwe, Alfred Bernard, Muhammad Sughis, Benoit Nemery, and Luc Int Panis. 2010. "Subclinical Responses in Healthy Cyclists Briefly Exposed to Traffic-Related Air Pollution: An Intervention Study." *Environmental Health* 9 (64) (January): 1–8. doi:10.1186/1476-069X-9-64.
- Jansen, Karen L., Timothy V. Larson, Jane Q. Koenig, Therese F. Mar, Carrie Fields, Jim Stewart, and Morton Lippmann. 2005. "Associations between Health Effects and Particulate Matter and Black Carbon in Subjects with Respiratory Disease." *Environmental Health Perspectives* 113 (12) (August 25): 1741–1746. doi:10.1289/ehp.8153.
- Johnson, Markey, V. Isakov, J.S. Touma, S. Mukerjee, and H. Özkaynak. 2010. "Evaluation of Land-Use Regression Models Used to Predict Air Quality Concentrations in an Urban Area." *Atmospheric Environment* 44 (30) (September): 3660–3668. doi:10.1016/j.atmosenv.2010.06.041.
- Katsouyanni, K, G Touloumi, E Samoli, A Gryparis, A Le Tertre, Y Monopolis, G Rossi, et al. 2001. "Confounding and Effect Modification in the Short-Term Effects of Ambient Particles on Total Mortality: Results from 29 European Cities within the APHEA2 Project." *Epidemiology* 12 (5) (September): 521–31.

- Kaur, S, and M J Nieuwenhuijsen. 2009. "Determinants of Personal Exposure to PM2.5, Ultrafine Particle Counts, and CO in a Transport Microenvironment." *Environmental Science & Technology* 43 (13) (July 1): 4737–43.
- Kaur, S., M. Nieuwenhuijsen, and R. Colvile. 2005. "Personal Exposure of Street Canyon Intersection Users to PM2.5, Ultrafine Particle Counts and Carbon Monoxide in Central London, UK." *Atmospheric Environment* 39 (20) (June): 3629–3641. doi:10.1016/j.atmosenv.2005.02.046.
- Kaur, S., M.J. Nieuwenhuijsen, and R.N. Colvile. 2007. "Fine Particulate Matter and Carbon Monoxide Exposure Concentrations in Urban Street Transport Microenvironments." *Atmospheric Environment* 41 (23) (July): 4781–4810. doi:10.1016/j.atmosenv.2007.02.002.
- King, E.A., E. Murphy, and Aonghus McNabola. 2009. "Reducing Pedestrian Exposure to Environmental Pollutants: A Combined Noise Exposure and Air Quality Analysis Approach." *Transportation Research Part D: Transport and Environment* 14 (5) (July): 309–316. doi:10.1016/j.trd.2009.03.005.
- Kingham, Simon, Ian Longley, Jenny Salmond, Woodrow Pattinson, and Kreepa Shrestha. 2013. "Variations in Exposure to Traffic Pollution While Travelling by Different Modes in a Low Density, Less Congested City." *Environmental Pollution* 181 (July 16): 211–218. doi:10.1016/j.envpol.2013.06.030.
- Larsen, Jacob, Zachary Patterson, and Ahmed M. El-Geneidy. 2013. "Build It. But Where? The Use of Geographic Information Systems in Identifying Locations for New Cycling Infrastructure." *International Journal of Sustainable Transportation* 7 (4) (June): 299–317. doi:10.1080/15568318.2011.631098.
- Li, Ning, Constantinos Sioutas, Arthur Cho, Debra Schmitz, Chandan Misra, Joan Sempf, Meiying Wang, Terry Oberley, John Froines, and Andre Nel. 2002. "Ultrafine Particulate Pollutants Induce Oxidative Stress and Mitochondrial Damage." *Environmental Health Perspectives* 111 (4) (December 16): 455–460. doi:10.1289/ehp.6000.
- Lusk, Anne C, Peter G Furth, Patrick Morency, Luis F Miranda-Moreno, Walter C Willett, and Jack T Dennerlein. 2011. "Risk of Injury for Bicycling on Cycle Tracks versus in the Street." *Injury Prevention: Journal of the International Society for Child and Adolescent Injury Prevention* 17 (2) (April): 131–5. doi:10.1136/ip.2010.028696.
- Martins, Leila Droprinchinski, Jorge A Martins, Edmilson D Freitas, Caroline R Mazzoli, Fabio Luiz T Gonçalves, Rita Y Ynoue, Ricardo Hallak, Taciana Toledo a Albuquerque, and Maria De Fatima Andrade. 2010. "Potential Health Impact of Ultrafine Particles under Clean and Polluted Urban Atmospheric Conditions: A Model-Based Study." *Air Quality, Atmosphere, & Health* 3 (1) (March): 29–39. doi:10.1007/s11869-009-0048-9.

- McNabola, Aonghus, B M Broderick, and L W Gill. 2008. "Reduced Exposure to Air Pollution on the Boardwalk in Dublin, Ireland. Measurement and Prediction." *Environment International* 34 (1) (January): 86–93. doi:10.1016/j.envint.2007.07.006.
- Pasquill, F. 1961. "The Estimation of the Dispersion of Windborne Material." *The Meteorological Magazine* 90 (1063): 33–49.
- Pope, C. Arden. 2000. "Epidemiology of Fine Particulate Air Pollution and Human Health: Biologic Mechanisms and Who's at Risk?" *Environmental Health Perspectives* 108 Suppl (August) (August): 713–23.
- Pope, C. Arden, and Douglas W. Dockery. 2006. "Health Effects of Fine Particulate Air Pollution: Lines That Connect." *Journal of the Air & Waste Management Association* 56 (6) (June): 709–742. doi:10.1080/10473289.2006.10464485.
- Pucher, John, and Ralph Buehler. 2005. "Cycling Trends & Policies in Canadian Cities." *World Transport Policy & Practice* 11 (1): 43–61.
- Pucher, John, Ralph Buehler, and Mark Seinen. 2011. "Bicycling Renaissance in North America? An Update and Re-Appraisal of Cycling Trends and Policies." *Transportation Research Part A: Policy and Practice* 45 (6) (July): 451–475. doi:10.1016/j.tra.2011.03.001.
- Pucher, John, Jennifer Dill, and Susan Handy. 2010. "Infrastructure, Programs, and Policies to Increase Bicycling: An International Review." *Preventive Medicine* 50 Suppl 1 (January): S106–25. doi:10.1016/j.ypmed.2009.07.028.
- Rivera, Marcela, Xavier Basagaña, Inmaculada Aguilera, David Agis, Laura Bouso, Maria Foraster, Mercedes Medina-Ramón, Jorge Pey, Nino Künzli, and Gerard Hoek. 2012. "Spatial Distribution of Ultrafine Particles in Urban Settings: A Land Use Regression Model." *Atmospheric Environment* 54 (July): 657–666. doi:10.1016/j.atmosenv.2012.01.058.
- Rojas-Rueda, David, Audrey de Nazelle, Marko Tainio, and Mark J Nieuwenhuijsen. 2011. "The Health Risks and Benefits of Cycling in Urban Environments Compared with Car Use: Health Impact Assessment Study." *British Medical Journal* 343: 1–8. doi:10.1136/bmj.d4521.
- Roorda, Matthew J., Rinaldo Cavalcante, Stephanie McCabe, and Helen Kwan. 2010. "A Conceptual Framework for Agent-Based Modelling of Logistics Services." *Transportation Research Part E: Logistics and Transportation Review* 46 (1) (January): 18–31. doi:10.1016/j.tre.2009.06.002.
- Ross, Zev, Paul B English, Rusty Scalf, Robert Gunier, Svetlana Smorodinsky, Steve Wall, and Michael Jerrett. 2006. "Nitrogen Dioxide Prediction in Southern California Using Land Use Regression Modeling: Potential for Environmental Health Analyses." *Journal of Exposure Science & Environmental Epidemiology* 16 (2) (March): 106–14. doi:10.1038/sj.jea.7500442.

- Ryan, Patrick H, and Grace K LeMasters. 2007. "A Review of Land-Use Regression Models for Characterizing Intraurban Air Pollution Exposure." *Inhalation Toxicology* 19 Suppl 1 (June 2006) (January): 127–33. doi:10.1080/08958370701495998.
- Sahsuvaroglu, Talar, Altaf Arain, Pavlos Kanaroglou, Norm Finkelstein, Bruce Newbold, Michael Jerrett, Bernardo Beckerman, Jeffrey Brook, Murray Finkelstein, and Nicolas L. Gilbert. 2006. "A Land Use Regression Model for Predicting Ambient Concentrations of Nitrogen Dioxide in Hamilton, Ontario, Canada." *Journal of the Air & Waste Management Association* 56 (8) (August): 1059–1069. doi:10.1080/10473289.2006.10464542.
- Samet, JM, F Dominici, FC Curriero, I Coursac, and SL Zeger. 2000. "Fine Particulate Air Pollution and Mortality in 20 US Cities, 1987–1994." *New England Journal of Medicine* 343 (24): 1742–1749.
- Sider, Timothy, Ahsan Alam, Mohamad Zukari, Hussam Dugum, Nathan Goldstein, Naveen Eluru, and Marianne Hatzopoulou. 2013. "Land-Use and Socio-Economics as Determinants of Traffic Emissions and Individual Exposure to Air Pollution." *Journal of Transport Geography* 33 (August): 230–239. doi:10.1016/j.jtrangeo.2013.08.006.
- Sider, Timothy, Gabriel Goulet-Langlois, Naveen Eluru, and Marianne Hatzopoulou. 2013. "Evaluating the Sensitivity of Transport Emission Inventories to the Level of Input Aggregation and Model Randomness." In *Proceedings 93rd Annual Meeting of the Transportation Research Board*.
- Strak, Maciej, Hanna Boogaard, Kees Meliefste, Marieke Oldenwening, Moniek Zuurbier, Bert Brunekreef, and Gerard Hoek. 2010. "Respiratory Health Effects of Ultrafine and Fine Particle Exposure in Cyclists." *Occupational and Environmental Medicine* 67 (2) (February): 118–24. doi:10.1136/oem.2009.046847.
- Strauss, Jillian, Luis Miranda-Moreno, Dan Crouse, Mark S. Goldberg, Nancy a. Ross, and Marianne Hatzopoulou. 2012. "Investigating the Link between Cyclist Volumes and Air Pollution along Bicycle Facilities in a Dense Urban Core." *Transportation Research Part D: Transport and Environment* 17 (8) (December): 619–625. doi:10.1016/j.trd.2012.07.007.
- Tsai, Dai-Hua, Yi-Her Wu, and Chang-Chuan Chan. 2008. "Comparisons of Commuter's Exposure to Particulate Matters While Using Different Transportation Modes." *The Science of the Total Environment* 405 (1-3) (November 1): 71–7. doi:10.1016/j.scitotenv.2008.06.016.
- Vélo Québec. 2010. "Bicycling in Québec in 2010."
- Wang, Yungang, Philip K. Hopke, David C. Chalupa, and Mark J. Utell. 2011. "Long-Term Study of Urban Ultrafine Particles and Other Pollutants." *Atmospheric Environment* 45 (40) (December): 7672–7680. doi:10.1016/j.atmosenv.2010.08.022.
- Weichenthal, Scott, William Farrell, Mark Goldberg, Lawrence Joseph, and Marianne Hatzopoulou. 2014. "Characterizing the Impact of Traffic and the Built Environment on near-

Road Ultrafine Particle and Black Carbon Concentrations.” *Environmental Research* 132 (July): 305–10. doi:10.1016/j.envres.2014.04.007.

Weichenthal, Scott, Ryan Kulka, Aimee Dubeau, Christina Martin, Daniel Wang, and Robert Dales. 2011. “Traffic-Related Air Pollution and Acute Changes in Heart Rate Variability and Respiratory Function in Urban Cyclists.” *Environmental Health Perspectives* 119 (10) (October): 1373–8. doi:10.1289/ehp.1003321.

Zuurbier, Moniek, Gerard Hoek, Marieke Oldenwening, Kees Meliefste, Peter van den Hazel, and Bert Brunekreef. 2011. “Respiratory Effects of Commuters’ Exposure to Air Pollution in Traffic.” *Epidemiology* 22 (2) (March): 219–27. doi:10.1097/EDE.0b013e3182093693.